NASA Contractor Report 165803

(NASA-CR-165803-Vol-1) LOW REYNOLDS NUMBER AIRFOIL SURVEY, VOLUME 1 Final Report (Low Energy Transport Systems) 106 p
HC A06/MF A01 CSCL 10A

N82-14059

Unclas
G3/02 08687

LOW REYNOLDS NUMBER AIRFOIL SURVEY
VOLUME I

B. H. Carmichael

LOW ENERGY TRANSPORTATION SYSTEMS
Capistrano Beach, California 92624

'hase Order L-40598
981

National Aeronautics and
Space Administration

Langley Research Center
Hampton, Virginia 23665

PREFACE

The location and collection of the large number of useful references pertaining to this highly specialized field was expedited through the generous and wholehearted cooperation of many enthusiastic researchers. The extensive airfoil design and testing by Drs. Althaus, Eppler and Wortmann of Stuttgart University, those of Dr. van Ingen and his associates at Delft University, The Netherlands, and those of Dr. Mueller and his associates at the University of Notre Dame are current and most useful. Although NASA Langley is not active in the critical Reynolds number field, discussions with Dr. Pfenninger, H. Phillips, and Dan Somers and Harry Shoaf of that facility have been helpful. Additional useful data have been obtained through Dr. Kramer of Göttingen University, Dr. Marsden of the University of Alberta, Dr. Miley of Texas A&M, Dr. Eggleston of the University of Western Ontario, Larrabee and Derilla of Massachusetts Institute of Technology, and Patrick of Cranfield University.

Aid was also received from Zipkin and Dr. Roy Smith of General Electric Corporation, John McMasters of Boeing Aircraft, Bob Liebeck of Douglas Aircraft, and Russ Osborne of Wright Field

The scientific free flight measurements of model aircraft builders, Maximillian Hacklinger of Germany, Gilbert Hoffmann, Andy Buaer, and Blain Rawdon of the United States have been inspiring.

Meeting and talking with Frank Zaic, whose Model Aircraft Yearbooks have disseminated the latest technology to model aircraft builders throughout the world for half a centure was a great joy and privilege. Discussions and correspondence with expert model builders such as Blanchard, Champine, Gieskieng, Gale, Hannan, Hines, Isaacson, Meuser, Meier, Ko, Pressnell,

Reid,Wagner, White, and Xenakis have helped to make the limitations of laboratory developed maximum performance airfoils when encountering the real world of rough air dynamic free flight painfully clear. The keen observational powers and empirical developments by free flight model builders have already arrived at a high technical plateau.

LOW REYNOLDS NUMBER AIRFOIL DATA SURVEY

TABLE OF CONTENTS

List of Illustrations

Nomenclature

SYMBOL	DESCRIPTION	UNITS
c	airfoil chord length	ft.
C_D	drag coefficient = $D/q \cdot S$	-
C_L	lift coefficient = $L/q \cdot S$	-
C_M	pitching moment coefficient = $M/q \cdot S \cdot c$	-
C_P	pressure coefficient = $(p_1 - p_o)/q$	
C_w	wetted area drag coefficient = $D/q \cdot S_w$	-
D	drag	pounds
f	camber or maximum mean line height above chord line	c
g	acceleration of gravity	ft/sec^2
h_t	height of bubble at transition	ft.
l	length	ft.
L	lift	pounds
L_b	total bubble length	ft.
m	velocity gradient parameter = $-\frac{\theta^2}{\nu}\cdot\frac{dU}{dx}$	-
M	pitching moment	ft.pounds
p_1	local surface pressure	$pounds/ft^2$
p_o	ambic pressure	$pounds/ft^2$
q	flight dynamic pressure = $\frac{\rho}{2}U_\infty^2$	$pounds/ft^2$
R	reattachment point	-
R_s	arc length Reynolds No. = $\frac{U s}{\nu}$	-
RN	chord Reynolds No. = R_c = $\frac{U_\infty c}{\nu}$	-
R_θ	momentum thickness Reynolds No. = $\frac{U\theta}{\nu}$	-
R_{θ_s}	R_θ at separation point = $\frac{U\theta_s}{\nu}$	-
s	arc length from stagnation point	ft.
S	wing area	ft^2

Nomenclature Continued

SYMBOL	DESCRIPTION	UNITS
S_w	wetted area	ft^2
SPL	sound pressure level	db
t	maximum airfoil thickness	ft.
T	transition point	-
T_u	turbulence level	% U_∞
u	velocity at height y in the boundary layer	ft/sec
U	velocity at outside edge of the boundary layer	ft/sec
U_∞	flight velocity	ft/sec
V	spanwise velocity	ft/sec
X	distance along stream direction	ft.
ΛX	laminar portion of bubble length	ft.
y	distance normal to surface	ft.
α	angle of attack - between chord line & relative wind	deg.
Δ	increment of distance	ft.
δ^*	displacement thickness = $\int_0^\delta (1 - \frac{u}{U})\, dY$	ft.
θ	momentum thickness = $\int_0^\delta \frac{u}{U}(1 - \frac{u}{U})\, dY$	ft.
γ	separation streamline angle from surface	deg.
σ	pressure recovery coefficient = 1 -	-
ρ	fluid density	$\frac{\text{pounds sec}^2}{ft^4}$
μ	absolute viscosity	$\frac{\text{pounds sec}}{ft^2}$
ν	kinematic viscosity	ft^2/sec

SUMMARY

Experimental aerodynamic properties of two dimensional airfoils in the critical chordlength Reynolds number range between 40,000 and 100,000 have been gathered from sources in nine countries of the world and from a seven decade time period. The differences in flow behavior in this regime compared with lower and higher Reynolds numbers are discussed. Information on flow separation, in particular, the large laminar separation bubble is discussed in detail in view of its important influence on critical Reynolds number airfoil behavior. The shortcomings of applying theoretical boundary layer computations found successful at higher Reynolds numbers to the critical regime are discussed. The large variation in experimental aerodynamic characteristic measurement due to small changes in ambient turbulence, vibration, and sound level is illustrated with experimental data. The variation in results from the best available laboratories and the problem of realistic laboratory simulation of free flight conditions is made clear. The difficulties in obtaining accurate detailed measurements in free flight are discussed.

Dramatic performance improvements at critical Reynolds number, achieved with various types of boundary layer tripping devices are discussed.

The included chronologies and bibliographies are intended to be the most complete available on this subject.

The aerodynamic parameters of airfoils in the critical Reynolds number range will be compared in the second volume of this study.

I BRIEF REVIEW OF APPLICABLE AERODYNAMIC PRINCIPLES

Boundary Layer

A comparatively thin sheet of decelerated fluid originating through friction along the surface of solids.

Boundary Layer - Laminar

The condition found at lower Reynolds numbers in which interchange of momentum between adjacent boundary layer levels does <u>not</u> occur. Surface friction and flow generated noise are low compared to ---

Boundary Layer - Turbulent

The condition found at higher Reynolds numbers in which interchange of momentum between adjacent boundary layer levels does occur. Surface friction and flow generated noise are high compared to the laminar condition.

Coefficient of Lift

The lift force (L) of a wing, non-dimensionalized on the basis of projected wing area (S) and flight dynamic pressure (q).

$$C_L = \frac{L}{S \cdot q}$$

Coefficient of Drag - Profile

The drag force (D) of a wing, non-dimensionalized on the basis of projected wing area (S) and flight dynamic pressure (q).

$$C_D = \frac{D}{S \cdot q}$$

Coefficient of Drag - Wetted

The drag force (D) of a wing, non-dimensionalized on the basis of wetted area $S_W = 2S$ and flight dynamic pressure (q).

$$C_W = \frac{D}{S_W \cdot q}$$

Coefficient of Moment

The pitching moment (M) of a wing, non-dimensionalized on the basis of projected wing area S, wing chord c, and flight dynamic pressure (q).

$$C_M = \frac{M}{S \cdot c \cdot q}$$

Coefficient of Pressure

The difference between local surface pressure at any point on a wing (P) and the free stream pressure (P_0), non-dimensionalized by flight dynamic pressure (q).

$$C_p = \frac{P - P_0}{q}$$

Density - Fluid

The mass density is equal to the weight per unit volume divided by the acceleration of gravity.

$$\rho = \frac{W}{V \cdot g}$$

Flight Dynamic Pressure

The kinetic energy of the relative airstream is equal to the product of one-half the fluid mass density and the square of the flight or free stream velocity.

$$q = \frac{\rho}{2} U_\infty^2$$

Pressure Gradient

The rate of rise or fall of local pressure with distance along the surface $\partial P/\partial s$

Reynolds Number - Chord

The ratio of inertial to viscous influences on the boundary layer. Large values help the boundary layer remain attached in spite of viscous induced retardation in the face of strong adverse pressure gradients. For a given fluid condition of density ρ and viscosity, μ, the Reynolds number is proportional to the product of wing chord c and true flight speed U_∞

$$R_c = \frac{\rho \cdot U_\infty c}{\mu} = \frac{U_\infty c}{\nu}$$

Reynolds Number - Boundary Layer

Prediction of the detailed behavior of the boundary layer is often correlated on the basis of either the displacement thickness RN R_{δ^*}, or the momentum thickness RN R_θ, where the local velocity U at the outer edge of the boundary layer is substituted for flight velocity.

$$R_{\delta^*} = \frac{U \delta^*}{\nu}$$

$$R_\theta = \frac{U \theta}{\nu}$$

Separation of the Boundary Layer - Laminar

At low Reynolds numbers the friction retarded flow near the surface has insufficient inertia or momentum to oppose adverse pressure gradients above a certain level, and is actually reversed in direction and separates from the surface causing large decrease in lift and large increase in drag. At Reynolds

numbers below about 50,000 there is insufficient distance for the flow to reattach prior to the trailing edge.

Separation Bubble - Laminar

At somewhat higher Reynolds numbers it is possible for the separated laminar boundary layer to go through transition to turbulent flow as a free wake, and then reattach to the surface as a turbulent boundary layer prior to the trailing edge. The region where this complex phenomena takes place is called the laminar separation bubble, and is so important for the range $50{,}000 < R_C < 4{,}000{,}000$ that an entire section of this report (III) will be devoted to it.

Separation of the Boundary Layer - Turbulent

It is also possible for a turbulent boundary layer to separate, causing a decrease in lift and a large increase in drag. This can be delayed by increases in chord Reynolds number, extensive laminar flow ahead of the start of pressure rise, and shaping the airfoil to produce an initial steep rise in pressure while the boundary layer is still relatively thin, then gradually decreasing the pressure gradient as the boundary layer thickens.

Suction Boundary Layer Control

Aerodynamic advantages can be achieved by sucking away the lower retarded layers. This method can be used to obtain large increases in maximum lift coefficient, or in the case of carefully distributed suction to retain attached laminar boundary layers even in the presence of strong adverse longitudinal and transverse pressure gradients to theoretically unlimited values of Reynolds number.

Thickness - Displacement

The boundary layer displacement thickness δ^* is the degree by which the potential flow is displaced from the wall by the boundary layer. δ^* can also be thought of as the required height of a layer which has lost all of its velocity with a mass flow loss equal to that integrated through the actual boundary layer.

$$\delta^* = \int_0^{\delta} \left(1-\frac{u}{U}\right) dy$$

Thickness - Momentum

The boundary layer momentum thickness θ is the height of a completely stagnant layer which would have the same loss in momentum as that integrated through the actual boundary layer. The momentum loss is equal to the drag.

$$\theta = \int_0^{\delta} \frac{u}{U}\left(1 - \frac{u}{U}\right)dy$$

Thickness - Kinetic Energy or Dissipation

This thickness follows the same reasoning as above but in terms of loss in kinetic energy. It is useful in certain correlative work.

$$\delta_3 = \int_0^{\delta} \frac{u}{U}\left(1 - \left(\frac{u^2}{U^2}\right)\right)dy$$

Transition - Boundary Layer

At sufficiently high combinations of Reynolds number and disturbance levels, the boundary layer which starts off in the laminar state goes through a complex transition to the fully turbulent state. It is not generally realized just how far this process can be delayed by reducing disturbance in the environment or those introduced by the vehicle. The earlier established flat plate transition line is still copied from text book to text book showing a transition at $R_X = 320{,}000$ in spite of the fact that $R_X = 3 \times 10^6$ was achieved in 1940 and $R_X = 5 \times 10^6$ more recently. If now a strong favorable pressure gradient is introduced, as on the forward part of thick low drag airfoils or low length to diameter ratio bodies of revolution, the transition length Reynolds number has been raised to 45,000,000 and for some cases could be even higher. As stated previously, there is no theoretical limit to laminar length Reynolds number with distributed suction flow control.

Tripping of the Boundary Layer

The boundary layer can be artificially induced to change state from the laminar to the turbulent case by introduction of various eddy producers either in the flow ahead of the wing or on the wing surface itself. This is done to mitigate the effects of the laminar separation previously discussed. In

some cases a drastic improvement in wing performance can be achieved. This subject is important enough to constitute a complete section (V) of this report.

Velocity - Flight or Free Stream

The velocity of the vehicle relative to the fluid U_∞. By reciprocity it is unimportant whether the vehicle moves through the fluid or the fluid streams past a stationary vehicle.

Velocity - Potential

The potential velocity distribution about a shape can be computed by inviscid methods, the Neumann being currently most popular. The shape should, however, be altered by adding the displacement thickness of the boundary layer and probably the wake. A new boundary layer calculation can now be computed from the altered pressure distribution. This iteration becomes increasingly important as the Reynolds number decreases. Where the laminar bubble attains significant size it would also be important to include its geometry. Recently the geometry of the laminar bubble (or at least certain types) has been defined.

Velocity - Boundary Layer

The velocity in the boundary layer U varies from zero at the wall to U or the potential value at the outer edge. The exact shape of velocity vs. height curve is important to laminar boundary layer stability. The concave profiles produced by strong favorable pressure gradients (flow acceleration) promoting high transition length Reynolds numbers. The linear lower profile found in zero pressure gradient has a much lower stability limit, while the inflected profiles found in adverse pressure gradients are even lower.

Viscosity - Absolute

The viscosity or stickiness of the fluid μ is the proportional constant linking the shear stress at the surface to the rate of change of velocity with distance from the surface. It is therefore in units of (pound)(second)/foot^2.

Viscosity - Kinematic

The kinematic viscosity ν is the ratio of the absolute fluid viscosity to the fluid mass density. Since the ratio appears in the Reynolds number, it is convenient to use ν for which values are available for air as a function of altitude in the earth's atmosphere and for water as function of temperature.

The short discussions given above are intended to help the reader in absorbing the main text of this report. The phenomena involved can be studied in greater detail in the following excellent references:

I-1 - Schlichting, Dr. Hermann - Boundary Layer Theory
First published in German language under the title "Grenzschicht-Theorie." 1951 McGraw-Hill Book Company, Inc. 4th Edition 1960.

I-2 - White, Frank M. - Viscous Fluid Flow McGraw-Hill Book Company, Inc. - New York 1974

II CHANGES IN FLOW PHENOMENA AND WING DESIGN TECHNIQUES WITH INCREASING REYNOLDS NUMBER

Although this report concentrates most heavily on Reynolds numbers between 20,000 and 200,000 it is believed helpful to present this regime as a band in the larger range of Reynolds numbers between 1 and 1,000 million so far explored by man. This is to show how the peculiarities of this region are a logical form of the beautiful and fascinating but ever-changing flow phenomena as one progresses through the "Realm of Reynolds."

Toward this end, the author has prepared Figure 1 which presents an outline of the flow phenomena variations, applications to motion in nature, and applications to man-made transportation devices as a function of Reynolds number.

The lowest straight line provides the laminar flat plate friction coefficient. The next line up extending from 10^5 to 10^9 provides the turbulent flat plate friction coefficient. The remaining two lines are the drag coefficients of spheres and cylinders converted from their normal frontal area form to wetted area form to be comparable with the plate coefficients. The marked decrease in the drag of cylinders and spheres at a Reynolds number of 400,000 occurs when transition to a turbulent boundary layer preceeds laminar separation. A similar effect is seen for a 10% thick Göttingen 801 airfoil at $\alpha = 12°$.

The critical Reynolds number is about 70,000 and a hysteresis loop is found. In approaching the critical condition from a lower Reynolds number, the drag stays high to a greater Reynolds number than that to which the drag stays low when backing down from a higher Reynolds number.

We shall now discuss twelve Reynolds number bands from lowest to highest with brief descriptions of the changing flow regimes and their significance to nature's and man-made attempts for efficient motion of solid bodies through fluids.

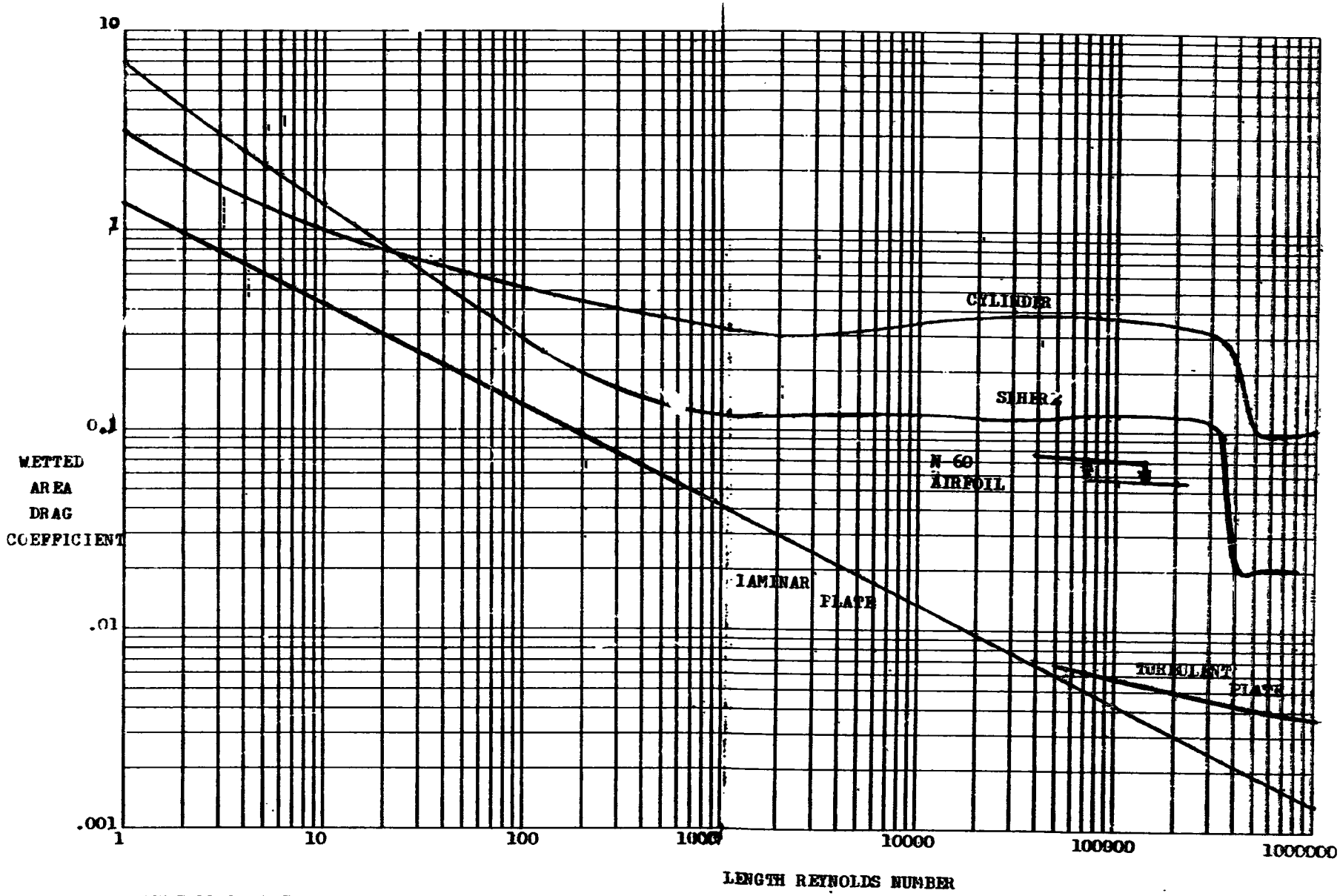

FIGURE 11-1- THE REALM OF REYNOLDS

(A) VERY LOW REYNOLDS NUMBER

At fractional Reynolds numbers, the flow is completely viscous. Fortunately, even in nature, wing design does not occur within this region. The practical considerations on Earth are the falling rates of smoke, dust, fog and pollen particles. This regime is outside the range of interest of this summary. For further information see Hoerner, reference II-1.

(B) REYNOLDS NUMBERS BELOW 150

This regime becomes of interest in the design of turbulence reducing screens II-3 and smoke streak producing wires II-4 for low turbulence wind tunnels. It is desired that these devices introduce a minimum disturbance to the flow. For Reynolds numbers less than 5 the flow is laminar and completely unseparated. Between 5 and 40 a fixed vortex pair is found just behind the wire. For values between 40 and 150, the laminar vortex street forms. In the case of smoke wires, a value of .25 has been found to introduce negligible disturbance to the stream. The critical RN at which screens produce troublesome eddies varies from about 30 to 60 depending on the screen solidity.

(C) REYNOLDS NUMBERS BETWEEN 1000 and 10,000

Here the flow is strongly laminar and it is very difficult to produce turbulent boundary layers artifically. Many insects must fly in this regime and nature has arrived at some unusual solutions. The dragonfly has a saw tooth single surface airfoil. It is speculated that eddies in the troughs help keep the flow attached (II-5). The common house fly wing, when viewed under the microscope, has large numbers of fine hair-like elements projecting normal to the surface. It is speculated that these promote eddy-induced energy transfer to prevent separation. Indoor model airplanes of the microfilm type operate in this regime. Single surface curved plates which have been found to be superior to flat plates or airfoils are employed. It has also been found that the blunt leading and trailing edge structurally required actually enhance the aerodynamic performance in this regime.

(D) REYNOLDS NUMBERS BETWEEN 10,000 AND 30,000

Bauer (II-7) has recently established in careful free flight testing that the total drag minus the induced drag of hand-launched glider models, non-dimensionalized on the basis of total wetted area give a coefficient equal to the laminar plate value. It seems that we have had 100% natural laminar flow aircraft in existence for some time! The other side of the coin is that these aircraft can only operate at lift coefficients of 0.5 or less. Even so, their lift-to-drag ratios are the best obtainable at this RN and their sinking speeds are phenomenally low (considering the small Reynolds number) due to their very low drag coefficient and in spite of the somewhat restricted lift coefficient. Trimming these models to higher lift coefficients produces a separated laminar boundary layer without reattachment. The lift falls, the drag rises by a very large factor, and the performance markedly deteriorates. To date, artificial tripping of the boundary layer has not been successful in this regime. Small rubber band powered indoor scale models called Peanut scale (II-8) also operate in this regime but their performance technology is not yet as highly developed as the hand-launched glider models.

(E) REYNOLDS NUMBERS BETWEEN 30,000 AND 70,000

This regime is of most interest to the technically oriented model aircraft builders and flyers. Both the Nordic A-2, tow-line launched model sailplanes and the Wakefield rubber powered models operate herein. These models are judged on endurance and must have as high as possible a ratio of $(\text{lift})^{3/2}/\text{drag}$. Induced drag considerations call for a high aspect ratio wing but this reduces the Reynolds number, so great care must be taken in the choice of the airfoil section-aspect ratio combination employed. Six percent thick airfoils can become supercritical near the upper end of this regime and the critical RN can be decreased toward the lower end by artifical boundary layer tripping. Under natural laminar separation conditions, the distance from separation to reattachment can be expressed as $RN_R - RN_S \simeq 50{,}000$. Thus, in the lower chord RN regime there is simply insufficient distance to the trailing edge for

reattachment to occur. Nevertheless, excellent performing wing sections have been developed for this regime.

This RN regime became suddenly of national interest in 1978 when JPL investigated the possibility of exploring the planet Mars by an aircraft flying in the thin Martian atmosphere (II-9). The RN fell right in this range. It is also of great interest for RPV aircraft operating at extreme altitude ➡100,000 feet (II-10) in the earth's atmosphere. To date, need for additional low turbulence laboratory work in this regime has not been responded to in the U.S. but a few European laboratories have continued their excellent earlier work.

(F) REYNOLDS NUMBERS BETWEEN 70,000 AND 200,000

At the lower end of this regime we find the bat in nature and small radio controlled model sailplanes and model power planes as man-made devices. Extensive laminar flow is easy to obtain and airfoil performance improves markedly in this regime. At the upper end, boundary layer tripping devices are no longer needed for sections as thick as 12%. Even a 19.6% thick section was made to deliver reasonable performance at a Reynolds number of 150,000 with the aid of a trip wire. There is a small data base for this regime but more work is justified in view of high altitude RPV and low altitude mini-RPV interest. The laminar separation bubble is still a significant potential performance robber in this region of flight. It should also be remembered that the pressure recoveries possible for an attached turbulent boundary layer are much less at low Reynolds number than at high.

(G) REYNOLDS NUMBERS BETWEEN 200,000 AND 700,000

In this regime we find man and nature together in flight. Large soaring birds of quite remarkable performance, large radio controlled model aircraft, foot launched ultra-light man-carrying hang gliders, and that super engineering triumph, the human power aircraft.

Again, extensive laminar flow is easy to obtain and airfoil performance continues to rapidly improve compared to that at

lower Reynolds numbers. There is little worry over reattachment failing to occur after mid-chord laminar separation, but the laminar separation bubble is still of significant relative length and does cost some performance. One must still be conservative in choice of the thickness-camber combination. Very little good data exists in this regime.

(H) REYNOLDS NUMBERS BETWEEN 700,000 AND 3,000,000

The aerodynamic data in this regime is very extensive and of very high quality. Two early NACA investigations have been supplemented by the excellent work at Stuttgart by Eppler, Wortmann and Althaus, by Marsden of Edmonton, by Liebeck of Douglas Aircraft, and by Somers of NASA.

In the high performance man-carrying sailplane we have marked performance improvement over the already highly refined WW II types through extensive natural laminar flow. This 30-year old technology is only now beginning to seep into the small powered aircraft field. Large RPV's designed for 55,000 foot altitudes also fall in this range of wing Reynolds numbers. The laminar bubble can still cause a ΔC_{D_o} of about 0.001 at a Reynolds number of one million, but becomes completely unimportant for RN $\geq 4 \times 10^6$. At the upper end of this regime, quite large combinations of airfoil thickness and camber are permissible together with far aft location of minimum pressure.

(I) REYNOLDS NUMBERS BETWEEN 3,000,000 AND 9,000,000

There is a large data base from the WW II era for this realm of racing planes and general aviation craft. Very low drag coefficients are possible through extensive natural laminar flow but it is important to fly at higher altitudes to keep the Reynolds number per foot reasonably low. Constructional and maintenance considerations are becoming increasingly stringent. The laminar separation bubble at mid chord is no longer a problem. The turbulent boundary layer on the aft part of the wing can stay attached through very severe adverse pressure gradients with the aid of modern airfoil design methods.

Various artificial boundary layer control schemes are effective in producing very high maximum lift (II-11).

(J) REYNOLDS NUMBERS BETWEEN 9,000,000 AND 40,000,000

It is still possible to obtain extensive natural laminar flow in this regime through strong favorable pressure gradients, for example, on thick laminar airfoils and on low fineness ratio bodies of revolution. This regime has very large payoff in performance for 100% laminar flow surfaces which can be achieved through use of artificial boundary layer stabilization (for example through distributed suction) (II-12). Suction is effective even in strong adverse longitudinal pressure gradients and in the presence of transverse pressure gradient induced cross flow instability caused by wing sweep. Net drag including the cost of suction can be reduced to about 1/8 that of turbulent boundary layer wings. Data base is appreciable. Small torpedoes and dolphins also operate in this regime (II-13).

(K) REYNOLDS NUMBERS BETWEEN 40,000,000 AND 10^9

Vehicles in this regime include large fast aircraft and small to moderate size submarines. Boundary layer flow is mostly turbulent. In nature, whales also operate in this regime. Little laboratory data is available to date. The new cryogenic tunnel at NASA Langley should provide data in the future.

(L) REYNOLDS NUMBERS GREATER THAN 10^9

Large nuclear submarines operate at these extreme values. The drag is primarily turbulent fraction drag. There is great interest today in finding practical ways to reduce the high Reynolds number turbulent friction drag in a practical manner applicable to extended cruising duration.

FLOW PHENOMENA BIBLIOGRAPHY

II-1 Hoerner, Sighard F. - Fluid Dynamic Drag - Published by the author, 148 Busteed Drive, Midland Park, New Jersey 07432 1965

II-2 Hoerner, Sighard F. and Borst, Henry V. - Fluid Dynamic Lift - Published by the authors, P.O. Box 342, Bricktown, N.J. 08723 1970

II-3 Schubauer, G. B. and Spangenberg, C. - "Aerodynamic Characteristics of Damping Screens" NASA TN2001 January 1950

II-4 Batell S. M. and Mueller, T. J. - "Visualization of the Laminar-Turbulent Transition in the Flow Over an Airfoil Using the Smoke-Wire Technique" AIAA Paper 80-0421 to be presented at 11th Aerodynamic Testing Conference - Colorado Springs, Colorado March 18-20, 1980

II-5 Hertel, Heinrich - Structure-Form-Movement - Reinhold Publishing Corporation, New York 1966

II-6 Shapiro, Asher H. - Shape and Flow The Fluid Dynamics of Drag - Doubleday & Company, Inc., Garden City, New York 1961

II-7 Bauer, Andrew B. - "The Laminar Airfoil Problem" National Free Flight Society Symposium Report 1975

II-8 Hannan, Bill - Peanut Power - Historical Aviation Album Publication - Temple City, California 1980

II-9 Seiman, Dr. Gerald R. - "A Concept Study of Remotely Piloted Vehicle for Mars Exploration" Final Technical Report under Jet Propulsion Laboratory Contract 955012 August 1, 1978

II-10 Carmichael, B. H. - Application of Sailplane and Low-Drag Underwater Vehicle Technology to the Long-Endurance Drone Problem" AIAA/MIT/SSA 2nd International Sympoisum on the Technology and Science of Low Speed and Motorless Flight. Cambridge, Mass. September 11-13, 1974

II-11 Lachmann, Dr. G. V. - Boundary Layer and Flow Control - Vol. I Pergamon Press New York 1961

II-12 Lachmann, Dr. G. V. - Boundary Layer and Flow Control - Vol. II Pergamon Press New York 1961

II-13 Carmichael, B. H. - "Underwater Vehicle Drag Reduction Through Choice of Shape" AIAA Paper No. 66-657 - Presented at Colorado Springs, Colorado June 13-17, 1966

III STATE OF KNOWLEDGE ON FLUID FLOW SEPARATION

Introduction

Fluid flow separation on man-made devices has been one of the most dangerous and persistent phenomena in the long history of fluid dynamics. The destructive dynamic response of blunt devices, i.e., power transmission lines, suspension bridge cables, and towing cables for underwater devices mark one end of the problem. The stalling of aircraft wings has instigated comprehensive study in this field for at least a half century. The attempts to provide reasonably good performance for model aircraft and high altitude manned aircraft are often aided by observation of nature's elegant solutions found on small to medium sized flyers in the insect and bird world.

The literature is so extensive that this report can only cover those references readily available to the author. The extensive bibliographies in the references quoted here may be used to delve further. It is inevitable that some very basic and helpful studies have been overlooked due to the short delivery time for this report.

The phenomena of laminar separation on lifting airfoils has a fundamental influence on the aerodynamic forces and moments. Even at very high Reynolds numbers, leading edge laminar separation can have a decisive influence on the stalling behavior of aircraft wings.

At chord Reynolds numbers below 50,000, laminar separation <u>without</u> reattachment can lead to large losses in lift and dramatic increases in drag. It is possible to design thin airfoils, e.g., $t/c \leq 6\%$ of quite good performance at chord Reynolds numbers down to 30,000. Use of artificial boundary layer tripping by various methods (as covered in Section V of this report) can improve the performance of thicker airfoils in this normally subcritical range. At Reynolds numbers between 700,000 and 1,500,000, the boundary layer can be converted to the turbulent form more elegantly through use of the shallow mid chord adverse pressure gradient (called instability gradient). This technique is widely used to improve the performance of laminar airfoils for man-carrying sail planes. At Reynolds above 4,000,000, this technique is no longer required and would lead to a loss in cruising performance if employed.

Studies of laminar separation with reattachment prior to the trailing edge (the so-called laminar separation bubble) have been vigorously pursued for the last four decades. It is now possible to define the bubble geometry and its influence on airfoil performance.

CHRONOLOGY
PRINCIPAL INVESTIGATORS AND MAJOR STEPS IN UNDERSTANDING

Year	Investigator	Contribution	Ref
1904	Prandtl	Discovery of the Boundary Layer	III-1
1914	Prandtl	Effect of Boundary Layer Transition Relative to Drag of Bluff Bodies	III-2
1933	Millikan and Klein	Effect of b.l. trans. relative to separation point on airfoil maximum lift coefficient	III-3
1934	Melvill-Jones	Described 3 types of stall. Turbulent b.l. sep. at t.e., leading edge sep. without reattachment, leading edge separation with reattachment	III-4
1934	von Kaman and Millikan	Discovered $R\delta sep./\sqrt{Rs\ lam.}$ is constant for a prescribed pressure distribution	III-5
1938	von Doenhoff	Discovered R sep to R trans = 50,000 R sep to R turb. reattach. = 70,000	III-6
1940	Schmitz	Airfoil behavior in critical RN range 21,000 to 168,000. Importance of stream turbulence, artificial b.l. tripping, choice of t/c, f/c, leading edge radius	III-7
1940 -43	Pfenninger	6% and 9% t/c extensively laminar airfoils at RN between 100,000 and 760,000. Improvements with surface steps and waves *and jirjets*	III-8
1948	Maekawa and Atsumi	Separation and transition study on bent plate R sep to R trans = 25,000 if $R\delta_{sep}$>1200. Reattachment fails when R length is too large	III-9
1951	Bursnall and Loftin	Found mid chord laminar bubble at low α on thick laminar airfoil	III-10
1951	McCullough and Gault	Defined: (1) stall preceeded by turb. b.l. sep moving forward from t.e. for thick airfoils, (2) laminar leading edge separation without reattachment (3) Laminar l.e. sep with reattachment which moves aft as α increases—thin airfoil stall	III-11

Year	Investigator	Contribution	Ref
1955	McCullough	Found 0006 airfoil reattached for all RN of $1.5 \times 10^6 \rightarrow 6 \times 10^6$ 0007 airfoil not reattached for RN > 6×10^6 0007.5 + 0008 airfoil not reattached for RN > 3×10^6	III-12
1955	Gault	Studied l.e. sep on 0010 and 66_1-018, t.e. sep. on 66_1 - 018. Found R_δ^* sep > 500 ΔX lam/ΔX sep = 0.75 → 0.85. ΔX lam decr by amb. turb and incr RN. Convergence angle θ as f(RN).	III-13
1955	Norbury and Crabtree	Mathematical prediction of pressure distribution on airfoil with a long bubble	III-14
1958	Chapman, Kuehn, Larson	Subsonic and Supersonic. 400 < Rℓ < 5,000,000 (1) Transition downstream of reattachment (2) Trans. between separation and reattachment (3) Transition prior to separation	III-15
1959	Moore	Experiment with stepped plate- low press. gradient For R_δ^* < 500 laminar reattachment. For R_δ^* > 500 turb reattach - pressure coefficient is independent of RN, bubble length ∝ 1/RN. For R_δ^* < 500 long bubble-large effect on pressure. For R_δ^* > 500 short bubble - no large effect on pressure. Long bubble length = f (shape and α) but not RN. Short bubble bursts to long when $(c_{p2} - c_{p1})/(1-c_{p1}) > 0.36$ even when R_δ^* >500	III-16
1959	Burrows and Newman	Suction within separation region reduces pressure at forward end of bubble and increases the pressure recovery coefficient. Size of bubble and b.l. thickness downstream are reduced by b.l. suction	III-17
1964	Tani	Confirmed bubble forms when R_δ^* > critical and pressure recovery coefficient < critical, R_δ^* critical different for cylinders and airfoils. Critical pressure recovery coefficient not universal.	III-18

Year	Investigator	Contribution	Ref
1964	Morkovin	Separation flow patterns behind a cylinder over complete Reynolds number range. Unexpected increase in drag at $R_d > 10^6$. Data on oscillatory lift as f(RN)	III-19
1967	Roshko	Discusses the limitations in present theory to define separated flows	III-20
1969	Gaster	$\frac{\theta_s^2}{\nu} \cdot \frac{\Delta U}{\Delta x} = f \frac{\theta_s U_s}{\nu}$ at bursting L short bubble length/θ_s = constant/R_{θ_s} R_l = 64,000 sep to reattachment R_l = 40,000 → 50,000 sep. to transition	III-21
1972	A.G.A.R.D.	Many fine papers on high lift systems and aircraft scaling	III-22
1972	Laine	Navier Stokes equations of laminar boundary separation over step in flat plate	III-23
1972	Dobbinga, van Ingen and Kooi	Defines angle of the separation streamline $\tan\gamma = -3\, d\theta_o/dx / \partial p/\partial x$ = K/Rθ sep. Defines pressure coefficient at reattachment	III-24
1975	van Ingen	Defines bubble geometry, bursting, pressure distribution--corelated with experiment. See figures which follow.	III-25
1977	van Ingen	Defines X trans. - X sep. as function of θsep., Rθ sep, and turbulence level. Corelation with experiments. See figures	III-26
1977	Young	Reviews knowledge on unswept and swept laminar separation bubbles. See figures	III-27
1978	Mueller	Flow visualization determined: separation pt. transition pt., and reattachment pt. on airfoil leading edge for 150,000< RN<420,000	III-28
1980	Batill and Mueller	Detailed profile and platform views of laminar separation and transition by smoke-wire technique on 66_3-018 airfoil at 50,000<RN<130,000	III-29
1980	Venkateswarlu and Marsden	Finite difference b.l. analysis together with some experimentally determined constants, define location and geometry of separation bubble at 60% to 70% chord on laminar airfoil at 500,000<RN<3,000,000. Predicts pressure distribution and b.l. velocity profiles downstream of reattachment	III-30

Discussion

The formulation of the boundary layer concept by Prandtl in 1904 solved the long-standing mystery concerning the differences in observed fluid behavior and the inviscid flow theory. By 1914, Prandtl was able to explain the large drag differences observed by different investigators for blunt objects such as spheres and cylinders on the basis of the condition of the boundary layer prior to the flow separation location. This effect was applied to the stalling of airfoils by Millikan and Klein in 1933.

In the Wright Brothers Memorial Lecture by Melvill-Jones in 1934, three distinct types of wing stall were described. The thick airfoil gentle stall in which turbulent flow separation gradually moves forward from the trailing edge, laminar flow separation from the leading edge without reattachment, and laminar leading edge flow separation with flow reattachment to the airfoil surface downstream of separation.

In 1938, von Doenhoff accurately described the laminar separation bubble in an adverse pressure gradient and found by experiment that the distance from the separation point to the transition point along the separated streamline can be defined as R transition - R separation $\approx$ 50,000 and the total bubble length as R reattachment - R separation $\approx$ 70,000.

In 1940, Schmitz published his classical work on low Reynolds number airfoil experiments in a low turbulence wind tunnel at Göettingen. He clearly pointed out the influence of stream turbulence, and artificial boundary layer tripping in extending good airfoil performance to lower Reynolds numbers. He also recommended optimum values of airfoil thickness, camber, and leading edge radius as a function of Reynolds number for flight in the low turbulence free atmosphere.

At about the same time, Pfenninger was exploring the limits of airfoil drag reduction through extensive laminar flow in a low turbulence wind tunnel at Zurich. He found that the performance of 6% and 9% thick propeller airfoil sections could be improved by boundary layer tripping using air jets normal to surface, large surface waviness, and backward facing steps in the surface.

There now followed intensive investigations of flow separation, laminar bubbles, and airfoil stalling behavior. In 1948, Maekawa and Atsumi in Tokyo discovered that flow reattachment did not occur when the bubble length Reynolds number exceeded a critical value of about 75,000. In the early to mid 1950s, McCullough and Gault were able to define the three types of airfoil stall first noted by Melvill-Jones in great detail in terms of the pertinent boundary layer parameters. They found that R_δ^* at separation had to exceed 500 for reattachment to occur in strong adverse pressure gradients. They found the laminar length in the separation bubble to be 75% to 85% of the total bubble length and defined the angle of closure of the flow with the surface after transition as a function of Reynolds number.

In 1959, Moore found that when R_δ^* at separation was less than 500, a long laminar bubble formed with very large effects on the pressure distribution, but that when R_δ^*sep. exceeded 500 a short bubble formed with only small local effect on the pressure distribution. They also found that even when R_δ^*sep. exceeded 500 and a short bubble initially formed, that it could burst to the long bubble type when the angle of attack was increased and the required pressure recovery following separation exceeded a value of

$$\sigma = (c_{p\ \text{recovery}} - c_{p\ \text{sep.}})/(1 - c_{p\ \text{sep.}}) > 0.36$$

In an extensive summary in 1964, Tani pointed out that R_δ^* critical at separation and the critical pressure recovery σ seemed to be different for cylinders and airfoils.

In 1969, Gaster further defined the conditions under which short bubbles could burst into long bubbles as $\left(\frac{\delta s^2}{\nu}\frac{\Delta U_1}{\Delta x}\right)_{\text{critical}}$ as a function of Re at separation.

From the early 1970s to the present time, van Ingen and his colleagues at Delft University in the Netherlands and Young and his colleagues at the University of London have made impressive strides in correlating various methods of computing the flow separation, bubble behavior, and resulting pressure distributions with carefully controlled experiments. Presently, Venkatesworlu and Marsden have applied powerful finite difference calculations to the problem with encouraging results. Mueller and his

colleagues at Notre Dame are continuing the excellent flow visualization work begun by the late F.N.M. Brown in wind tunnels of very low turbulence level providing excellent details on separate boundary layer transition and reattachment at chord Reynolds numbers of 50,000 to 420,000. The clearest photographs of flow separation from both blunt objects such as spheres, and on airfoils at angle of attack may be found in F.N.M. Brown's remarkable book, See The Wind Blow, ref. III-32. The text is also one of the most illuminating to be found in the long history of fluid dynamics.

It must be emphasized that it is still necessary to proceed in a semi-empirical manner in predicting separation for a new case, and inevitably there are disappointments just when one feels that things are well enough defined for engineering purposes. In 1972, Laine at the University of Helsinki solved the Navier Stokes equations for the separated flow from a rearward facing step on a flat plate. Thompson of Mississippi State University, reference III-31, is presently attempting to correlate similar exact solutions with the experimental work of Mueller at Notre Dame. The computer requirements are formidable but such calculations should eventually provide realistic results for even the most complex flow separation problems.

Calculating Flow Behavior Involving Laminar Separation

It is desired to calculate:

1. The location of laminar separation.
2. The angle of the separation streamline with the surface.
3. The length along the separation streamline to transition.
4. The angle of closure of the separated boundary layer with the surface following transition.
5. The location of reattachment with the surface.
6. The length of run after reattachment required for the boundary layer velocity profile to return to normal.
7. The criteria for which reattachment does not occur.
8. The effect of the foregoing on the pressure distribution.
9. The effect of the separation bubble on boundary layer velocity profiles.
10. The penalties in drag, lift, and moment for those cases where reattachment does occur.

The separation bubble geometry as outlined above is shown in Figure III-1, from the initial von Doenhoff concept of 1938 through several intermediate experimenters and concluding with the detailed 1980 description of Venkatesworlu and Marsden shown in Figure III-2.

1. The location of laminar separation is shown in the upper plot of Figure III-3 in terms of the boundary layer shape parameter $H_{sep} = 3 + 0.0713/m_{sep}$ as a function of $m = -\frac{\theta^2}{\nu}\frac{dU}{dX}$. The intersection of the laminar boundary layer H history with the critical value gives the desired location. Some typical values of R_δ* at separation found on spheres and cylinders as a function of Reynolds number based on diameter are shown in the middle figure. Values of R_δ* at separation found for various airfoil, angle of attack, chord RN combinations are shown in the lower figure.

2. The tangent of the angle of the separation streamline with the surface tan γ is shown as a function of Re at separation on a logarithmic plot, upper figure III-4 and in cartesian form in lower figure III-4. The scatter is small and the definition quite good for objects as diverse as cylinders, flat plates, and airfoils. Correlation with smoke line flow visualization on a Wortmann airfoil figure III-5 is seen to be excellent.

3. von Doenhoff found during his low turbulence plate measurements under adverse pressure gradients that the Reynolds number (based on local potential flow velocity and the length from separation to transition) was about 50,000. Some recent measurements on a Wortmann airfoil give values which range from 37,000 at $Re_{sep} = 175$ to 70,000 at $Re_{sep} = 415$. Figure III-6. The values found for bubbles on swept wings vary from 42,000 to about 60,000, while those found on a cylinder were much higher than those found on airfoils.

   An excellent correlation is provided by van Ingen in the form $10^4/Re_{sep.}$ vs. $\Lambda\gamma/\theta_{sep.}{\cdot}Re_{sep.}$ with an assisting variable in the form of ambient turbulence level expressed as a % of stream velocity. The experimental values fell on prediction curves obtained by integrating the amplification of small disturbances

to ratios which vary with the ambient turbulence level. The results appear here as figure III-7.

4. von Doenhoff in his original concept of the laminar bubble suggested a closure angle of 15° from the separation streamline based on the typical spreading angle of the turbulence. Maekawa and Atsumi found a value of 17° to fit better with their observations on separation over a sharply bent plate. Gault found in his study of the NACA 0010 and 66_3-018 airfoils over a range of angles of attack of 4° to 15° and chord Reynolds numbers between $2X10^6$ and $6X10^6$ that the closure angle varied from 15° at high Reynolds number to as high as 52° at low RN. These values were based on the assumption that the separation streamline left tangent to the surface and later work has shown this assumption to be incorrect.

5. A constant bubble length Reynolds number (based on the potential flow velocity and distance from separation to reattachment) of 70,000 was suggested by von Doenhoff. Experimental values for the 0006 airfoil are 48,000→59,000. For the 0009 airfoil 72,000→79,000, and for the 66018 airfoil 62,000→114,000. The value for mid chord bubbles on thick airfoils are 120,000 to 240,000. See figure III-8.

6. The distance required for the reattached boundary layer to recover to a normal turbulent form following the bubble was first noted in the excellent summary paper of Young as being equal to $100\theta_{sep.}$ for the case of unswept wings, 100 to $150\theta_{sep.}$ for a 26.5° swept wing and 150 to $300\theta_{sep.}$ for a 45° swept wing.

7. The point of most practical interest to the struggling applied aerodynamist who must predict stalling behavior is to define when a short bubble (which has rather limited effects on pressure distribution and therefore on lift, drag, and pitching moment) will burst to the long bubble form. The first condition is that R_δ^* at separation must exceed 500 if a short bubble is to form. For lower values, the bubble is long and in many cases reattachment is not possible. Even

when $R\theta_{sep}$ exceeds 500, the resulting short bubble will eventually burst to the long bubble type when angle of attack is increased sufficiently. In 1959, Moore in his experiments on a stepped flat plate found that this occurred when the difference between the pressure coefficient at reattachment and the pressure coefficient at separation divided by (1 - the pressure coefficient at separation) exceeded a value of 0.36. $(C_{p_{reattachment}} - C_{p\ sep}) > 0.36$. See figure III-9-A. In 1969 Gaster put it in terms of the adverse gradient (which is nearly always linear) for the same region between separation and reattachment.

$\frac{\theta_s^2}{\nu} \cdot \frac{\Delta U}{\Delta x}$ = a function of $R\theta_{sep}$. Some experimental results of non-bursting bubbles obtained in tests of a Wortmann airfoil are compared with Gasters limiting line in figure III-9-B for values of $R\theta_{sep}$ less than 500. The σ value for bursting are given for McGregor's airfoil at three angles of attack for chord RN between 0.7×10^6 and 2.7×10^6 in figure III-9-C and for a Piercy airfoil at $R_c = 1.7 \times 10^6$ in figure III-9-D. The More criteria of $\sigma_{crit} = 0.36$ seems to be adequate.

8. Pressure distributions on wings at very high Reynolds numbers in the absence of flow separation can be accurately predicted by inviscid flow calculations. At lower Reynolds numbers, in the absence of flow separation, a more accurate prediction can be made by adding the boundary layer displacement thickness to the wing profile and re-computing the pressure distribution for this combined shape.

   A short laminar separation bubble will cause a local flattening of the pressure gradient in the region of the laminar portion of the bubble, followed by a steep pressure gradient in the turbulent bubble region. At reattachment the pressure recovers to the same value present in the absence of the short bubble.

A long bubble causes very large changes in the pressure distribution. The negative pressure peak ahead of the bubble is greatly diminished as is the lift. Figure III-10-C clearly shows the difference between long and short bubbles. Figure III-10-A shows the difference in the pressure distribution on a cylinder with transition preceeding and following separation. Figure III-10-B shows the pressure distribution change on a thick airfoil as one proceeds from a moderate Reynolds number with a short bubble to a lower Reynolds number with a long separation bubble which does not reattach. Figure III-10-D provides pressure distributions for a 45° swept wing with short separation bubble along the complete span, E shows short bubble inboard and long bubble outboard, and F shows long bubble along the complete span.

Computation of the pressure distribution under long bubbles with either reattachment or non-reattachment is probably academic since one wishes to design to avoid this condition. Under a short bubble, a good engineering approximation can often be obtained by using the data on separation point, angle of the separation streamline, length to transition, closing angle, and total bubble length previously presented to define the geometry of the bubble. Then assume an almost constant pressure value from separation to transition equal to the separation value. Next draw a linear pressure rise from transition to the reattachment point where the reattachment pressure is equal to the value with bubble absent.

A more exact solution may be found in reference III-30 and will be discussed at the end of this section.

9. Detailed measurements of the distorted boundary layer velocity profiles within short and long bubbles on a 45° swept wing in both chordwise and spanwise direction are shown in figure III-11.

   Correlation of measured with predicted chordwise boundary layer velocity profiles for a mid chord bubble on a thick airfoil will be presented in a following section.

10. For the case of short bubbles with reattached flow the pressure distribution is not altered enough to markedly affect lift and movement. For leading edge short bubbles one often finds a change of lift curve slope and moment slope at the angle of attack where the bubble forms. The small changes which do occur could be accounted for by integrating the slightly altered pressure distribution. Short bubbles cause a small but measureable increase in drag which has been found by Marsden to be about $\Delta C_{D_0} = 0.001$ at $R_c = 1 \times 10^6$ for mid chord bubble on thick laminar airfoils.

A Comparison of Experiment With the Most Complete Separation Bubble Calculations to Date

Reference III-30 by Venkatesworlu and Marsden is certainly the culmination of the long effort to understand and predict laminar separation bubbles. The reader will have noted a great deal of experimentally guided empiricism in most of the foregoing discussion. Reference III-30 reduces this to a minimum and uses finite difference calculations to provide an improved theoretical prediction. The case covered is the mid chord laminar separation bubble on a thick laminar NACA 66_3-018 airfoil Comparison of theoretical predictions were made with experiments at $R_c = 0.8 \times 10^6$, $\alpha = 2°$, and a turbulence level of 0.02% at Edmonton, and with experiments at $R_c = 1.7 \times 10^6$, $\alpha = 0°$, and a turbulence level 0.2% from the NACA measurements of reference III-10. The schematic diagram of the bubble is given in figure III-2. The total length of separation (figure III-12) compared with three experiments can be expressed as $L_b = 75/R\theta_s$. The corresponding bubble height at transition (figure III-13) is expressed by $\frac{ht}{\delta^*} = \frac{4.8 \times 10^6}{\frac{U}{U_\infty}\left(\frac{\delta^*}{c}\right)_s R_e^2}$ The excellent agreement of computed b.l. profiles with those measured at Edmonton is shown in figure III-14, including the region downstream of reattachment. This is most important for the calculation of the drag with a bubble present. Excellent agreement is found in figure III-15 between the predicted and experimental pressure

distribution. The history of the boundary layer shape parameter H is given in figure III-16. Comparisons of predicted and experimental (reference III-10) boundary layer profiles including the region following reattachment are shown in figure III-17. This fine study reference III-30 presently available only from the University of Alberta has been submitted for publication to the Royal Aeronautical Society of the United Kingdom.

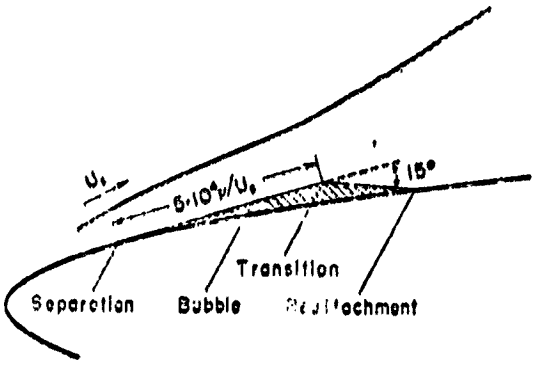

Von Doenhoff's concept of bubble formation.

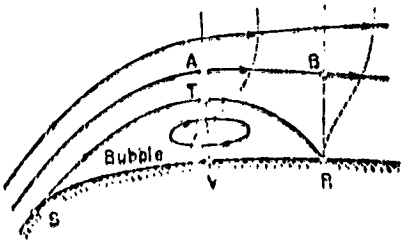

Norbury and Crabtree's simplified model of flow pattern with a bubble.

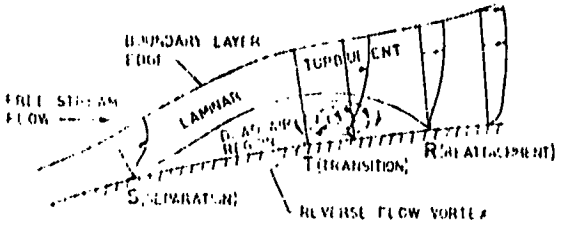

Two dimensional short laminar separation bubble (not to scale)

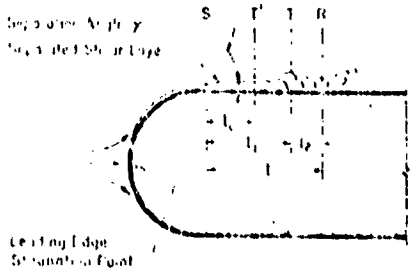

b) Sketch of Smoke Flow Showing the Locations of Separation, S, the Onset of Transition, T', the Completion of Transition, T, and the Reattachment, R.

a) The Separation Bubble From Smoke Visualization Experiments.

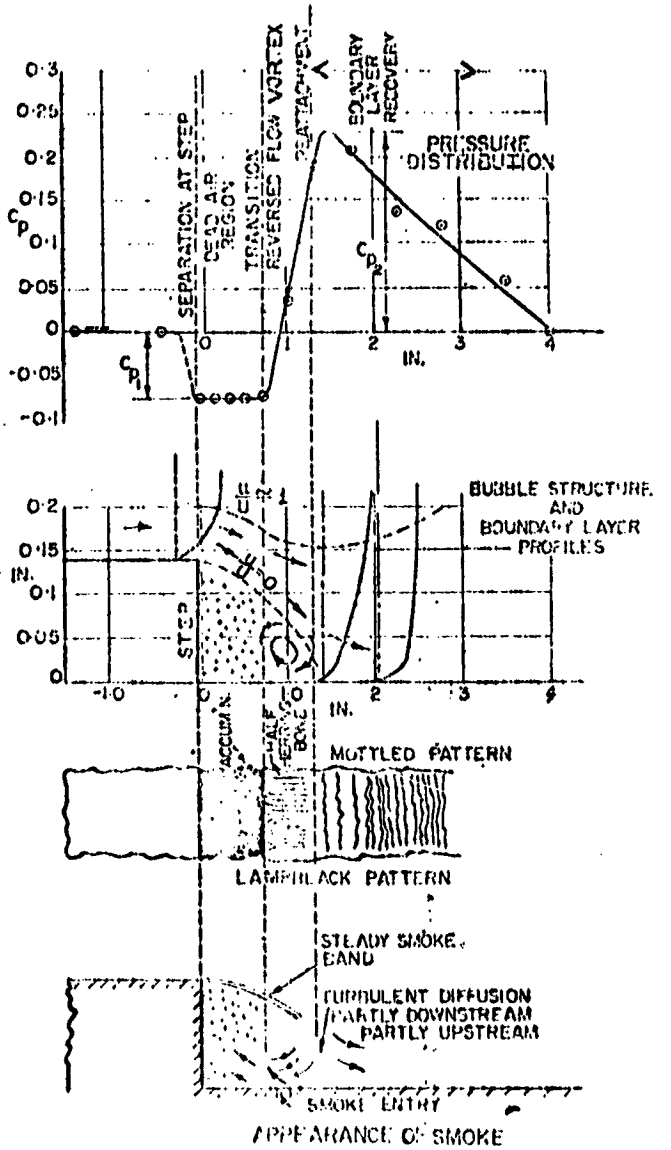

APPEARANCE OF SMOKE

The structure of a bubble illustrated by the flow over a step. Step height = 0.138 in. Distance of step from leading edge = 6.3 in. U_0 = 50 ft./sec. R_δ = 620.

FIGURE III-1 LAMINAR BUBBLE GEOMETRY

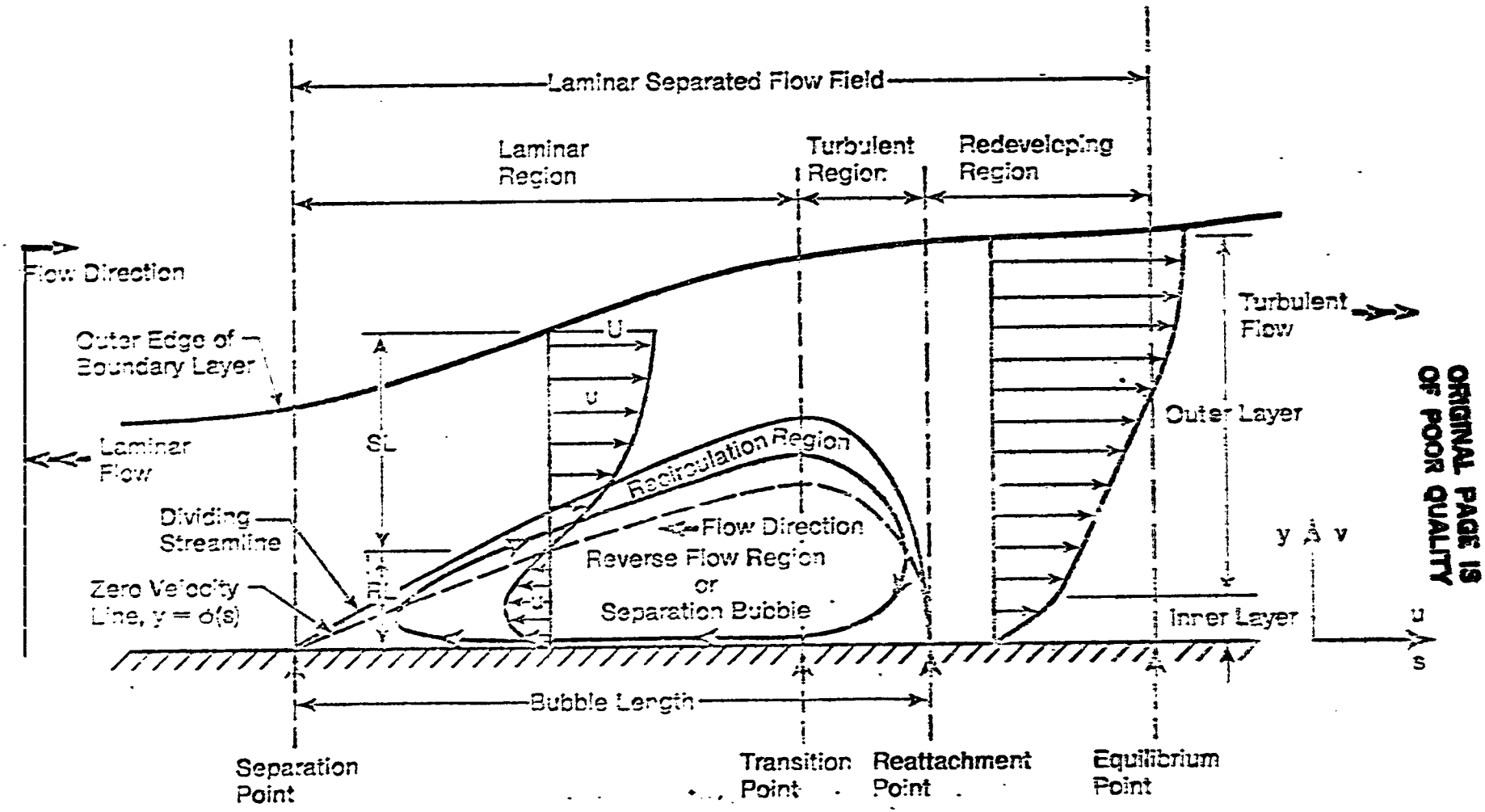

FIGURE III-2 - Schematic diagram of Laminar Separation Bubble

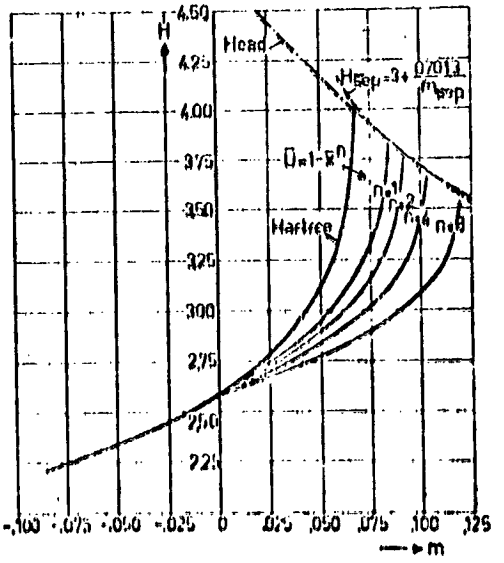

H(m) for some special exact solutions of the boundary layer equations.

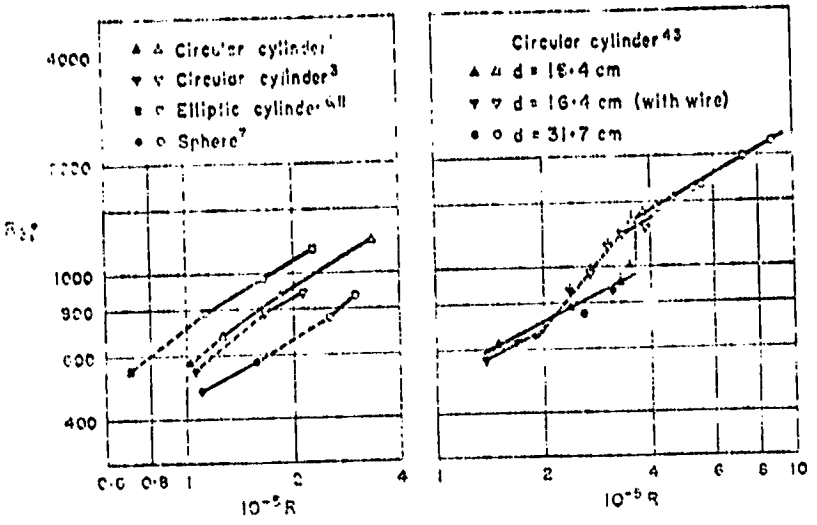

Calculated boundary-layer Reynolds number at separation on circular cylinder, elliptic cylinder and sphere.

Boundary-layer Reynolds Number at Separation

Aerofoil (NACA)	R	α	R_{δ_2}	σ	Type of bubble	Reference
63-009	$5{\cdot}8 \times 10^6$	8·5°	893	0·22	short	18, 22
		9·0°	477		long	
64A006	$5{\cdot}8 \times 10^6$	4·5°	516	0·22	short	19, 22
		5·0°	393		long	
0006	$2{\cdot}7 \times 10^6$	6·0°	520	0·29	short	28
		6·5°	350		long	
	$4{\cdot}6 \times 10^6$	6·5°	671	0·24	short	28
		7·0°	392		long	
	$6{\cdot}8 \times 10^6$	6·0°	774	0·23	short	28
		6·5°	480		long	
0008	$2{\cdot}0 \times 10^6$	8·0°	532	0·27	short	28
		8·5°	352		long	
	$4{\cdot}0 \times 10^6$	9·0°	812	0·24	short	28
		10·0°	426		long	

FIGURE III-3 LAMINAR SEPARATION PREDICTION

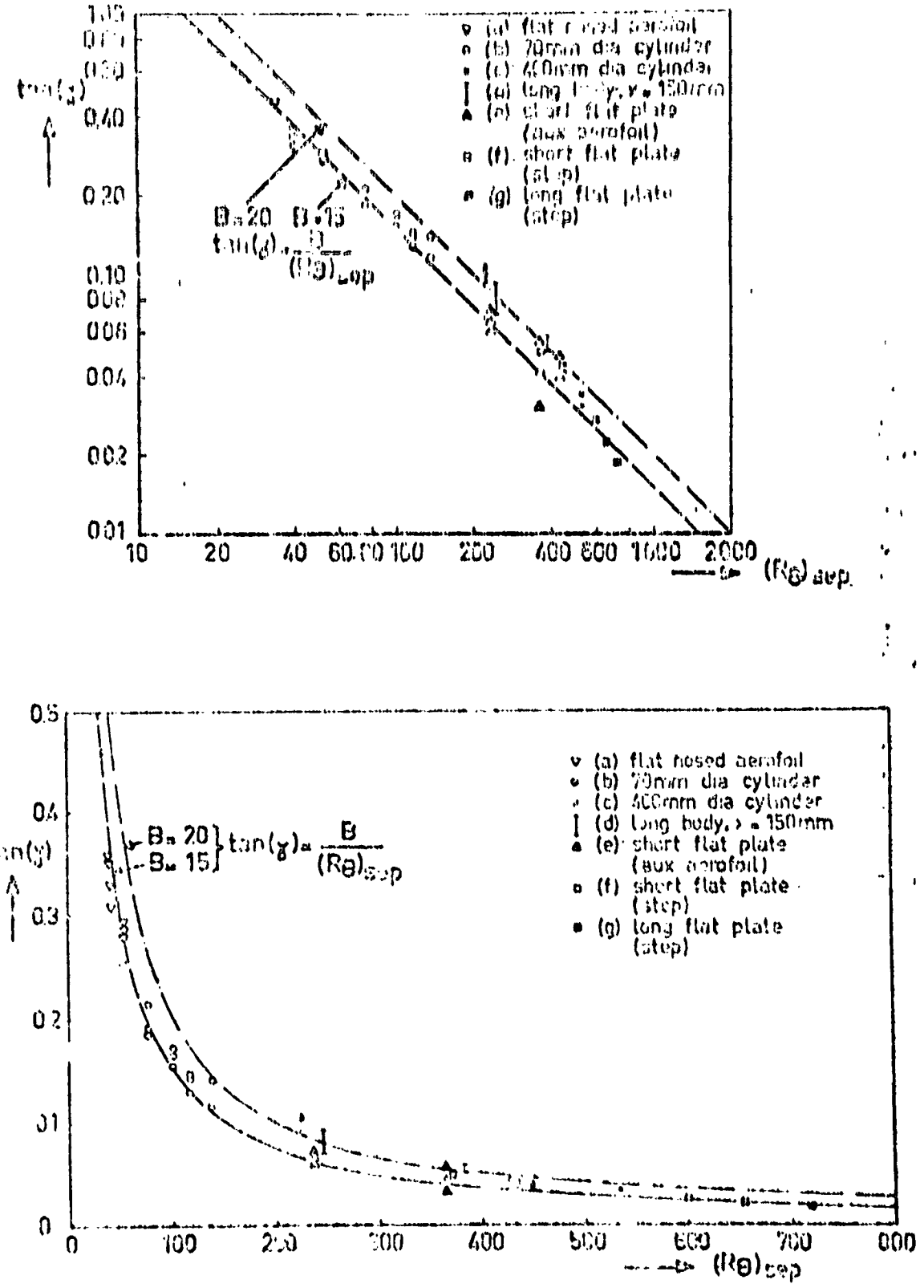

FIGURE III-4 SEPARATION STREAMLINE ANGLE

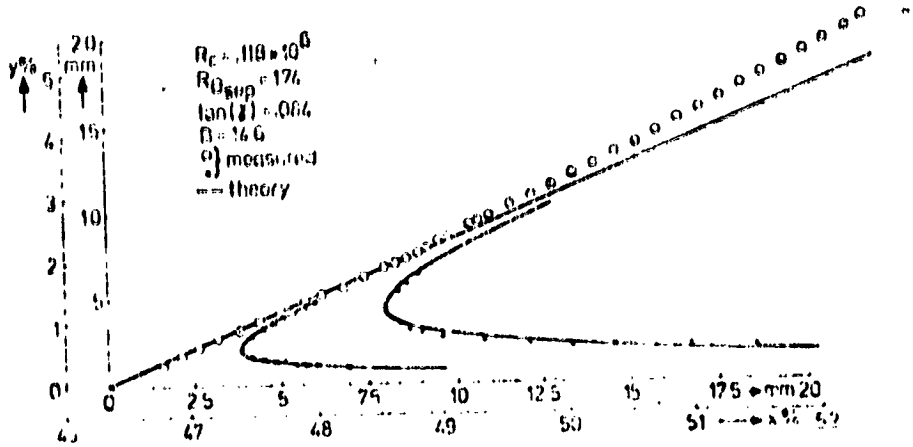

One of the suction pictures obtained for the Wortmann airfoil at conditions in Fig. (8).

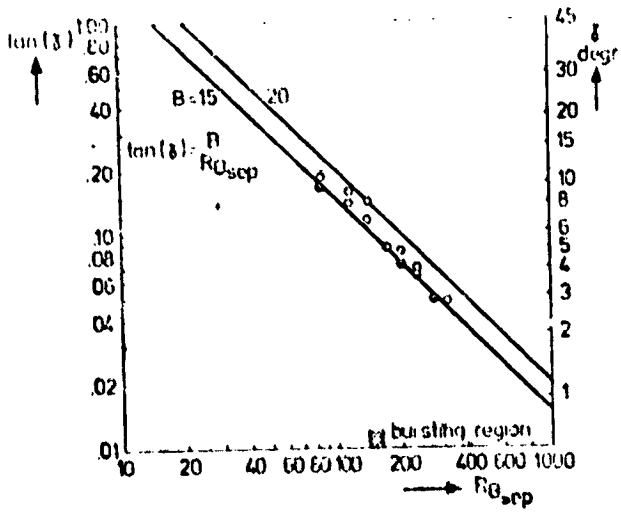

tan(γ) vs. $R\theta_{sep}$ for the Wortmann airfoil.

FIGURE III-5 SEPARATION STREAMLINE ANGLE

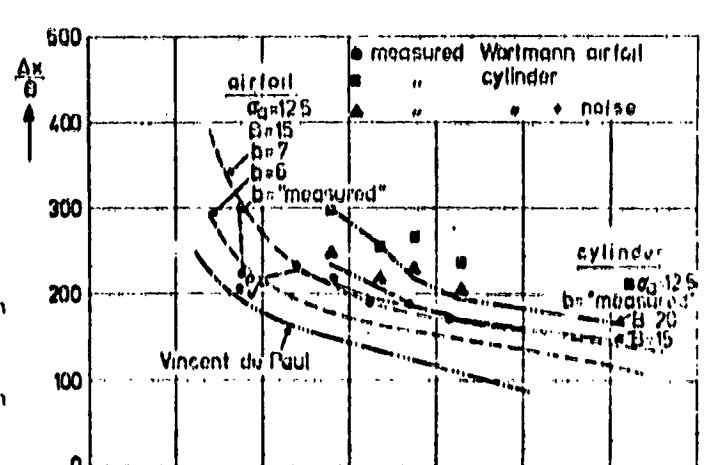

$\Delta x/\theta_{sep}$ as function of $(R_\theta)_{sep}$ Measured points for the Wortmann airfoil (●) and the cylinder with (▲) and without (■) extra noise. Curve labelled "Vincent du Paul" denotes the correlation curve used in ref. (18).

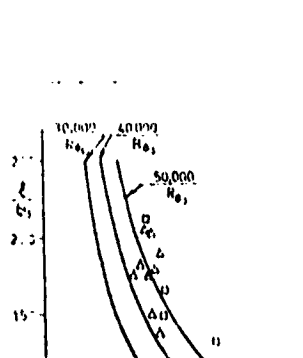

Variation of transition bubble length with Reynolds number for swept bubbles

FIGURE III-6 TRANSITION BUBBLE LENGTH

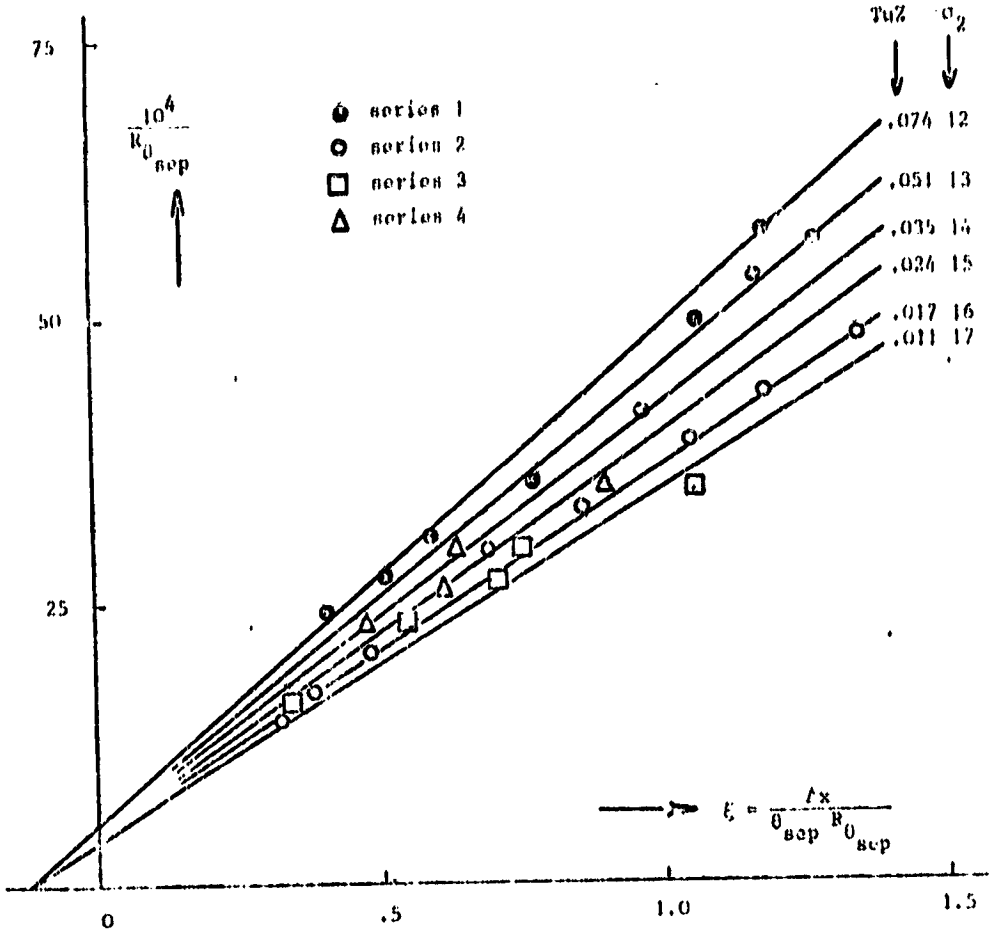

FIGURE III-7

Length of the laminar part of the bubble correlated with "effective Tu" and σ_2.

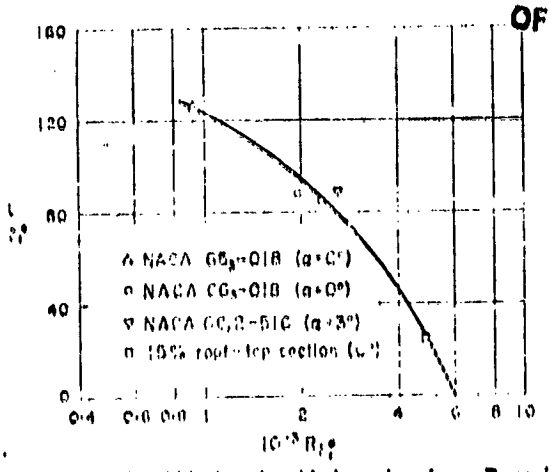

Fig. Variation of bubble length with boundary-layer Reynolds number at separation for aerofoil sections at incidence in the low-drag range.

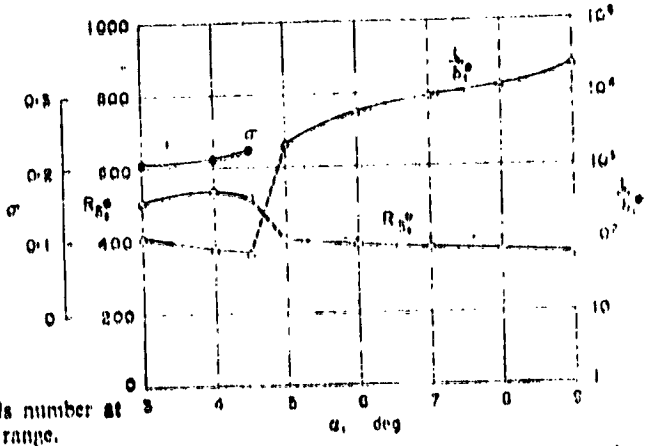

Fig. Calculated boundary-layer Reynolds number at separation, length of bubble and pressure recovery coefficient for NACA 64A006 aerofoil section. $R = 5{\cdot}8 \times 10^6$.

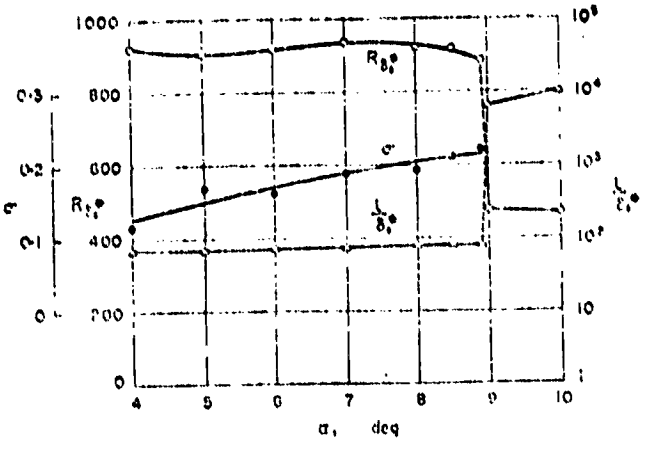

Calculated boundary-layer Reynolds number at separation, length of bubble and pressure recovery coefficient for NACA 63-009 aerofoil section. $R = 5{\cdot}8 \times 10^6$.

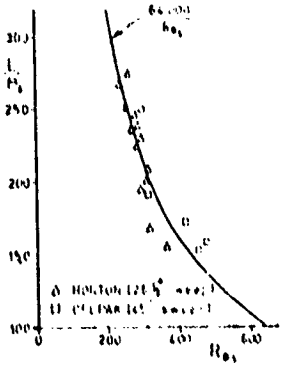

Variation of theoretical bubble length with separation Reynolds number for swept-back wing

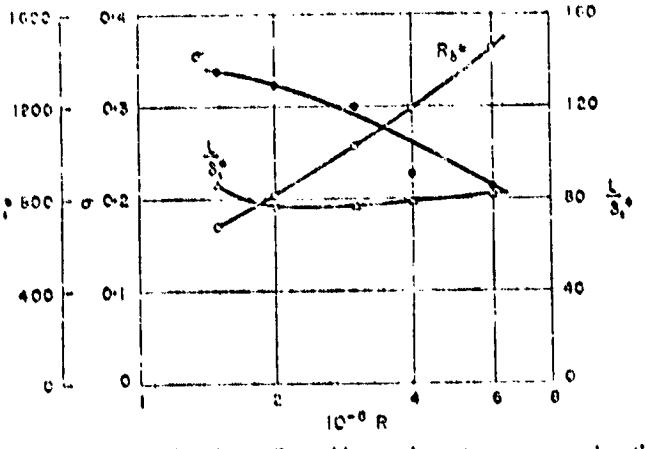

Calculated boundary-layer Reynolds number at separation, length of bubble and pressure recovery coefficient for NACA 66$_3$-018 aerofoil section at $\alpha = 15°$.

FIGURE III-R TOTAL BUBBLE LENGTH

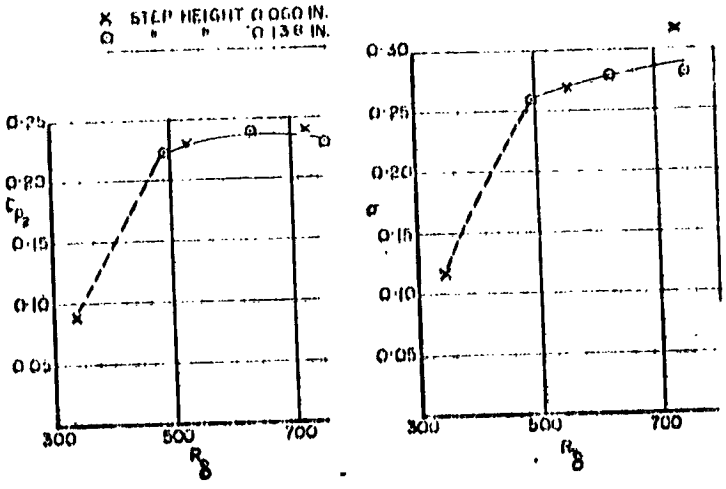

A
Variation of C_{p_s} and σ with R_δ.

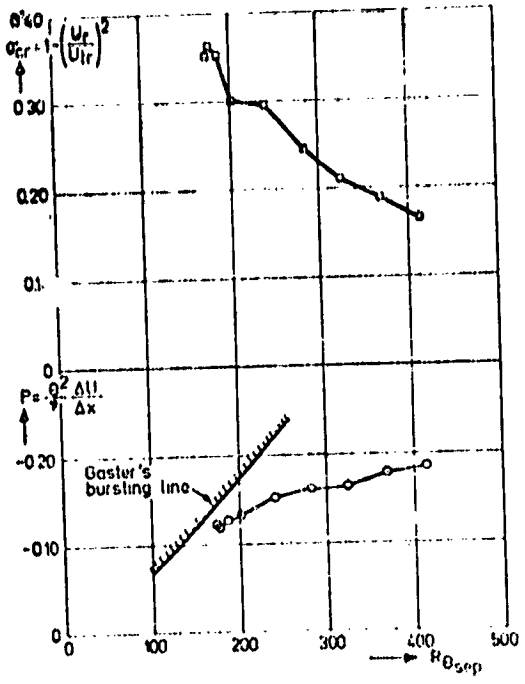

B
Pressure recovery coefficient σ_{cr} (Eq. 31) and Gasters pressure gradient parameter for closed separation bubbles on the Wortmann airfoil.

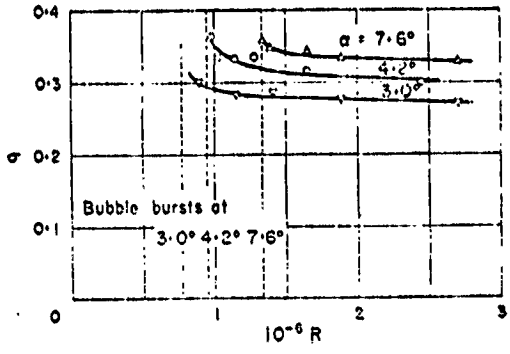

C Variation of pressure recovery coefficient with Reynolds number at constant incidences. Crabtree's analysis[11] of experimental data on McGregor's test model.

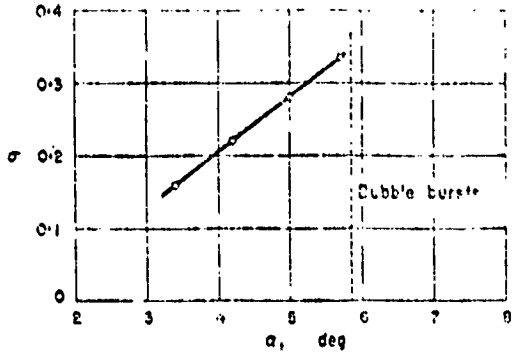

D Variation of pressure recovery coefficient with incidence at $R = 1{\cdot}7 \times 10^6$. Crabtree's analysis[11] of McGregor's experimental data on a Piercy aerofoil.

FIGURE III-9 CRITICAL BURSTING PRESSURE COEFFICIENT

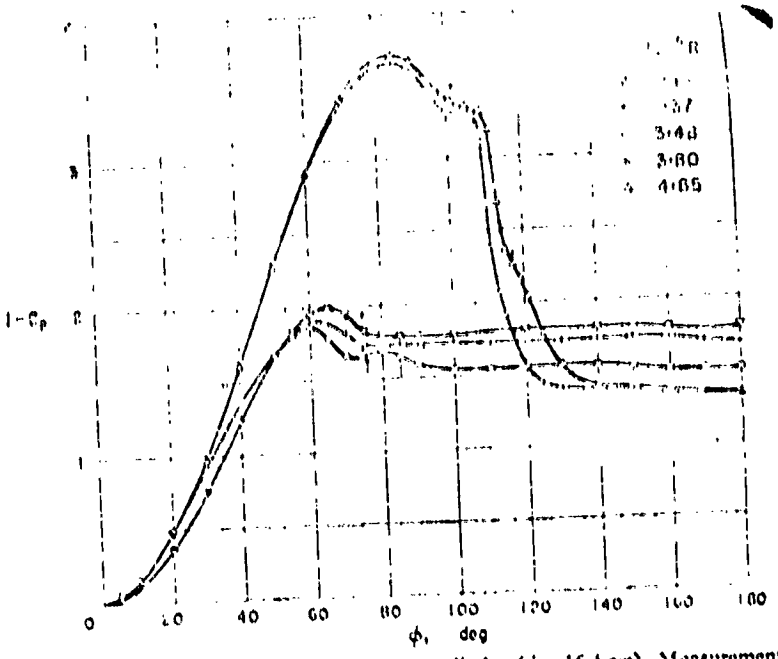

A. Pressure distribution on circular cylinder (d = 16·4 cm). Measurements by Yamamoto and Iuchi[43]. Corrected for tunnel-wall constraint.

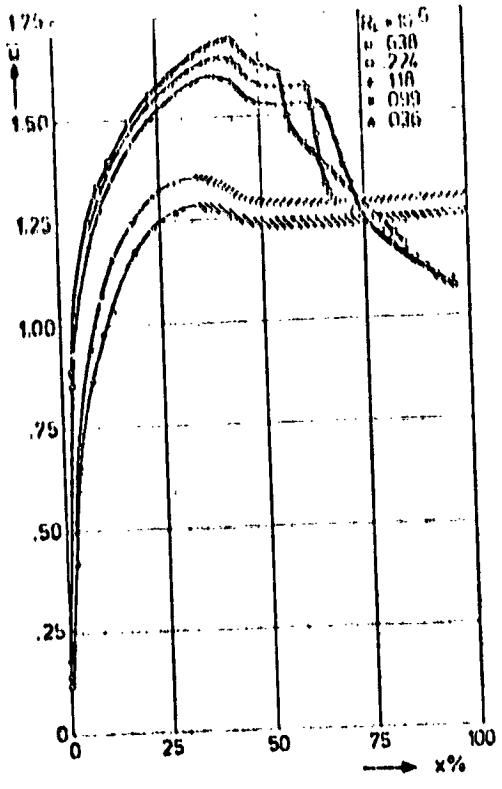

B Some of the measured pressure distributions for the Wortmann airfoil (for $R_c \leq .099 \times 10^6$ the bubble bursts).

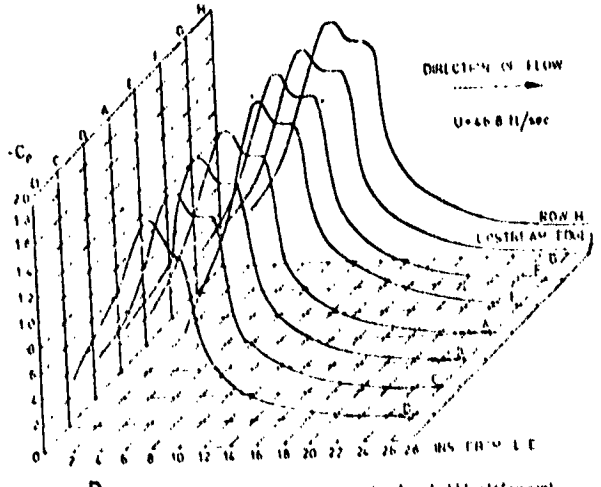

D Pressure distributions along the span for short bubble (45° sweep)

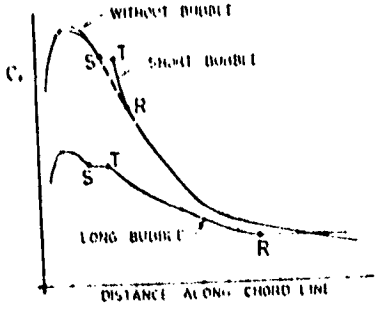

C Sketch illustrating pressure distributions on a wing section with short and long separation bubbles
S = separation, T = transition, R = reattachment

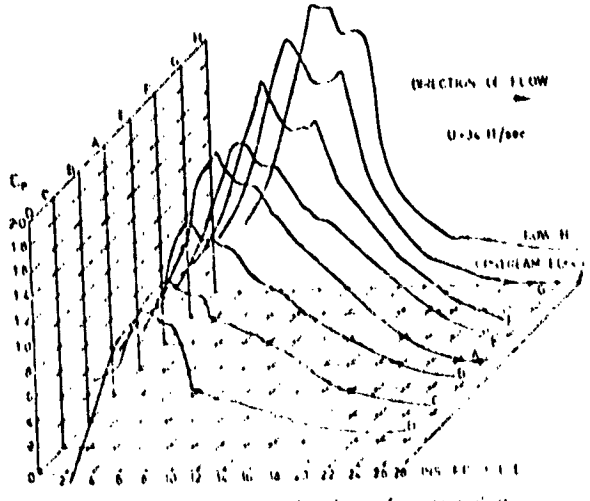

E Pressure distributions along the span for part-span short bubble and part-span long bubble (45° sweep)

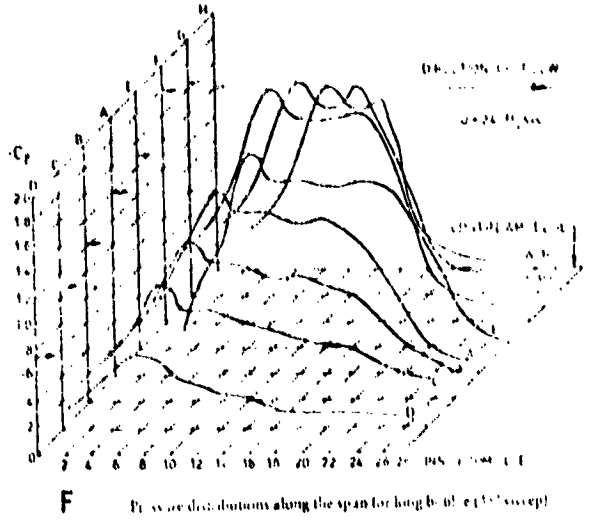

F Pressure distributions along the span for long bubble (45° sweep)

FIGURE III-1. BUBBLE EFFECTS ON PRESSURE DISTRIBUTION

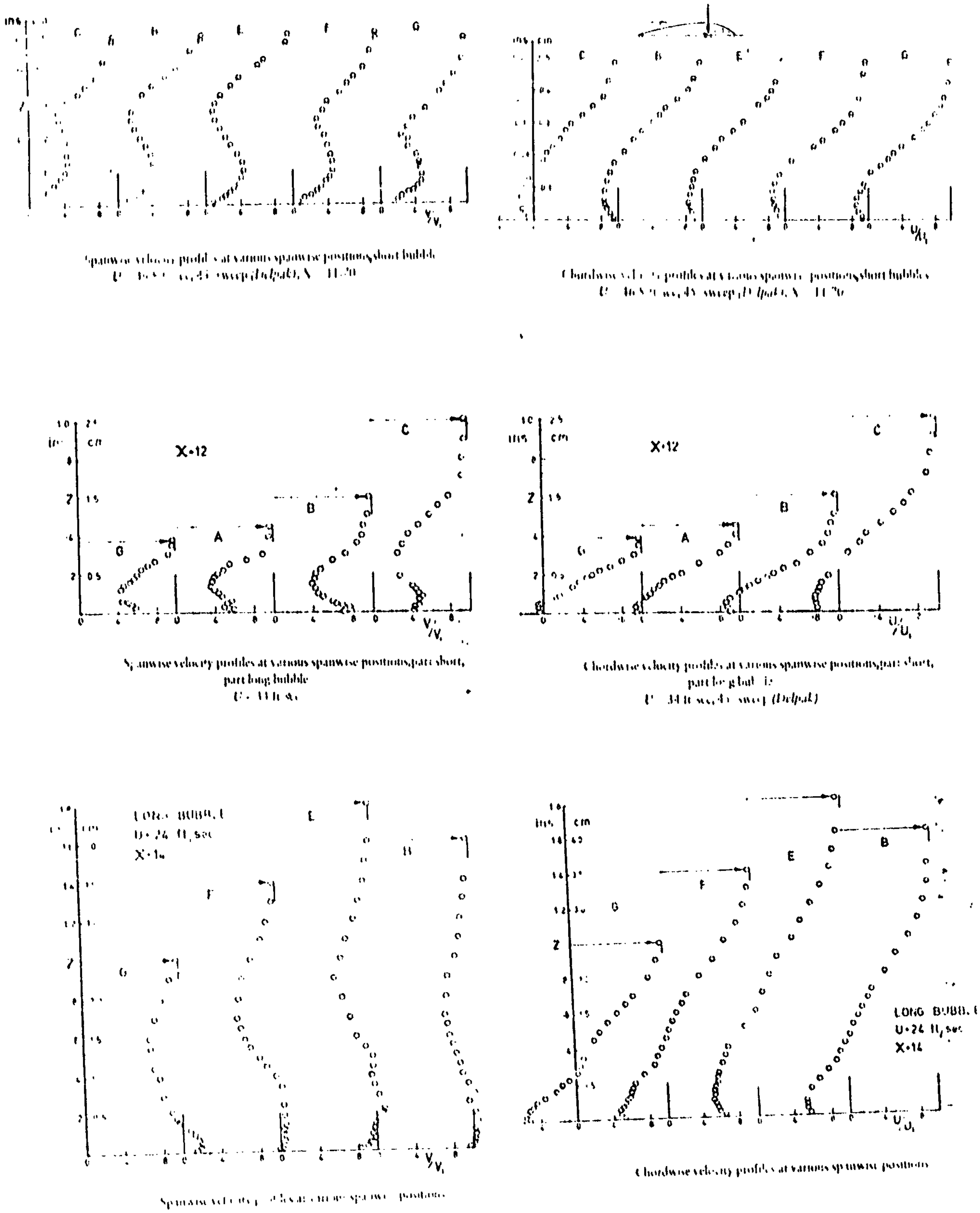

FIGURE III-11 BOUNDARY LAYER VELOCITY PROFILE

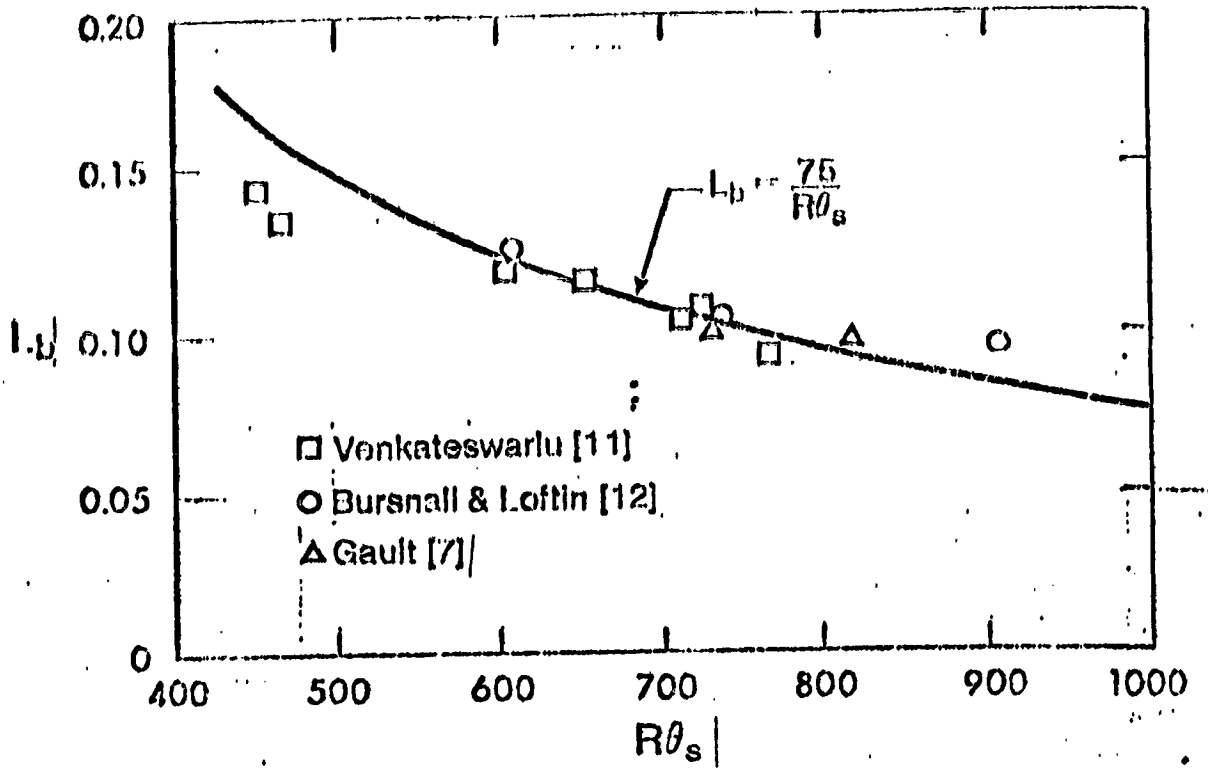

FIGURE III-12 - Bubble Length

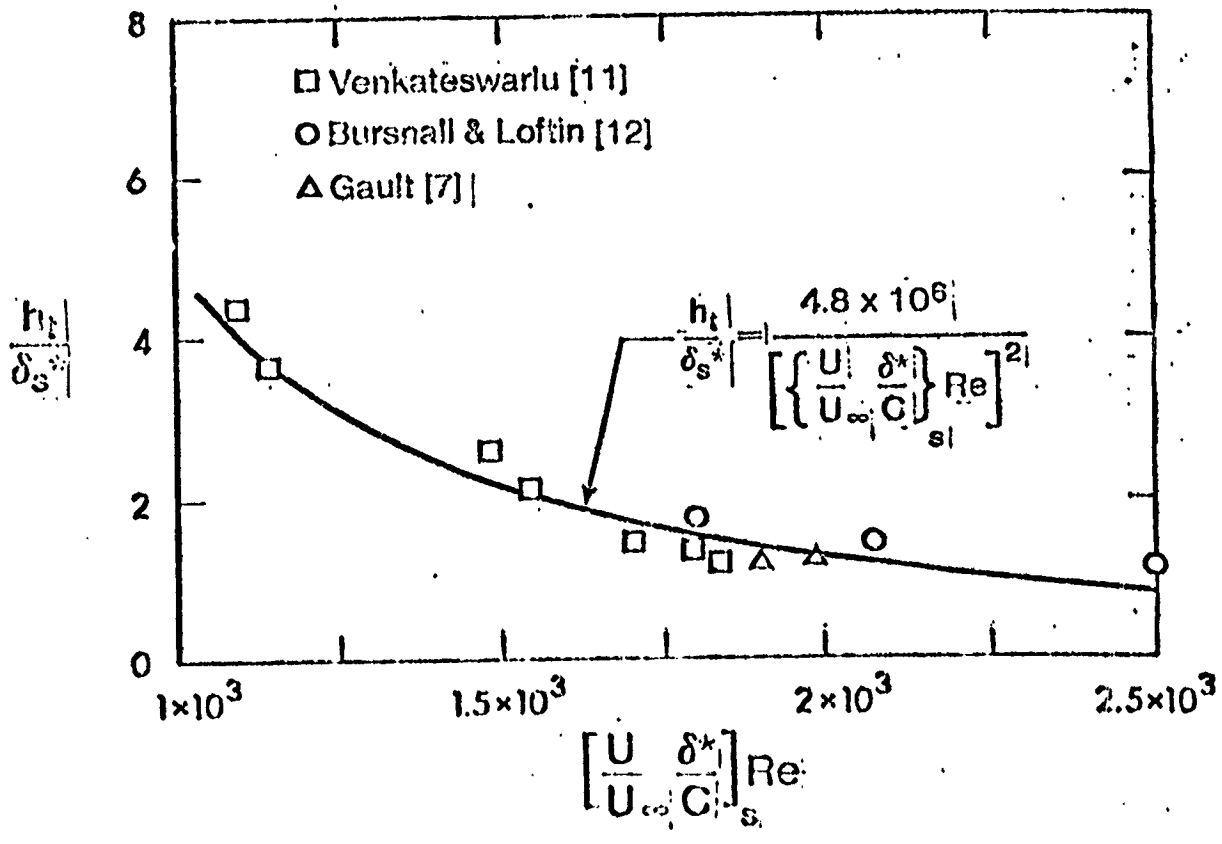

FIGURE III-13 - Transition Criterion Based on Bubble Height and Reynolds Number.

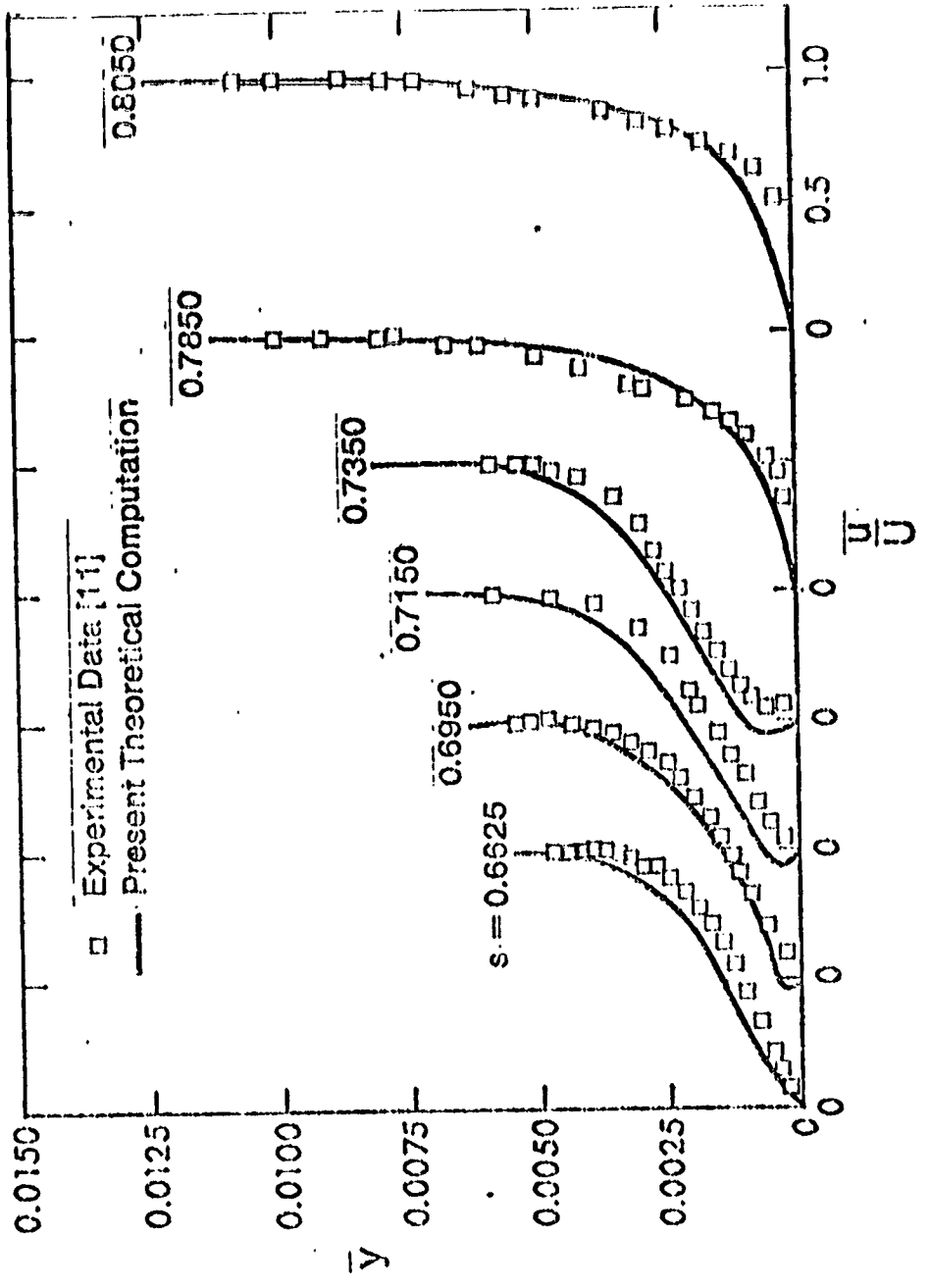

FIGURE III-14
- Velocity Distributions in Separation Bubble, NACA 66_3018

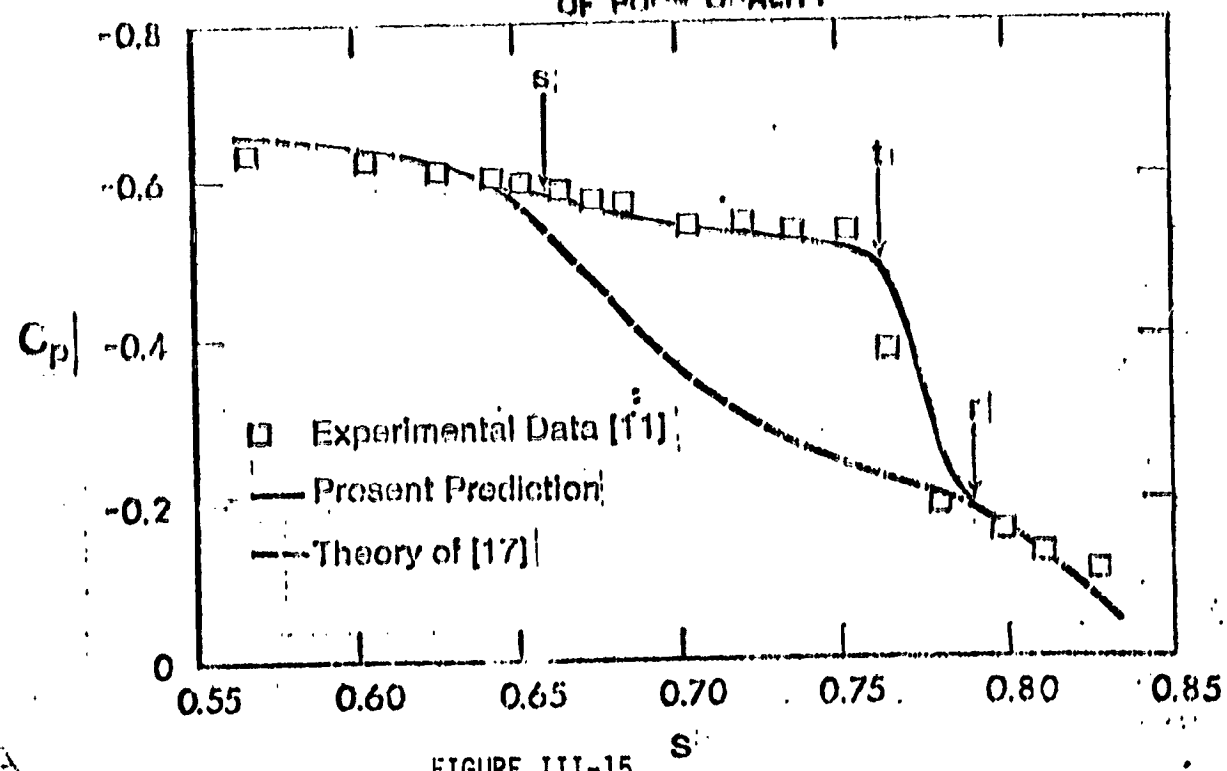

FIGURE III-15
- Pressure Distribution over Separated Region

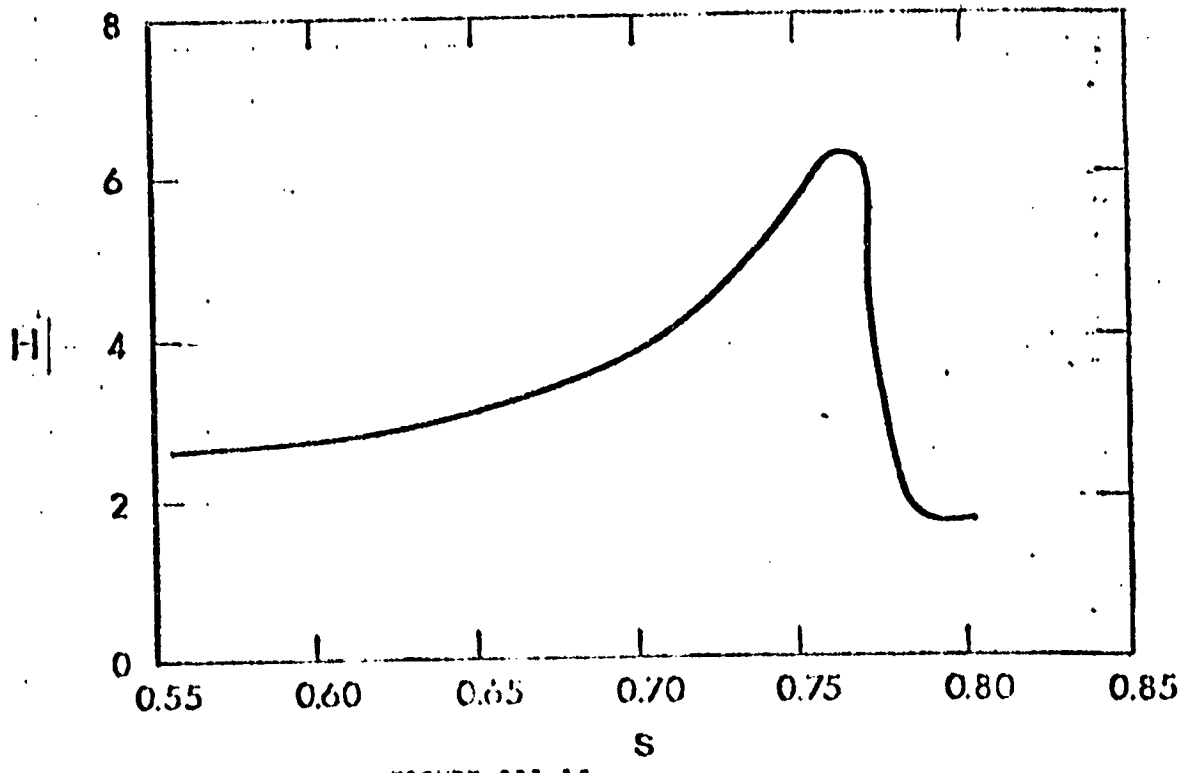

FIGURE III-16
- Variation in Shape Factor, $H = \frac{\delta^*}{\theta}$

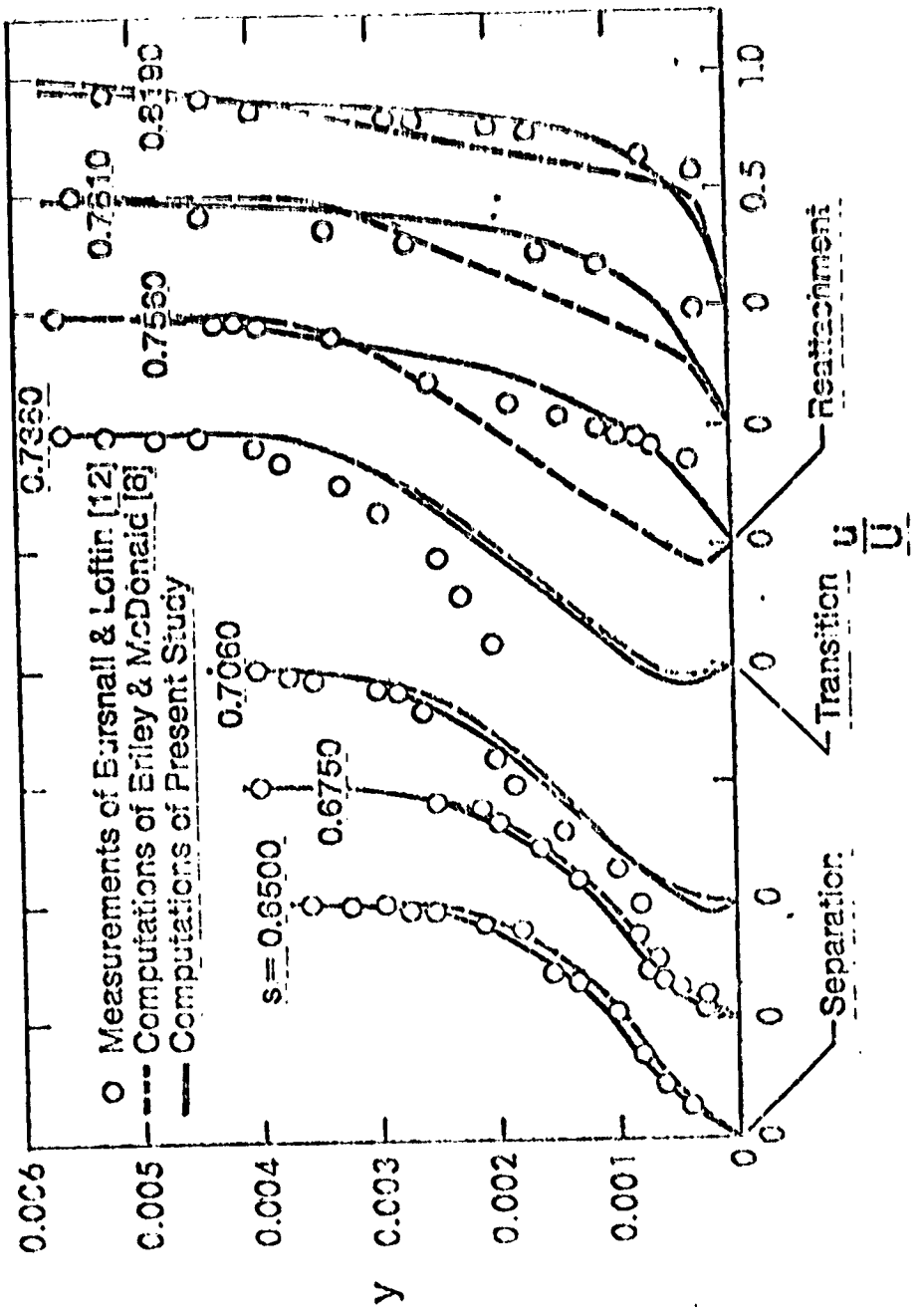

FIGURE III-17
- Comparison of Calculated Velocity Distributions

FLOW SEPARATION BIBLIOGRAPHY

III-1 Prandtl, L. - Verh. 3d Int. Math Kongr - Heidelberg
Translated as NACA Technical Memorandum 452

III-2 Prandtl, L - Strömungslehre, 4th Edition.
Friedr. Vieweg & Sohn, Braunschweig 1944

III-3 Millikan, C. B. & Klein, A. L. - "The Effect of Turbulence"
Aircraft Engineering, Vol. 5, No. 8, August 1933, p. 169-174

III-4 Jones, B. Melville - "Stalling" - Journal of the Royal
Aeronautical Society, Vol. 38, No. 285, Sept. 1934, p. 753-770

III-5 von Karman, Th. & Millikan, C. B. - "On The Theory of Laminar
Boundary Layers Involving Separation", NASA Rep. No. 504, 1934

III-6 von Doenhoff, Albert E. - "A Preliminary Investigation of Boundary
Layer Transition Along a Flat Plate with Adverse Pressure Gradient",
NACA TN639, 1938

III-7 Schmitz, F. W. - Aerodynamics of The Model Airplane. Part 1-
Airfoil Measurements, Ludwig Prandtl Prize for 1941, translation
by Redstone Scientific Information Center

III-8 Pfenninger, W. - "Investigations on Reductions of Friction
on Wings, In Particular By Means of Boundary Layer Suction"
ETH Zurich - Translated as NACA TM No. 1181

III-9 Maekawa,T. & Atsumi, S. - "Transition Caused by the Laminar
Flow Separation" - NACA TM 1352

III-10 Bursnall, W. J. & Loften, L. K. - "Experimental Investigation
of Localized Regions of Laminar Boundary Layer Separation",
NACA TN 2338, April 1951

III-11 McCullough, G. B. & Gault, D. E. - "Examples of Three
Representative Types of Airfoil-Section Stall at Low Speed",
NACA TN 2502, September 1951

III-12 McCullough, George B. - "The Effects of Reynolds Number on the
Stalling Characteristics and Pressure Distributions of Four
Moderately Thin Airfoil Sections". NACA TN 3524, November 1955

III-13 Gault, Donald E. - "An Experimental Investigation of Regions
of Separated Laminar Flow", NACA TN 3505, 1955

III-14 Norbury, J. F. & Crabtree, L. F. - "A Simplified Model of the
Incompressible Flow Past Two-Dimensional Aerofoils with a Long
Bubble Type of Flow Separation", RAE Tech. Note. No. Aero 2352,
June 1955

III-15 Chapman, Dean R., Kuehn, Donald M. & Larson, Howard K. "Investigation of Separated Flows in Supersonic and Subsonic Streams With Emphasis on the Effect of Transition", NACA Report 1356, 1958

III-16 Moore, T. W. F. - "Some Experiments on the Reattachment of a Laminar Boundary Layer Separating From a Rearward Facing Step on a Flat Plate Aerofoil"

III-17 Burrows, F. M. & Newman, B. G. - "The Application of Suction to a Two-Dimensional Laminar Separation Bubble", Miss. State University Aerophysics Dept. Report #27, Oct. 1959

III-18 Tani, Itero - "Low Speed Flows Involving Bubble Separations", Progress in Aeronautical Science, Vol. 5, p. 70-103, Pergamon Press, 1964

III-19 Morkovin, M. V. - "Flow Around Circular Cylinder - A Kaleidoscope of Challenging Fluid Phenomena" Symposium on Fully Separated Flows. ASME Conference, Philadelphia, PA, May 18-20, 1964

III-20 Roshko, A. - "A Review of Concepts in Separated Flow", Canadian Congress of Applied Mechanics, Quebec, May 1967

III-21 Gaster, M. - "On The Stability of Parallel Flows and the Behavior of Laminar Separation Bubbles", PhD Thesis, University of London, 1963. Also see British ARC R&M 3595, 1969

III-22 A.G.A.R.D. - "Fluid Dynamics of Aircraft Stalling" Conference Proceedings Lisbon, Portugal, April 1972

III-23 Laine, S. K. - "A Theoretical Study of the Effect of a Step in a Flat Plate Upon the Laminar Boundary Layer. Numerical Solutions of the Navier Stokes Equations", Dr. of Technology Thesis, Helsinki University, Finland, 1972

III-24 Dobbinga, E., van Ingen, J. L., Kooi, J. W. "Some Research on Two Dimensional Separation Bubbles", Found in Reference III-22, 1972

III-25 van Ingen, J. L. - "On the Calculation of Laminar Separation Bubbles in Two Dimensional Incompressible Flow", AGARD Symposium at Gottingen, May 1975, AGARD CP 168

III-26 van Ingen, J. L. - "Transition, Pressure Gradient, Suction Separation, and Stability Theory", AGARD Conference Proceedings No. 224, Laminar-Turbulent Transition, 1977

III-27 Young, A.D. - "Some Special Boundary Layer Problems" 20th Ludwig Prandtl Lecture, Copenhagen, May 1977 Z. Flugwiss, Weltraumforsch 1 1977 Heft 6

III-28 Mueller, T. J. - "Visualization of the Separation and Subsequent Transition Near the Leading Edge of Airfoils", ATAR Conference Langley Research Center, March 1978

III-29 Batill, S. M. & Mueller, T. J. - "Visualization of the Laminar-Turbulent Transition in the Flow Over an Airfoil Using the Smoke-Wire Technique", AIAA Paper 80-0421, March 1980

III-30 Venkateswarlu, K. & Marsden, D. J. - "Prediction of Boundary Layer Development in the Presence of a Laminar Separation Bubble", University of Alberta, Edmunton, Canada, 1980

III-31 Thompson, J.F., Turner, L., Bearden, J. H., Kwon, J. H., and Long, W. S. - "Numerican Solution of the Navier-Stokes Equations for Arbitrary Two-Dimensional Multi-Element Airfoils." Langley Research Center ATAR Conference, March 7-9, 1978

III-32 Brown, F.N.M. - See The Wind Blow
University of Notre Dam, Fort Wayne, Indiana, copyright 1971, F.N.M. Brown

III-33 Russell, J. M. - "Length and Bursting of Separation Bubbles", NASA Conference on Science and Technology of Low Speed and Motorless Flight, March 29-30, 1979

III-34 Herring, R. N. & Ely, W. L. - "Improved Prediction of Laminar Leading Edge Separation", NASA Advanced Technology Airfoil Research. Vol. 1 CP-2045, Hampton, VA, March 7-9, 1978

III-35 Gross, L. W. - "The Prediction of Two Dimensional Airfoil Stall Progression", NASA Advanced Technology Airfoil Research Vol. 1 CP-2045, Hampton, VA, March 7-9, 1978

IV. LOW REYNOLDS NUMBER AIRFOIL CHARACTERISTICS

A. LABORATORY TEST DATA

Historical Review

In the first two decades of the century, the early state of wind tunnel development occasioned testing at sufficiently low Reynolds numbers to be of interest to this study. References IV-1, 2, and 3 are from this era. The turbulence levels of these facilities were lower than those for this period in the United States, but even so required some correction to an effective Reynolds number higher than the actual test Reynolds number. Although not a rigorous correction, the data shown in Figure IV-1 indicates good correlation of higher turbulence test data shifted only in RN with accurate low turbulence test data.

Reference IV-1 is a very early set of systematic data showing the effects of thickness and undercamber on sharp nosed airfoils at a Reynolds number of 40,000. These results might have been lost in the mist of time were it not for the sharp eyes of Krouse in Reference IV-C, D and H.

Likewise the systematic airfoil developments of WWI of reference IV-2 might have been lost to American model airplane builders, had not Dr. Alexander Lippisch remembered them. He spent many hours pouring over the old data and selecting the most suitable for model airplanes. His gift to American model builders, reference IV-7, lacked only the correction to effective Reynolds number. This led to somewhat optimistic performance predictions.

The first real understanding of the low Reynolds number problem on wing sections came with the work of Schmitz, reference IV-4. Continuous wind tunnel refinement to a turbulence level near that of free flight revealed the difficulty of obtaining good airfoil performance at low Reynolds number (17,000→80,000) in the absence of high ambient turbulence. He discovered hysteresis loops in the lift and drag values of airfoils in the critical flow regime and the effectiveness of artificial turbulence produced by a wire in decreasing the critical Reynolds number. He provided the first attempted recommendation of optimum values of airfoil thickness and camber, and their positions as well as leading edge radius, all as a function of R_c. Reference IV-4 is the one fundamental book which should appear in any low Reynolds number library.

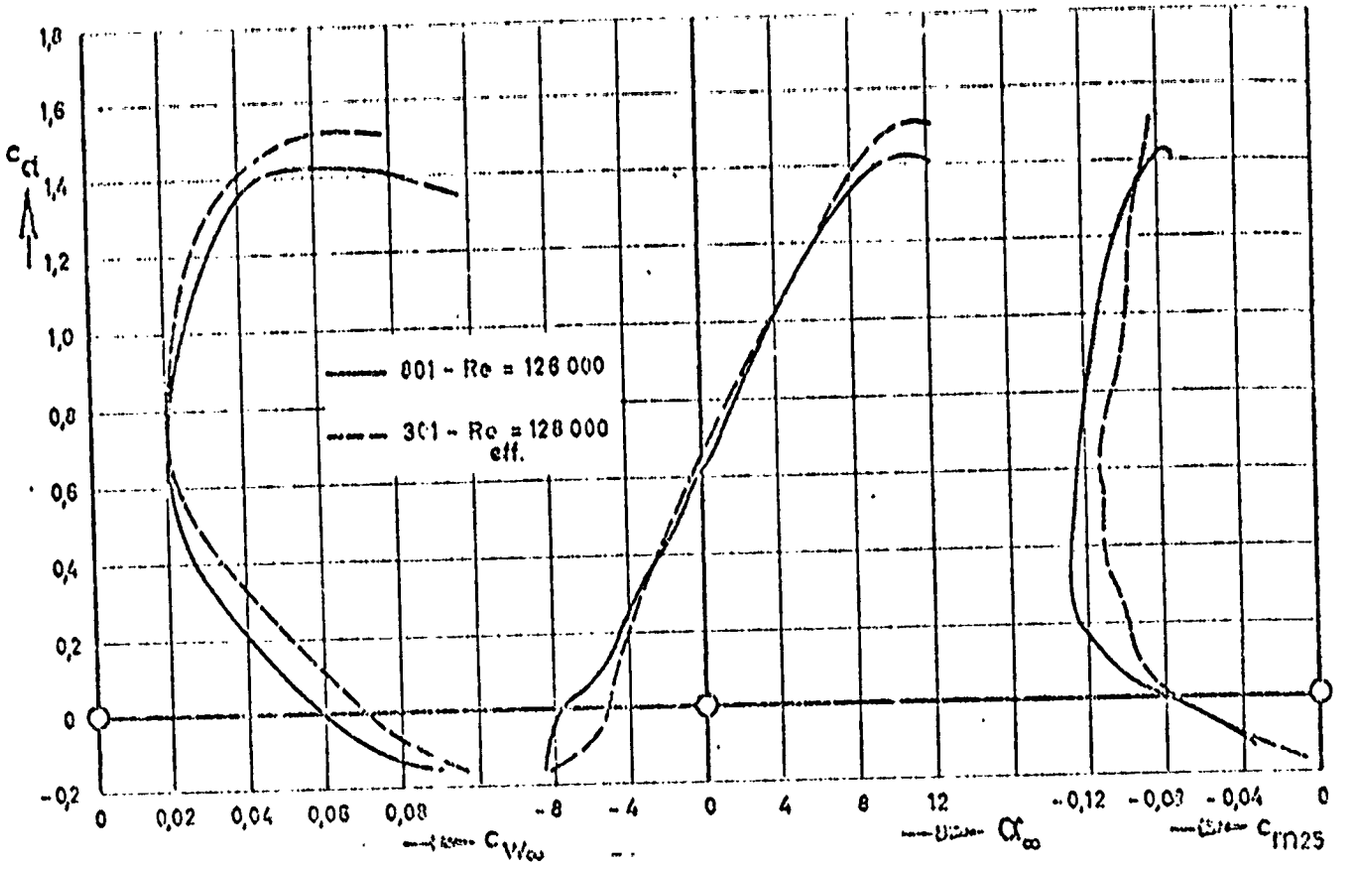
1,8
1,6
c_{ci}
1,4
1,2
1,0
0,8
0,6
0,4
0,2
0
-0,2
001 - Re = 126 000
301 - Re = 128 000 eff.
0
0,02
0,04
0,06
0,08
c_{Wo}
-8
-4
0
4
8
12
α_∞
-0,12
-0,08
-0,04
0
c_{m25}

FIGURE IV-1

Pfenninger in Zurich studied airfoils with extensive laminar flow, IV-5 with and without distributed suction at Zurich in the early 40's. These experiments in a low turbulence wind tunnel showed remarkably low drag values for 6% and 9% thick laminar airfoils at Reynolds numbers between 100,000 and 760,000. He also showed the effectiveness of leading edge air jets, surface waviness, and rearward facing steps in the upper surface in reducing the drag at certain Reynolds numbers.

The sole contribution of NACA to airfoil information at RN<700,000 (once the importance of ambient turbulence was recognized) is the data of reference IV-6 on a thick laminar airfoil showing the decrease in performance as the Reynolds number is decreased to a value of 230,000.

Suzuki of Japan attempted free air testing by use of a whirling arm. He experienced difficulties in reducing the data to absolute numbers but felt the comparative data was valuable. IV-8.

Following WWII, a group of model aircraft enthusiasts in England did extensive low RN aerodynamic work in three different low turbulence wind tunnels. Reference IV-9 and IV-19.

A very large systematically derived series of airfoils was developed at G.E. in 1954 and tested at the wind tunnel at West Virginia University. The data was shifted to an effective Reynolds number greater than test RN and is believed by this writer to be valid. This data is most useful in studying systematic variations in thickness, camber, and form over a RN range of 70,000 to 565,000. IV-10.

Pfenninger returned with a remarkable test of a 4.8% thick, 4.2% camber laminar airfoil in 1956, reference IV-11. These experiments were done in a flow tube of very low turbulence at a single angle of attack over a RN range of 20,000→92,000. He was able to show the beneficial effect of multiple spanwise running chrodwise spaced tape strips on the upper surface and the necessity for placing the first strip further forward as the Reynolds number decreases.

Charwat, reference IV-12, continued work started with Pfenninger on the bird-like airfoil section of Vladamir Seredensky and obtained an excellent set of test data for 30,000→RN<110,000.

An extremely thorough set of tests were conducted by Kraemer who had worked with Schmitz at Göettingen and may be thought of as a continuation of the earlier Schmitz work. Data from four different airfoils with and without artificial turbulence wires is presented in reference IV-13. Additional systematic and detailed measurements on Göettingen airfoils of 8, 12, 16 and 20% thickness were performed by Musemann in 1959. Reference IV-14.

The measurements at Mississippi State University, reference IV-15, were conducted in an unusual facility with the wing extending spanwise beyond the edges of a free jet.

An excellent review of a few airfoils suitable for model aircraft were reviewed by Thies in reference IV-16. The review by Rabel on 29 MVA airfoils with Reynolds numbers adjusted to correct effective values plus 18 later Göettingen sections from low turbulence tunnel experiments represents the best set of easy-to-read airfoil polars available. Reference IV-17.

Stan Miley chose the design of low Reynolds number airfoils as his Doctorate Thesis at Mississippi State University in 1972. He made some measurements with a model airfoil mounted on a sailplane in the turbulence free atmosphere to confirm his design theory. See Reference IV-18.

In 1971 Patrick summarized some of the work of the British Low Speed Research Group in an American publication, IV-19, since the limited reports of LSARA had long been unavailable.

Although Wortmann of Stuttgart had been primarily involved in sailplane airfoil development at RN = 700,000 to 3 X 10^6, he did investigate an excellent airfoil, the FX 63-137 at RN between 280,000 and 700,000, IV-20. This section was used on the British Puffin man power aircraft.

A large number of airfoils have been tested in a small wind tunnel in Milano, Italy, by Bosco and reported in 1972. IV-21.

Data from a low turbulence tunnel in Czechoslovakia on the low cambered Gö 795 was made available to model builders in 1974 as well as the NACA 4412. IV-22, -23.

Also in 1974 Hendricks was able to test a complete A/2 model sailplane in the low turbulence tunnel at Delft University in the Netherlands. IV-24.

In the same year De Laurier and Harris at the Battelle Institute put to rest the furor over the Kline-Fogleman stepped airfoil reputed to have magical properties by measuring it as inferior to everything in sight. IV-25

Model builders received some very useful new results in 1976 when Phillips on sabbatical in England tested both the popular American Gard Linstrum Phillips airfoil and the Eppler 387 in the low turbulence wind tunnel at Cranfield. IV-26. This work was continued by Patrick. IV-28.

Meanwhile, a group at the University of Western Ontario in Canada were attempting to develop low Reynolds number airfoils from theory. A few were tested in a low turbulence tunnel and reported in reference IV-27.

The finest measurements at low Reynolds numbers are presently being obtained at Delft University. Tests of five airfoils were reported in reference IV-29 in 1977. These results were compared to Gö 795 results in a paper by Girsberger. Reference IV-30.

In 1978 the writer presented some long lost data on the thin laminar Pfenninger 048 airfoil with multiple upper surface trippers to modellers in reference IV-32. In the same year, he summarized all available low Reynolds number, low turbulence airfoil data in connection with the Mars aircraft project. Reference IV-31.

Prof. Marsden of the University of Alberta has developed two different low drag airfoils with slotted flaps for high performance sailplanes and light power planes. His measurements extend down to R_c = 500,000, where these relatively thick airfoils are still performing well. IV-33.

McMasters at Boeing has recently developed a thick symmetrical strut fairing for RN between 250,000 and 1,000,000. Tests have been conducted and correlated with theory. Reference IV-34.

In 1979, Patrick of England presented a fine paper to the Bristol International RPV Conference showing data from the Cranfield tests and new free flight data obtained in the U.S. on radio controlled sailplane models. Reference IV-28.

In 1980, Derilla of MIT sent data obtained on the Lissaman 7769 Liebeck type airfoil used on the McCready cross-Channel man powered airplane. The tests were conducted in an open jet wind tunnel at a RN of 277,200. IV-35.

In February 1980, Dr. van Ingen sent the latest data from Delft University on a curved plate windmill airfoil with tubular spar, reference IV-36, and the eagerly awaited test data on the very promising Eppler E-61, reference IV-36. This thin, cambered, theoretically derived (reference Book No. 9) section was recommended for testing by the writer in 1978 as having the most interesting potential for efficient flight in the critical Reynolds number range. The preliminary results are most interesting and a more complete report will be available when Mr. deVries returns from military duty.

McMasters in reference IV-38 presents a fascinating collection of aerodynamic data on flying devices ranging from insects at RN = 100 to aircraft at RN = 10,000,000. His Low Speed Airfoil Bibliography reference IV-39 is useful mainly for the Reynolds number regime of 700,000 and above.

Gooden, reference IV-40, extended the measurements on a popular thick Wortmann sailplane airfoil down to RN = 500,000 in a very detailed study in the excellent Delft University low turbulence wind tunnel.

References IV-41, IV-42, IV-43 and IV-45 present measurements at Reynolds numbers greater than 700,000 but are valuable in bounding the region of interest to this report.

Althaus in reference IV-46 presents wind tunnel measurements on airfoils with flaps, down to a Reynolds number of 700,000.

In 1980 a large catalog, reference IV-46, containing coordinates and performance data for 30 airfoils in the model aircraft Reynolds number range became available. The measurements were made by Dr. Dieter Althaus in the small low turbulence wind tunnel at the University of Stuttgart in West Germany. A model chord of 4.72 inches allows measurement down to a chord Reynolds number of 40,000 while a 7.85 inch model chord allows measurement up to 250,000. The turbulence level is 0.08% of free stream velocity.

Eleven of the 30 clean airfoils were also tested with a single two dimensional trip strip on the forward upper surface. Three of the models were tested with trailing edge flaps at several deflections. Thickness ratios varied evenly from 5.2% to 15% with an additional 33% symetrical section. Camber varied from 0 to 6.7%. Location of maximum thickness varied from 19.6 to 33.9% and location of maximum camber from 30.9 to 56.5% of chord.

Six sections were designed by Dr. F. X. Wortmann, three by Dr. D. Althaus and nine by Dr. R. Eppler, all of Stuttgart. Also included were two old Göttingen sections, six old NACA sections, two Clark Y sections, plus the Sokolov and K-2 Russian sections. This catalog is unique in having so many sections accurately measured in the same facility. Many of the older sections are of interest because they have been used by model builders in the past. The new Stuttgart sections are of interest since they have been based on modern boundary layer analysis concepts.

Mueller of Notre Dame has been doing basic research on low Reynolds number laminar separation bubbles in an excellent low Reynolds number smoke tunnel. In reference IV-48 he describes leading edge separation on an NACA 66_3-018 airfoil at Reynolds numbers of 50,000 and 130,000.

At the author's instigation, Dr. Mueller directed graduate student T. F. Burns, reference IV-49, to measure the performance of the Eppler 61 and Pfenninger 048 airfoils. Using a force balance for drag, the measured performance of these sections was markedly lower than previous wake rake drag determinations performed at Delft and at Stuttgart. These discrepancies in data from three different but excellent low turbulence tunnels are now being actively studied by Mueller. Resolution of this problem may have far-reaching consequences on future experimental airfoil performance measurement methods.

PRINCIPAL INVESTIGATORS, LABORATORIES, REYNOLDS NUMBER RANGES AND AIRFOILS

YEAR	INVESTIGATOR	LABORATORY	R.N.	AIRFOILS	REF
1912	Bairstow & Jones	Natl. Physics Lab England	~40,000	Flat bottom sharp nose various t/c. Mid t/c upper surf. with various under-camber.	IV-1
1917	Munk & Hückel	Göettingen Germany	106,000 128,000 eff. 170,000	MVA 29 airfoils various thickness and camber	IV-2
1920-1932	Langer & Schrenk	Göettingen Germany	400,000 680,000 eff?	Large families of airfoils of various thickness and camber	IV-3
1937-1939	Schmitz	Göettingen Germany	17,000 to 380,000	Flat plate, curved plate, 12%t 4%f and 20%t 6%f airfoils	IV-4
1940-1943	Pfenninger	ETH Zurich, Switzerland.	100,000 760,000	Laminar t/c = .06 f/c = .027 Laminar t/c = .09 f/c = .029	IV-5
1944	Quinn & Tucker	NASA Langley USA LTT, TDT, & 7'x1 0'	230,000 to $9X10^6$	NACA 65_3-418 a = 1.0 NACA 0012	IV-6
1950	Lippisch	Göettingen Germany	106,000 128,000 170,000	Review of Munk and Hückel data 29 MVA airfoils	IV-7
1948 1952	Suzuki	Whirling Arm Japan	45,000 120,000	Clark Y, 6409, 6412, Gö 500, 227 M6, R series, curved plate	IV-8
1954	Patrick & Keating	Battersea Polytechnic England	25,000-630,000	ISACSON 64009 M.A.R.P. 6309e	IV-9
1954 1955	Deslauriers	Univ. of W.Va. USA	70,000-565,000	27 systematic variations in t/c and f/c + NACA 65-410 65-(12)10 BR·10C4/25C50	IV-10
1956	Pfenninger	Low Turbulence Flow Tube USA	20,000-92,000	Laminar t/c = 0.048 f/c = 0.042	IV-11

YEAR	INVESTIGATOR	LABORATORY	R.N.	AIRFOILS	REF
1957	Charwat	Low Turbulence W.T. at USC,USA	30,000-110,000	Seredensky-bird airfoil t/c = 0.10 Sharp l.e.	IV-12
1957	Kraemer	Göettingen Germany	21,000 170,000	Gö 801 t/c = 0.1 f/c = 0.07 Gö 801 paper covered Gö 801 with lower l.e. cut-out Gö 803 t/c = 0.06 f/c = 0.07 Gö 804 t/c = 0.06 f/c = 0.067	IV-13
1959	Musemann	Göettingen Germany	17,000-410,000	Go 795 796 797 798 t/c = 0.08 0.12 0.16 0.20	IV-14
1959	Murphree	Miss. State Univ, USA	150,000	Eppler No. 49 t/c = 0.07 f/c = 0.07	IV-15
1963	Thies	Göettingen Germany	42,000 168,000	MVA 123, 301, Go 795 Go 801, 801 paper covered, 803	IV-16
1965	Rabel	Göettingen Germany	21,000 380,000	29 MVA airfoils 18 Gö airfoils	IV-17
1972	Miley	Miss. State Univ, USA	600,000	Miley MO 6-13-128	IV-18
1971	Patrick	3 wind tunnels in England	32,000 55,000	LDC 2, LSARA Droopsnoot, Gö417a Benedek B-8258b, B-8356b, NASA 6409	IV-19
1972	Althaus	Stuttgart Germany	280,000-700,000	Wortmann FX63-137	IV-20
1972	Bosco	Milano, Italy	41,800-60,000	Bo 545-310 Clark Y Eppler 385, 387, 392, Fukuda 10 Gö 496, 500, 546, Hill SR2 NACA 0009, 0012, 4212, 4412, 6412, 6409	IV-21
1974	Horeni & Lnenicka	Czechoslovakia	20,000-250,000	Gö 795	IV-22

YEAR	INVESTIGATOR	LABORATORY	R.N.	AIRFOILS	REF
1974	Lněnička	Czechoslovakia	20,000-250,000	NACA 4412	IV-23
1974	Hendricks	Delft Univ. The Netherlands	39,600-50,800	Geronimo t/c = .0761 f/c = .0724	IV-24
1974	DeLaurier & Harris	Battelle Insti. Columbus, Ohio USA	23,000	Flat plate, stepped wedge, NACA 0012, Circ. Arc	IV-25
1976	Phillips	Cranfield Institute Bedford, Eng.	25,000-80,000	Gard, Linstrum, Phillips Eppler 387	IV-26
1976	Eggleston	Univ. of Western Ontario, Canada	66,000	(A) t/c = .06 Recovery from 17% (B) t/c = .06 Recovery from 71%	IV-27
1976 1977	Patrick	Cranfield Institute Bedford, Eng.	?	Eppler 387	IV-28
1977	Volkers	Delft Univ. The Netherlands	60,000-500,000	Double wedge, curved plate, FX66-S-196VI Eppler 385 and 387	IV-29
1977	Girsberger	Göettingen Germany	20,000 250,000	Gö 795 and Eppler 387	IV-30
1978	Carmichael	Capistrano Beach, Calif. USA	20,000 100,000	Survey of 27 Low RN Airfoil Characteristics	IV-31
1978	Carmichael	Capistrano Beach, Calif. USA	23,000 90,000	Pfenninger 048	IV-32
1979	Marsden	Univ. of Alberta Canada	500,000-1,200,000	Marsden SF 154 $c_{f/c}$ = 0.17 t/c = 0.154	IV-33
1980	McMasters	Boeing AC USA	250,000-1,000,000	Symmetrical t/c = 0.288 at .31c	IV-34
1979	Patrick	Delft Univ.	60,000-200,000	Eppler 387 on all	IV-28
		Cranfield Insti	40,000-100,000		
		R/C Free Flight	62,000-320,000		
1980	Derilla	MIT Open Jet Wind Tunnel	277,200	Lissaman 7769	IV-35

Year	Investigator	Laboratory	RN	Airfoils	Reference
1972	Liebeck, R.	McDonald Douglas	10^6	Liebeck laminar Liebeck turbulent	IV-45
1978	Althaus, D.	Stuttgart, Germany	500,000 to 1,500,000	60-126 H-2 065137 64,-012 LIII-142K	IV-46
1979	Bruining, A.	Delft University The Netherlands	60,000 100,000 200,000	Circ. ARC Plate 10% Camber 6.67% C Tube Spar	IV-37
1980	deVries, J.	Delft University The Netherlands	50,000 80,000	Eppler E-61	IV-36
1980	Althaus, D.	Stuttgart, Germany	40,000 to 250,000	30 Airfoils	IV-47
1980	Mueller, T. J. Batill, S. M.	University of Notre Dame	70,000	NACA 66018	IV-48
1981	Burns, T. F.	University of Notre Dame	46,000 to 210,000	Eppler 61 Pfenninger 048	IV-49

DISCUSSION

In predicting free flight performance through use of wind tunnel airfoil data one must be aware of the pitfalls. Small changes in ambient turbulence, tunnel noise, model vibration, and model surface contamination can have large effects on aerodynamic performance in the critical Reynolds number range.

The data referenced in this report has been limited to experiments in low turbulence facilities or, in some cases, to data where the Reynolds number has been adjusted upward by a factor based on the ratio (sphere test critical Reynolds number in free flight over sphere test critical Reynolds number in the particular wind tunnel).

When performance critical parameters such as maximum lift coefficient, maximum lift/drag, maximum $(\text{lift})^{3/2}/\text{drag}$ or minimum drag of various airfoils are compared one could easily be led into a poor choice of airfoil for a particular application. It is necessary to examine the complete lift vs. angle of attack curves and lift vs. drag polar as well as pitching moments vs. angle of attack for the entire Reynolds number regime of the application in order to make a wise choice. Some examples of low Reynolds number irregularities follow.

Lift vs α and Lift Drag Polar Shapes

In the critical Reynolds number range, lift vs. angle of attack and lift vs. drag curves undergo distortions relative to the forms to which we are accustomed at high Reynolds number. One can classify the forms in five categories, shown in Figure IV-2 and discussed below.

C_D vs. C_L Form	Description
A	Almost constant drag over a large lift range
A^1	Smooth drag increases above and below design point
B	Smooth drag decrease to a high C_L design point
C	Noticeable drag increase in the mid C_L range
D	As in C with a measurable hysteresis loop
E	Rapidly increasing drag toward very limited C_L max

C_L vs. α Form	
A	Linear, well behaved as at high Reynolds number
B	Non-linear in the mid C_L range
C	Hysteresis loop in the mid C_L range
D	Hysteresis loop at or beyond C_L max
E	Very limited C_L max

Various degrees of the above distortions appear. It is possible that some C form polars are actually D type but that insufficient data points were available to reveal the hysteresis loop. The same might be said for the B and C lift vs. α curves. In general, a given airfoil's characteristics will regress from the A or B types at higher Reynolds number to the C, D, and E types as the Reynolds number is decreased. At a given Reynolds number, excessive thickness and/or camber is more likely to result in distorted lift and drag curves than a more judicious choice. The B and C type polars will often give the highest L/D and $L^{3/2}/D$ values.

LIFT DRAG POLAR FORMS

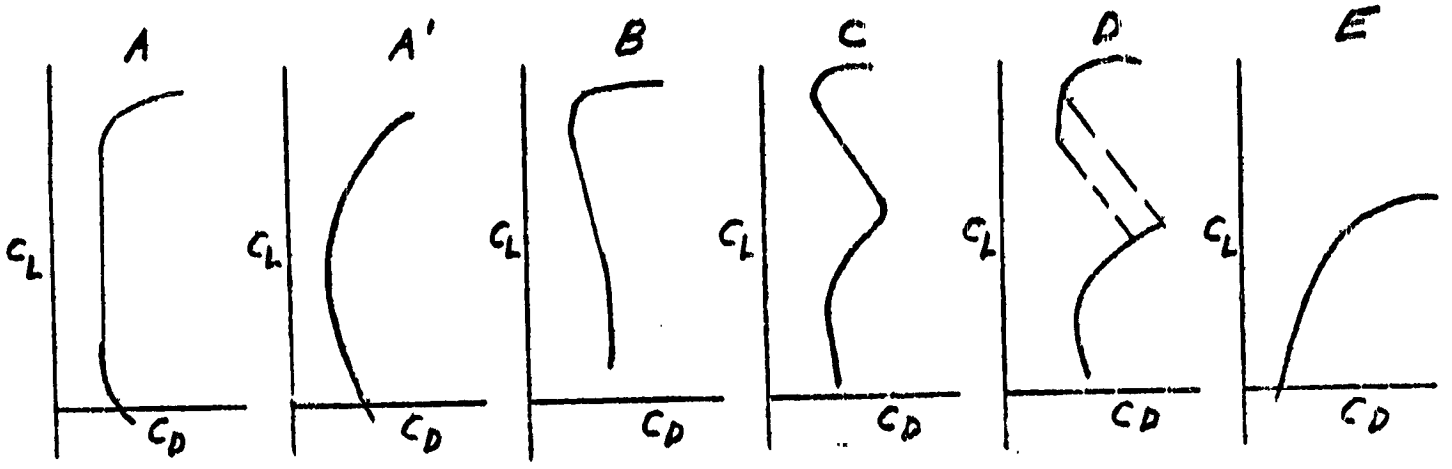

LIFT VS. α FORMS

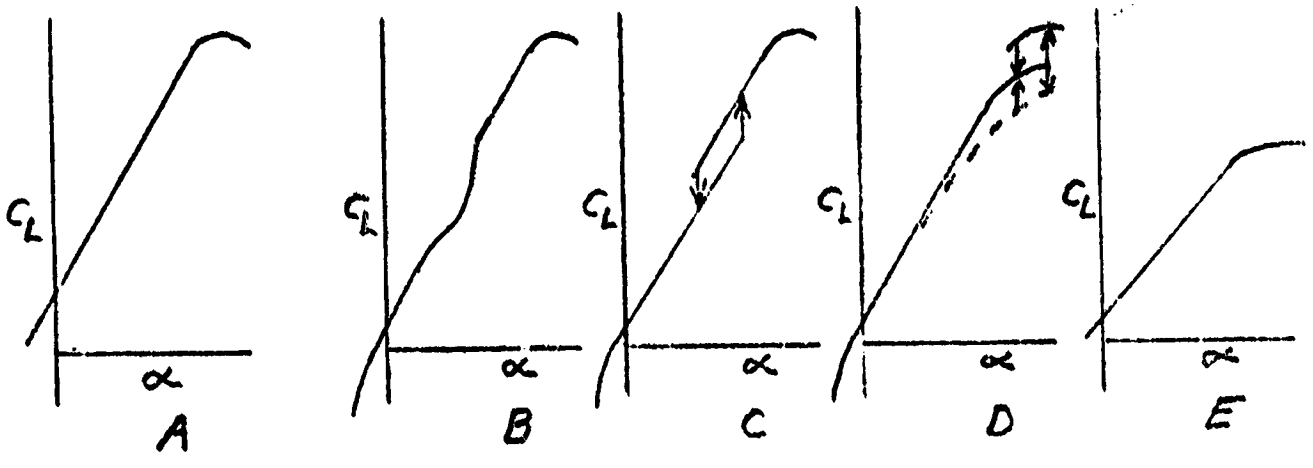

FIGURE IV-2 - LIFT VS. DRAG AND LIFT VS. α FORMS

E type behavior (very low performance) can occur with a too thin, too little camber section as well as with a too thick section and should be avoided in the range 20,000< R<100,000. D type behavior should also be avoided because of possible wild flight dynamics. A moderate amount of C behavior seems to be associated with the highest L/D and $L^{3/2}/D$ airfoils when the Reynolds number is just critical and can perhaps be tolerated.

A very steep lift curve slope is often found at negative angles of attack in the critical RN range. This has been explained by the beautiful smoke pictures taken at Notre Dame by Burns, Jansen, and Mueller, IV-49. The flow is unable to follow around a thin, cambered airfoil nose at negative α. The separation causes a symmetrical shape of the outer flow lines. It is as if the camber has been removed and a steep drop in lift occurs over a small angle of attack range.

b. EPPLER E-61 RESULTS IN THREE LOW TURBULENCE TUNNELS

Introduction

The survey conducted by the author and published in reference IV-31 pointed out the desirability of testing the Eppler 61 since theory predicted it to have low Reynolds number performance superior to any sections tested to date. deVries, Hegen and Boermans, working under the direction of Dr. van Ingen at Delft University, IV-36, in the Netherlands, and Thomas F. Burns, working under the direction of Dr. Mueller at Notre Dame University, IV-49, have both conducted such tests. The Eppler 61 was also included in the large number of airfoils tested at the University of Stuttgart, IV-47, by Althaus.

Characteristics at R_c = 50,000

Lift drag polars from the three facilities are compared in Figure IV-3 at a chord Reynolds number of 50,000. The Delft data were taken at 50,000, the Notre Dame data at 46,421 and the 40,000 and 60,000 data were averaged to produce the Stuttgart curve. Rather pronounced C type behavior is noted. The Delft data give higher lift and lower drag at optimum lift than the other two tunnels, and come very close to Dr. Eppler's theoretical predictions, IV-D-9. The Stuttgart results are very similar but optimum C_L is lower and

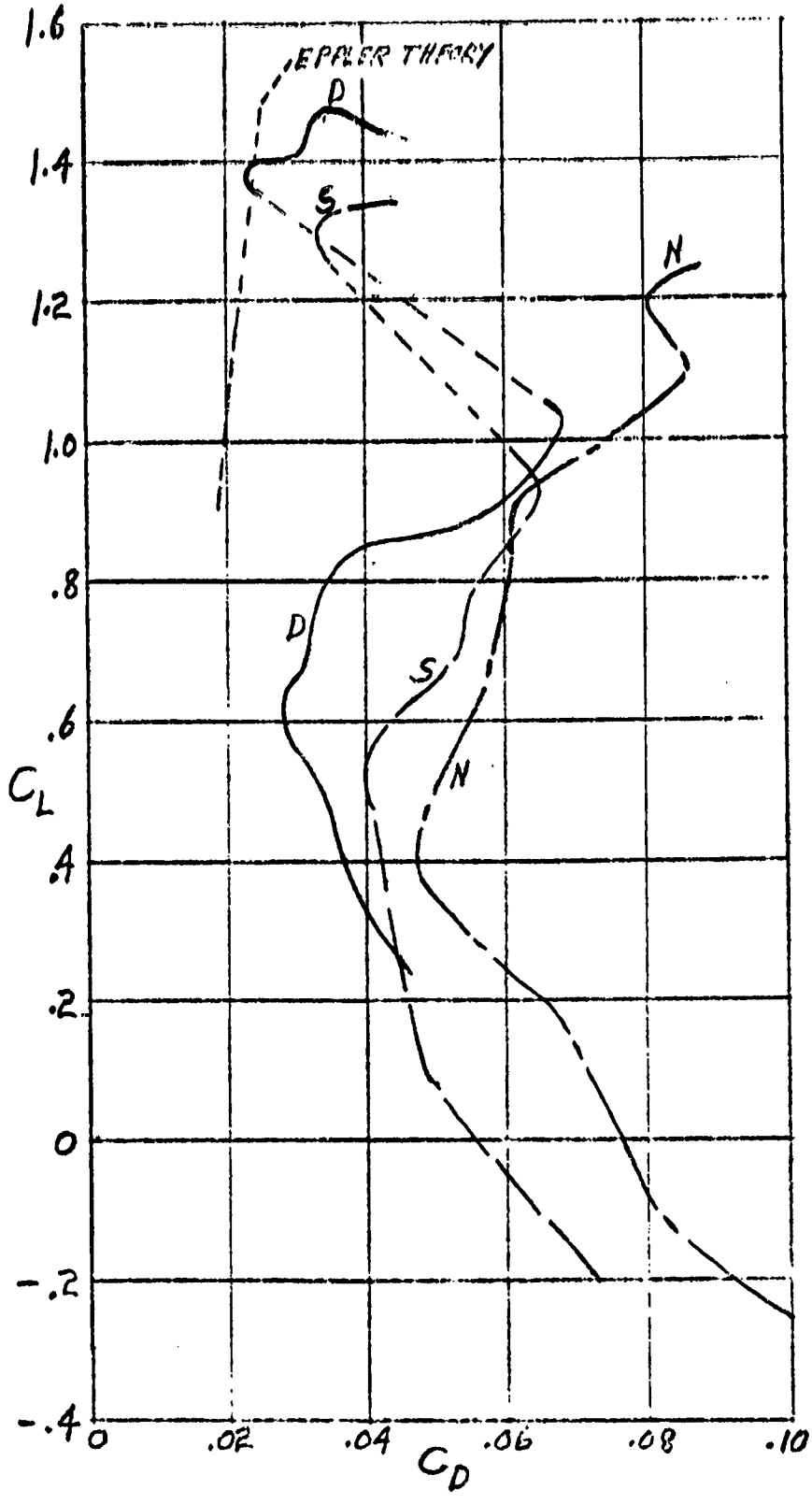

FIGURE IV-3 - EPPLER 61 IN THREE WIND TUNNELS AT REYNOLDS NUMBER = 50,000.

drag at optimum C_L is higher than at Delft. The Notre Dame data agree with the other two at $C_L = 0.9$, but the drag at optimum lift does not fall back to a greatly reduced level as in the other two tunnels. Differences in (L/D) max and ($L^{3/2}/D$) max are appreciable.

Facility	Optimum C_L	Maximum L/D	Maximum $L^{3/2}/D$
Delft	1.39	61.8	72.8
Stuttgart	1.31	39.7	44.9
Notre Dame	1.20	14.8	16.2

Characteristics at $R_c = 80,000$

The comparison at 80,000 R_c appears in Figure IV-4. The behavior is still distinctly C type. The Delft and Stuttgart data are similar but the Notre Dame data do not show any drag decrease above $C_L = 0.9$. The Delft and Stuttgart max performance numbers are now reasonably close but the Notre Dame numbers indicate much lower performance.

Facility	Optimum C_L	Maximum L/D	Maximum $L^{3/2}/D$
Delft	1.4	63.6	75.3
Stuttgart	1.3	61.0	69.6
Notre Dame	1.2	23.1	25.3

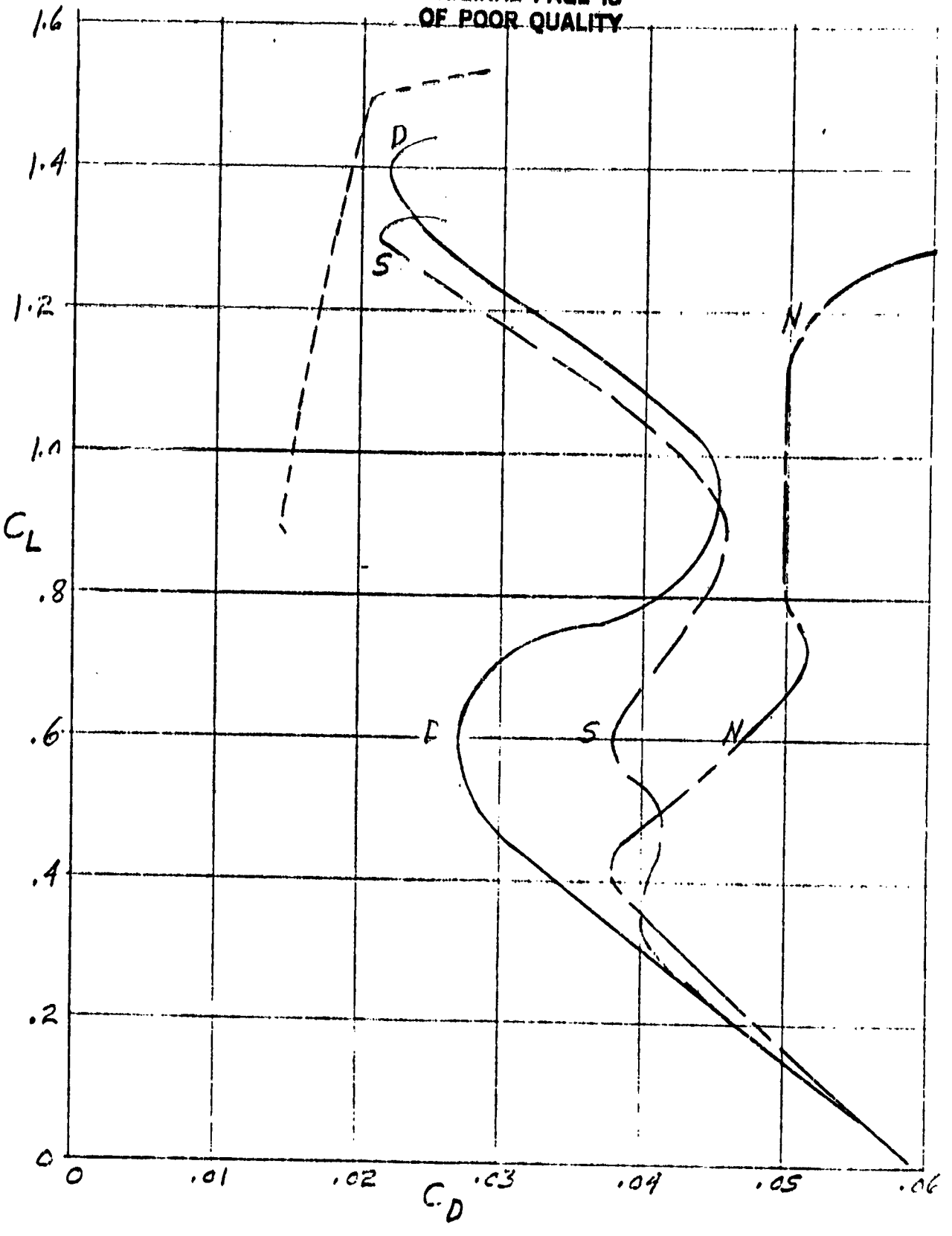

FIGURE IV-4 - EPPLER 61 IN THREE WIND TUNNELS AT REYNOLDS NUMBER = 80,000.

Description of the Three Wind Tunnels

Item	Delft	Stuttgart	Notre Dame
Type	?	Non-return	Non-return
Cross Section	Octagonal	Rectangular	Rectangular
Height	4.1 ft	1.21 ft	2.0 ft
Width	5.9 ft	1.97 ft	2.0 ft
Length	?	2.62 ft	6.0 ft
Cross Sectional Area	22.3 ft^2	2.38 ft^2	4.0 ft^2
Power	?	1.0 H.P.	15 H.P.
Turb. Level	.025% at 131 fps	0.08%	29.5<U_∞<88.6 fps
Lift Measurement	Strain Gage Balance	Strain Gage Balance	Strain Gage Balance
Drag Measurement	Wake Rake	Wake Rake	Strain Gage Balance
Moment Measurement	None	None	None
Other	Oil Film	--	Smoke Streams

The measurement of drag by the balance method at Notre Dame could be the explanation of the low indicated performance. However, they did do a lot of work on repeatability and study of edge effects. While complete data was not available, the previous table reveals that all three facilities are of reasonably low turbulence level. Since the Notre Dame turbulence is slightly higher than the other two tunnels, we cannot challenge the better performance numbers at Delft and Stuttgart on the basis of a turbulence induced increase in effective Reynolds number over Notre Dame. As will be discussed in V, the ambient noise level can provide a large benefit in the critical Reynolds number range similar to a trip wire. At present, I do not have noise level measurements for Stuttgart and Notre Dame and only limited data for Delft.

As mentioned in the historical review, work is now in progress by Mueller of Notre Dame which may shed light on the discrepancies between low Reynolds number airfoil drag measurements using strain gage or wake rake.

We can also compare results of tests of two other Eppler airfoils in the Delft, IV-29, and Stuttgart, IV-47, tunnels.

Airfoil	Reynolds No.	(L/D)Max		$(L^{3/2}/D)$Max	
		Delft	Stuttgart	Delft	Stuttgart
E-385	60,000	38	47.5	46.5	48
	100,000	63	53	73	55
E-387	60,000	38	36	38	34
	100,000	55	54	55	58

The agreement is quite good for the E-387. The differences are greater for the more heavily cambered 385. The differences are not predominately in favor of either wind tunnel at either of the two Reynolds numbers.

(c) Other Test Methods

It is apparent that performance measurements of high performance airfoils in the critical Reynolds number range is tricky even using modern low turbulence tunnels and instrumentation. One would like to obtain the data in the noiseless low turbulence regime of free flight. Free flight gliding of complete models as discussed in IV-B provides the proper flow regime but is complicated by:

(1) Launching and flight dynamics

(2) Atmospheric motions (if tested outdoors)

(3) Uncertainties in calculation of induced and parasite drag

One would like to see a test section developed (with strain gage balance for lift and moment and strain gage plus wake rake for drag) and mounted on some sort of noiseless vibrationless carriage. Perhaps a tensioned wire guided scheme with falling weight drive? The space requirements, time at steady speed, and data recording/storage plan all constitute complications. One could well find new disturbance sources as serious as the noise and turbulence problems of the present tunnels. Still, the scheme does not appear impossible.

(d) Airfoil Performance Comparisons

The very large amount of low Reynolds number airfoil data available from the last seven decades and from nine different nations will be presented in convenient form for the design engineer in Volume II of this study.

LABORATORY DATA BIBLIOGRAPHY

IV-1 Bairstow, L. and Jones, B. Melvill - "Notes on the Properties of Airfoils as Deduced From the Results of the Various Aeronautical Laboratories". British R&M No. 53, March 1912

IV-2 Munk, M. and Hückel - "Messergebnisse aus den Technischen Berichten T.B.I und II der Flugzeugmeisterei". Göttingen 1917-18

IV-3 Langer, R. and Schrenk, O. "Neuere Profilunstersuchungen" and "Untersuchung weiterer Joukowsky-Profile" In - Ergebnisse der Aerodynamischen Versuchsanstalt Zu Göttingen IV Leiferung Munchen und Berlin 1932

IV-4 Schmitz, F. W. - Aerodynamics of the Model Airplane Part I - Airfoil Measurements - Translation by Redstone Arsenal Nov. 22, 1967 - Original Publication - Göttingen 1942

IV-5 Pfenninger, W. - "Investigations on Reduction of Friction on Wings, In Particular by Means of Boundary-Layer Suction" Translated as NACA TM No. 1181, 1946

IV-6 Quinn, J. H. and Tucker, W. A. - "Scale and Turbulence Effects on the Lift and Drag Characteristics of the NACA 653-418 a = 1.0 Airfoil Section." NACA ACR No. L4HII. WR L-138. 1944

IV-7 Lippisch, A. M. - "Wing Sections for Model Planes" Air Trails Pictorial Magazine - April and May 1950

IV-8 Suzuki, S. - "Whirling Arm Airfoil Testing" Work done in Japan. Reported in Model Aeronautic Year Book by Frank Zaic 1955-56

IV-9 Keating, F. A. and Patrick T. - "Airfoil Test Work of the Model Aerodynamics Research Project." 1954 M.A.R.P. Symposium Report. Also reported in British Model Aircraft Magazine, Feb. 1956

IV-10 Deslauriers, E. J. - "A Simple Blade Profile Systematic" General Electric Tech. Information Series DF54A6T498 12-15-54 and "Blade Performance at Low Reynolds Numbers" G.E. Tech. Information Series R54AGT605 1-14-55

IV-11 Pfenninger, W. - "Experimental Investigation of an Airfoil With High Lift to Drag Ratios at Low Reynolds Numbers." Northrup Aircraft Inc. NAI 56-188 Report No. BLC-84 Feb. 1956

IV-12 Charwat, A. F. - "Experiment on the Variation of Airfoil Properties With Reynolds Number." Journal of the Aeronautical Sciences May 1956

IV-13 Kraemer, K. - "Airfoil Profiles In a Critical Reynolds Number Region" Göettingen Report Forschung auf dem Gebiete des Ingerieurwesens Bd 27, 1961 Nr. 2 S 33/46

IV-14 Muesmann, G. - "Measurements and Boundary Layer Observations on a Thickened Blower Profile as a Function of the Reynolds Number" Z Flugwiss 7 (9), 253-264 1959

IV-15 Murphree, D. L. - "Measurements On A Highly Cambered Model Airfoil Section And Experimental Techniques" Aerophysics Dept. Research Note #8, Miss. State University, April 1959

IV-16 Thies, W. - "Flügelprofile mit gerader Unterseite" Swiss Aero Revue - January 1963 and February 1963

IV-17 Rabel, H. "Modellflug Profile" - Munchen 1965

IV-18 Miley, S. - "An Analysis of the Design of Airfoil Sections For Low Reynolds Numbers." Mississippi State University Ph.D. 1972 - University Microfilms, Ann Arbor, Mich.

IV-19 Patrick T. J. - "The Low Speed Aerodynamic Research Association 1947-1954" Fourth Annual Symposium of the National Free Flight Society. 1971

IV-20 Althaus, D. - "Stuttgarter Profilkatalog I." Institut fürAerodynamik und Gasdynamik der UniversitätStuttgard 1972

IV-21 Bosco, A. - "Airfoil Sections for Flying Models" Associazione Sportiva Aeromodellistica 20081 Abbiategrasso Milano Italy, December 1972

IV-22 Horeni, B. and Lnenicka, J. - "Aerodynamika Opravdus Modelarska" Modelar Mogazine 4/1974

IV-23 Lnenicka, J. - "Report to Pierpont of NASA Langley on the Critical Reynolds Number of the NASA 4412 Airfoil." Czechoslovakia April 1974

IV-24 Hendricks, F. - "Aerodynamic Measurements on the Wing of the Geronimo A-2." The National Free Flight Society Seventh Annual Symposium 1974

IV-25 DeLaurier, D. and Harris, J. M. - "An Experimental Investigation of the Aerodynamic Characteristics of Stepped-Wedge Airfoils at Low Speed." Aermican Institute of Aeronautics and Astronautics. 1974

IV-26 Phillips, W. H. - "Low Speed Wind Tunnel Tests of Two Airfoils Suitable for Models." Ninth Annual Symposium of the National Free Flight Society. 1976

IV-27 Eggleston, B. - "The Design of Airfoils for High Lift/Drag Ratios at Low Reynolds Numbers." CASI Symposium on Recreational Aircraft. Toronto, Canada. September 1976

IV-28 Patrick, J. T. - "Airfoils Down to Critical Reynolds Numbers And the Performance of Remotely Controlled Gliders", Briston UK Remotely Piloted Vehicles International Conference, 3-5 Sept. 1979

IV-29 Volkers, D. F. - "Preliminary Results of Windtunnel Measurements on Some Airfoil Sections at Reynolds Numbers Between 0.6 x 10^5 and 5.0 x 10^5." Delft University of Technology, Dept. of Aerospace Engineering - Memo M-276. The Netherlands. June 1977

IV-30 Girsberger, R. - "Ergebnisse von Wind-kanalmessungen an Modellflugprofilen." Swiss Aero Review. 12, 1977

IV-31 Carmichael, B. H. - "Survey of Two Dimensional Airfoil Data Between Reynolds Numbers of 20,000 and 100,000." Study for Developmental Sciences Incorporated. City of Industry, Calif. 91744, April 1978

IV-32 Carmichael, B. H. - "A Significant Increase in Lift to Drag Ratio of Airfoils at Low Reynolds Number Through the Use of Multiple Trippers and Low Drag Laminar Flow." Annual National Free Flight Symposium Report For 1978

IV-33 Marsden, D. - "Wind Tunnel Tests of a 15.4% Thick Laminar Airfoil With Slotted Flap at Reynolds numbers of 0.5 x 10^6 to 1.2 x 10^6." University of Alberta, Edmonton, Canada. Unpublished Notes. 1979

IV-34 McMasters - "Thick Streamlined Strut Test Results." Private Communication. February 1980

IV-35 Derilla, M. - "Tests of the Lissaman 7769 Airfoil at a RN of 277,200 in the M.I.T. Open Jet Wind Tunnel." Private Communication. February 1980

IV-36 deVries, J., Hegen, G. H. & Boermans, L.M.M. - "Preliminary Results of Wind Tunnel Measurements at Low Reynolds Numbers on Airfoil Section E-61." Dept. of Aerospace Engineering, Delft University of Technology. Private Communication from Dr. J. L. van Ingen, February 18, 1980

IV-37 Bruining, A. - "Aerodynamic Characteristics of a Curved Plate Airfoil Section at Reynolds Numbers 60,000 and 100,000 and Angles of Attack From -10 to +90 Degrees." Delft University of Technology, Report LR-281, May, 1979.

IV-38 McMasters, J. H. - "An Analytical Survey of Low Speed Flying Devices - Natural and Man-Made". Proceeding of the 2nd International Symposium on the Technology and Science of Low-Speed and Motorless Flight. Mass. Inst. of Technology, September 11-13, 1974

IV-39 McMasters, J. H. - "Low Speed Airfoil Bibliography". Technical Soaring, Vol. 3, No. 4. Fall 1974

IV-40 Gooden - "Experimental Low Speed Aerodynamic Characteristics of The Wortmann FX66-S-196 VI Airfoil". Technical Soaring, Vol. 5, No. 3, March 1979

IV-41 Bingham, G. J. and Noonan, K. W. - "Low Speed Aerodynamic Characteristics of NASA 6716 and NACA 4416 Airfoils with 35-Percent-Chord Single-Slotted Flaps". NASA TMX 2623

IV-42 Jacobs, E. N. - "Preliminary Report on Laminar-Flow Airfoils and New Methods Adapted for Airfoil and Boundary-Layer Investigations". NACA ACR, April 25, 1939

IV-43 Loftin, L. K. and Smith, H. A. - "Aerodynamic Characteristics of 15 NACA Airfoil Sections at Seven Reynolds Numbers From 0.7×10^6 to 9.0×10^6". NACA TN 1945, 1949

IV-44 Quinn, J. H. and Tucker, W. A. - "Scale and Turbulence Effects on the Lift and Drag Characteristics of the NASA 65_3-418 α - 1.0 Airfoil Section". NACA ACR No. L4H11, 1944

IV-45 Liebeck, R. - "Wind Tunnel Tests of Two Airfoils Designed for High Lift Without Separation in Incompressible Flow". Douglas Aircraft Company Report MDC J5667/01, August 1972

IV-46 Althaus, D. - "Measurements on Airfoils With Flaps at Medium Reynolds Numbers". Technical Soaring, Vol. V. No. 2. December 1978

IV-47 Althaus, D. - Profilpolaren Für Den Modelflug N V. Neckar - Verlag - Villingen - Schweinningen 1980

IV-48 Mueller, T. J. and Batill, S. M. - "Experimental Studies of the Laminar Separation Bubble on a Two Dimensional Airfoil at Low Reynolds Numbers". AIAA Paper 80-1440, July 1980

IV-49 Burns, T. F. - "Experimental Studies of Eppler 61 and Pfenninger 048 Airfoils at Low Reynolds Numbers". Graduate Thesis - Notre Dame University - Indiana. January 1981

(B) DISCUSSION OF FREE FLIGHT TESTING

It is more difficult to obtain reliable experimental airfoil data in the critical Reynolds number regime than at higher Reynolds number. An excellent comparison of three different experimental methods is given by Phillips in Reference IV-59. The first is the laboratory or wind tunnel approach covered in the previous section. The remaining two involve measurements in free flight. The first consists of straight glides in a large room or out of doors, in which distance covered, altitude lost, and time are recorded. The glide ratio can be obtained from the forward speed and the sinking speed, and, knowing the wing loading, one can reduce the results to a lift, drag polar for the complete aircraft. By subtracting the theoretical induced drag and the estimated parasite drag due to fuselage, tail and trim, one can obtain the two dimensional airfoil lift, drag polar. The majority of the references in this section employ this method. The development of a refined method of this type is described in Reference IV-54. This writer was privileged to witness this development, in which the student Hoffman encouraged by Dr. Gus Raspet and aided by Guy Storer (all of Mississippi State College) slowly discovered the problems and came up with increasingly improved solutions. A special launching rail with falling weight accelerator was used to improve the steady state, on speed, on glide path launch, so necessary to prevent longitudinal oscillations. The use of two reference horizon lights, a light in the side of the model aircraft, an open camera placed before a whirling interrupter disk, coupled with launching in a darkened large room, constituted the final refinement. The slope of the interrupted light trace with respect to the reference horizon gave the glide path angle and the interruption pattern gave the flight speed. This type of testing was simultaneously and independently carried to the same degree of refinement by Maximillian Hacklinger who obtained a minimum sinking speed of 25.1 cm/sec and maximum glide ratio of 17 on a Nordic A/2 model sailplane, References IV-35 and IV-71. Even when glide tests are carried out in a large room one must be careful that the results are not influenced by possible micrometeorologic effects. When conducted outdoors, this problem becomes very difficult just as in the performance testing of ma.. carrying sailplanes. As glider performance improves, (flatter glide slopes and lower sinking speeds) the percent error introduced by vertical air motion and also horizontal wind in ground referenced

measurements becomes larger. The advantage of this simple type of test is most pronounced for very low Reynolds numbers testing where glide slopes are steep, room size requirements are modest, and internal instrumentation is not possible. See for example Hacklinger IV-71, tailless microfilm model RN = 1150, Gibo and Pallett, deceased butterfly RN = 2700, IV-70, Hacklinger IV-58, Indoor Microfilm 3120→7310, Raspet-Zanonia Seed RN = 6000, IV-53, Harland, Microfilm indoor model 5,200→12,900, IV-64, McBride IV-30, Indoor Microfilm model RN = 12,800, Bauer IV-66, hand launched glider RN = 15,000, and Newman, IV-68, artificial dragonfly wing, 12,000→60,000.

A somewhat less precise method often used by model builders is to time several descents from the top of a tow launch line of known length in the early morning when vertical air currents are not likely to be large. This is only useful for comparison of different configurations and is fraught with uncertainties. Nevertheless, it was used as the basis for the statistical analysis of Reference IV-61 in an attempt to define the most suitable airfoil selection parameter values for A/2 model sailplanes. A more refined outdoor glide test has recently been developed for radio controlled model sailplanes by Rawdon, IV-69. Each model is flown several times at a given longitudinal trim setting over a course. Ground based recording of start time and altitude and finish time and altitude are made for consecutive passes, 180° different in heading. The latter cancels out the horizontal wind but scatter is still introduced by small vertical air currents.

Phillips in IV-59 describes a method which is insensitive to air mass motion. It obtains the model drag to lift ratio as the tangent of the sum of a free floating vane angle and a pendulum angle where the former is measured from the longitudinal body axis and the latter from the normal to this axis. It is necessary to place the vane outside the upwash field to the wing or to correct for it, and it is necessary to damp the pendulum and only read when it is steady. Although this method has not been widely used as yet for either model or man carrying sailplanes, it would seem to hold great promise for free flight measurements.

FREE FLIGHT TESTING

YEAR	INVESTIGATOR	TYPE OF MODEL	WING SECTION	RN	REF
1934	McBride	Indoor Microfilm	Curved Plate		IV-50
1950	Holbrook	Hand launched glider	Seredensky Airfoil Diffuser Tip Flying Wing	300,000	IV-51
1951	Jex	Tow line glider	SL 6205 NACA 6409 LSARA S II and S II Reversed	60,000	IV-52
1953	Raspet	Zanonia Seed	Membrane - Single surface AR = 2.65		IV-53
1954	Hoffmann	Tow line glider	NACA 4612 5" chord 45" span	40,000 60,000	IV-54
1955	Hacklinger	Nordic A-2 Model Sailplane	Hacklinger	30,000	IV-55
1956	Hindes	Tow line glider	NACA 6409 4" chord 48" span	40,000	IV-56
1957?	Anon	Model Sailplane	Flat bottom t/c = 0.093 AR = 8.4		IV-57
1964	Hacklinger	Indoor Microfilm	Curved Plate		IV-58
1970	Phillips	R/C Model Sailplane Nordic Model Sailplane	Not Given	200,000 30,000	IV-59
1971	Ovelmen & Meuser	Wakefield	NACA 6407.5 Aspect Ratio - 19.2	30,000	IV-60
1970	Allnut & Kaczauowski	Nordic A/2 Model Sailplanes	21 Successful Airfoils	40,000	IV-61
1974	Hartman	Nordic A/2 Model Sailplane	Eppler 58 & 59 plus three other camber mods.	40,000	IV-62
1973	Nippert	3 Nordic A/2 model Sailplanes	Not Specified	40,000	IV-63

YEAR	INVESTIGATOR	TYPE OF MODEL	WING SECTION	RN	REF
1975	Harlan	Indoor Microfilm	Curved Plate	5,200 12,900	IV-64
1975	Hadas	Nordic A/2 Model Sailplane	B-8456-f at Root B-6456-f at TIP	42,800	IV-65
1975	Bauer	Paper hand-launched Gliders	Thin Plate Section	30,000	IV-66
		Balsa hand-launched Gliders	2 Element Airfoils	15,000	
		3 Nordic A/2 Sailplanes	One with 2 element airfoil	40,000	
1976	Bauer	Nordic A/2 Sailplanes	AR-500 & CH407	80,000	IV-67
		FAI Power Model	2 Element Airfoils	70,000	
1976	Newman, Savage & Schouella	Indoor Glider 40" span 5" chord	McBride B-7 Curved plate	35,000	IV-68
			Dragonfly	60,000	
1977	Rawdon	Radio Controlled Sailplane Models	NACA 6412 2R-12	62,000	IV-69
			Rawdon 12.5% t 3% f	320,000	
1979	Gibo & Pallet	Deseased Butterfly	Flat Plate	2700 4900	IV-70
1955	Hacklinger	Nordic A/2 Model Sailplane	HA-12	39,000	IV-71
1961	Hacklinger	Nordic A/2 Model Sailplane	HA-12	39,000	IV-72
		Microfilm Tailless	Curved Plate	1150	

IV-50 McBride, J. W. - "Some Technical Notes on the Present Indoor Airfoil" - In Junior Aeronautics Year Book - By Frank Zaic Ed. 1934

IV-51 Holbrook, C. T. - "Some Studies on Flying Wings." IAS Student Branch Meeting at Tuscaloosa, Alabama. April 21-22, 1950

IV-52 Jex, H. - "Narwhal Glide Test Results at Reynolds Number = 60,000." Tests Conducted at Mass. Inst. of Technology - 1950-1951

IV-53 Raspet, A. - "Glide Polar of a Zanonia Macrocarpa Seed." Indoor glide tests conducted at Mississippi State College, 1953

IV-54 Hoffman, Gilbert - "Aerodynamic Measurements at Reynolds Numbers Below 100,000 Obtained by a Free Flight Glide Technique." Presented at 5th Annual Southeastern IAS Student Branch Meeting. April 1954

IV-55 Hacklinger, M. - "Effect of Turbulators on the Glide Performance of an A-2 Model Sailplane." Presented at the 1955 Low Speed Aeronautical Research Association Meeting. R.Ae.S. Library - London, England. November 12, 1955

IV-56 Hindes, S. - "Glide Tests Results on a Model Sailplane." Presented at the 1956 Low Speed Aeronautical Research Association Meeting. London, England. M.A.R.P. Report

IV-57 Anon - "Glide Tests of the Basilisk Model Sailplane." Basler Schulen - Swiss Aero Review

IV-58 Hacklinger, M. - "Theoretical and Experimental Investigation of Indoor Flying MOdels." Journal of the Royal Aeronautical Society. November 1964

IV-59 Phillips, W. H. - "Experiments on Methods of Measuring the Lift Drag Ratio of Airfoils." National Free Flight Symposium Report. 1970

IV-60 Ovelmen, S. and Meuser, R. - "The Flight Testing of 13 Wakefield Propellers." - Includes glide test of model. Fourth Annual Symposium of the National Free Flight Society. 1971

IV-61 Allnut, P. J. and Kaczauowski - "A Relationship Between Basic Airfoil Parameters/Aspect Ratio and Rate of Sink of Nordic A/2 Gliders." National Free Flight Society, Third Annual Symposium Report. 1970

IV-62 Hartman, P. A. - "Intuitive Airfoil Theory and Construction of Solid Wings." National Free Flight Society. Seventh Annual Symposium Report. 1974

IV-63 Nippert, V. - "Indoor Nordic Glider Tests." National Free Flight Society Digest. November 1973.

IV-64 Harlan, R. B. - "Drag Elements of Indoor Models" National Free Flight Society Symposium Report for 1975

IV-65 Hadas, A. - "Aerodynamic Characteristics of a High Lift Two Element Wing - An Experimental Study." National Free Flight Society Symposium For 1975

IV-66 Bauer, A. B. - "The Laminar Airfoil Problem." National Free Flight Society Symposium Report for 1975

IV-67 Bauer, A. B. - "Fun and Games with FAI Flappers." Ninth Annual National Free Flight Society Symposium Report for 1976

IV-68 Newman, B. G., Savage, S. B., and Schouella, D. - "Model Tests on a Wing Section of an Aeschna Dragonfly." McGill University, Montreal, Canada. 1976

IV-69 Rawdon, B. - "Preliminary Report on L/D Trials." Private Communication (to be published in the 1981 National Free Flight Society Symposium Report). 1979

IV-70 Gibo, D. L. and Pallett, M. J. - "Soaring Flight of Monarch Butterflies, Danaus Plexippus (Lepidoptera: Danaidae), During the Late Summer Migration in Southern Ontario." Canadian Journal of Zoology, Vol. 57, No. 7. 1979

IV-71 Hacklinger, M. - "Flergmessung an einem Segelflugmodell" Aerodynamische Versuchsanstalt Göttingen Dated 30.4.1957. Tests Performed in 1954. Also presented at LSARA Meeting R.Ae.S. Library, London, England Nov. 12, 1955

IV-72 Hacklinger, M. "Gelöste und ungelöste Fragen der Modellflugtechnik" Winner of Otto-Lilienthal and Ludwig Prandtl Prize. Das Buch der Luftfahrt und Raumfahrt, Bond VI, Deutsche Verlags-Anstalt Stuttgard 1961

IV-73 Czepa - "Czepa on Airfoils" - Model Airplane News, August, September-1957

(C) LOW REYNOLDS NUMBER AIRFOIL DESIGN

Until quite recently, the design of airfoils for Reynolds numbers below about 1×10^6 has been primarily empirical in nature, guided by observations of nature's solutions for insects, birds, and small fish, and aided by inputs from low Reynolds number smoke tunnel flow visualization and force measurements. In the early years, considerable optimism was generated by the beneficial effect of tunnel turbulence level in artificially raising the critical Reynolds number of airfoils which operate well at increased RN but have very low performance in free flight at the true value of lower Reynolds numbers. The brilliant pioneering effort of Schmitz (reference IV-4) introduced realism to the game. Technical aeromodellers, armed with the Schmitz results, now began an empirical development which, due to their competitive spirit and keen powers of observation led to some remarkably good airfoils which work well in the real world of free flight at low Reynolds numbers in the earth's atmosphere.

The question now arises as to whether the presently available powerful analytical airfoil design procedures can lead to dramatic additional improvements over the present empirical state of the art as had occurred in the Reynolds number range of 1×10^6 to 3×10^6.

Systematic series of aircraft airfoils were originally designed by NASA by wrapping the best thickness fairings about the best camber lines where both had come from long years of empirical experience. This work of the 20's and 30's was followed in the late 30's by the development of laminar airfoils with improved favorable pressure distributions forward of more aft minimum pressure points and improved linear pressure recoveries aft of minimum pressure through rear surface cusping. See Reference IV-A. These airfoils were excellent at Reynolds numbers above 4×10^6 but often gave disappointing results at RN's of 0.7×10^6 to 2.5×10^6. The performance in this regime was remarkably improved by the efforts of Wortmann, Reference IV-J, and Eppler, Reference IV-L, and together with smooth, wave-free composite construction led to large improvements in the performance of man-carrying high performance sailplanes for the past 25 years. (To date, these advantages have been avoided by all but a few European power plane builders and some American homebuilders.

The brilliant application by Liebeck (Reference IV-K), of the Stratford (Reference IV-B) concave pressure recovery led to drag reduction and lift increases at RN = 1 x 10^6 to a level previously thought to be impossible.

Meanwhile, technical aeromodellers continued to design improved airfoils for 20,000 < RN < 300,000 using empirical guidance from the few low turbulence low RN tests available, and checking every step of the way with what worked in the real world of free flight contests. See References IV-C, D, E, F, G, H, O and IV-51.

In 1972, Miley investigated the theoretical lower limit of Reynolds number for which the Wortmann, Stratford, and Liebeck techniques might apply and set a lower limit of R_c = 300,000. He conducted tests of the Miley MO-6-128 airfoil designed according to theory in the free atmosphere mounted on a sailplane with excellent comparison with theory at R_c = 600,000.

To date only R. Eppler and W. H. Phillips have attempted to predict the lift-drag polars of airfoils at Reynolds numbers less than 300,000. They have both used the Eppler method IV-L and IV-R. Results may be found in IV-T, IV-U, and Aeromodeller Book (9). The calculations cease upon separation. To date the calculations have not been iterated for the boundary layer displacement thickness nor is there yet provision for including the effects of a separation bubble with reattachment. Comparison of theory and experiment for the Eppler 387 is seen in Figure IV-5 to be quite good at R_c = 200,000 but further in error at R_c = 100,000.

An excellent review of the prospects for the application of modern airfoil design technology to the low Reynolds number regime was provided by Russell in 1975, Reference IV-P, and clearly points out the problems associated with separation. He suggested that the exact solution of Navier Stokes equations as applied by Laine, Reference III-23, in 1972 to the flow over an aft facing step on a plate could eventually be applied to the low RN airfoil problem. Since the computer requirements are so formidable, it is more likely that the approach of Venkateswarlu and Marsden, Reference III-30, will be attempted first.

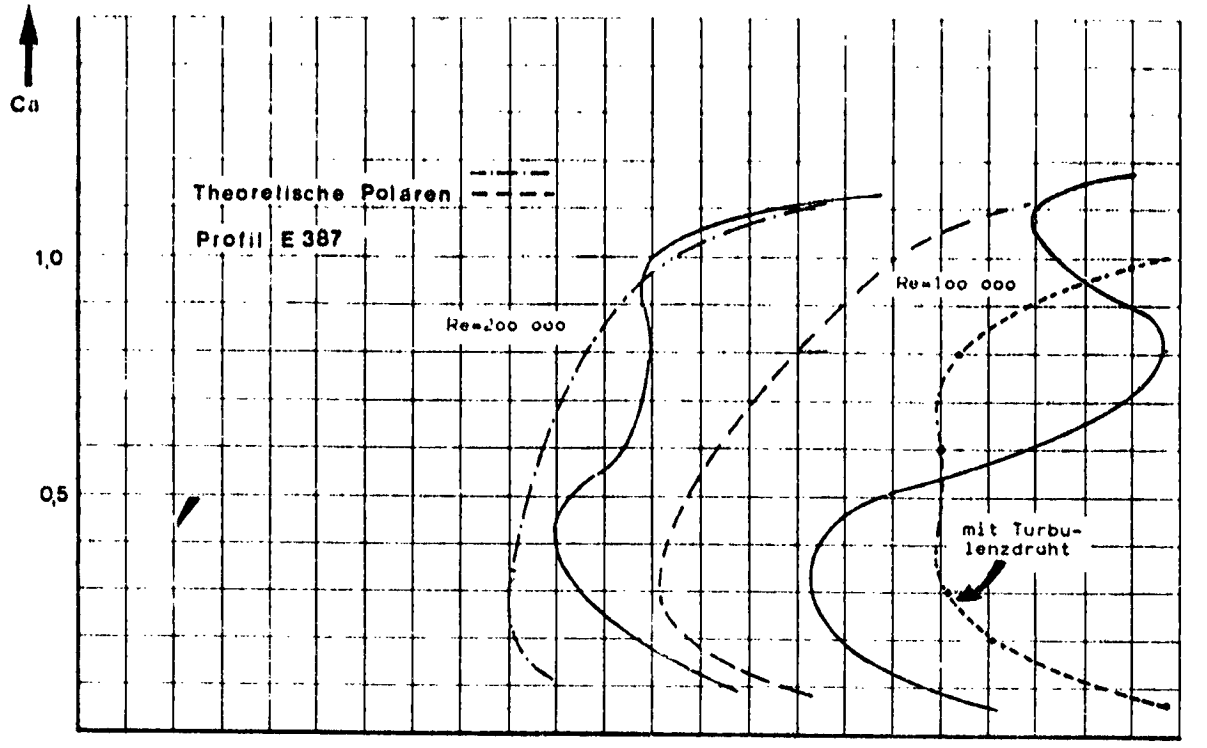

Vergleich der theoretischen Polaren mit den in Delft gemessenen Polaren

FIGURE IV-5

The Eppler type calculations seem to be fastest, and equally accurate when compared with others at $RN \geq 10^6$. Some aspects of the methods given in IV-M, N, Q and S may constitute additional refinements. The most helpful technique in reducing time and cost of airfoil design at $RN \geq 10^6$ is given in reference IV-V. The man must definitely be kept in the loop to keep from being swamped with useless computer printout.

Recently, McMasters and Henderson, VI-W and IV-X, have been exploring the possibility of extending theoretical airfoil development to lower Reynolds numbers. It is highly likely that significant improvements will evolve from this talented team.

At present, summer of 1981, John Roncz has been using a modified Eppler program to optimize the design of canard surfaces for sailplanes and sport planes at chord Reynolds numbers down to 380,000. He also closely follows the laminar bubble studies of Dr. Mueller at Notre Dame. John is fascinated with the entire Reynolds number range and it is his hope that laminar separation bubble characteristics derived from the smoke stream photographs and measurements of Mueller can be added to the Eppler airfoil design method and by keeping the man in the loop it may eventually be possible to predict analytically the lift curve and lift drag polar distortions which are found experimentally at $40{,}000 < RN < 380{,}000$

It would appear that the theoretical airfoil design calculations so nobly started by Eppler may soon be refined to allow accurate predictions in the critical Reynolds number range. It may just be that when we arrive there we will have rediscovered the better airfoils already empirically developed by the technical aeromodellers.

LOW REYNOLDS NUMBER AIRFOIL DESIGN BIBLIOGRAPHY

Discussions of the problems peculiar to the design of airfoils in the critical Reynolds number regime may be found in the books on Technical Aeromodelling at the end of this section and in the previously cited references:

I-1, 2 II-1, 2, 5, 6, 7, 9 III-1, 2, 6, 7, 8, 18, 23, 25

III-27, 28, 29, 30, 31, and 32

IV-5, 6, 7, 9, 10, 11, 12, 13, 14, 15, 18, 19, 26, 27, 28, 29, 30, 31, 32, 33, 34

The following references are directed specifically to the actual airfoil design problem.

IV-A - Abbott, I. H. and von Doenhoff, A. E. - Theory of Wing Sections Copyright 1949. Dover Publication New York, NY 1959

B - Stratford, B. S. - "The Prediction of Separation of the Turbulent Boundary Layer." Journal of Fluid Mechanics Vol. 5 1959

C - Krouse, J. R. - "Effect of Undercamber on Endurance" Third Annual Symposium of the National Free Flight Society 1970

D - Krouse, J. R. - "Effect of Airfoil Parameters on Flight Duration" National Free Flight Symposium 1971

E - Bogart, C. W. - "A New Family of Free Flight Airfoils for all Occasions" Fourth Annual Symposium of the National Free Flight Society 1971

F - Monson, D. - "Some Aspects of Airfoil Geometry" National Free Flight Symposium 1971

G - Monson, D. - "Some Aspects of Airfoil Geometry - Part II" Fifth Annual Free Flight Symposium Report 1972

H - Krouse, J. R. - "Airfoil Leading Edge Bluntness, Good or Bad" Fifth Annual Free Flight Symposium 1972

I - Miley, S. J. - "An Analysis of the Design of Airfoil Sections for Low Reynolds Numbers" Mississippi State University Dissertation 1972

J - Wortmann, F. X. - "A Critical Review of the Physical Aspects of Airfoil Design at Low Mach Numbers" NASA CR-2315 1973

K - Liebeck, R. H. - "A Class of Airfoils Designed for Highlift in Incompressible Flow" Journal of Aircraft, Vol. 10 October 1973

IV-L - Eppler, R. - "Direct Calculation of Airfoils From Pressure Distribution" NASA TTF-15, 417 1974

M - Bonner, E and Gingrich, P. - "Prediction of Airfoil Real Fluid Characteristics at Subsonic Speeds" Rockwell International L.A. Division NA-73-771 April 1974

N - Hicks, R. M., Murman, E. M., and Vanderplaats, G. N. - "An Assessment of Airfoil Design by Numerical Optimization" NASA TM-X-3092 1974

O - Bauer, A. B. - "The Laminar Airfoil Problem" National Free Flight Symposium 1975

P - Russell, J. - "Prospects For The Application of Modern Airfoil Design Technology to the Low Reynolds Number Flow Regime" National Free Flight Symposium Report 1975

Q - Narramore, J. C., Olander, R. D., and Stearman, R. O. - "The Development of a Computer Aided Airfoil Design Procedure Including Preliminary Wind Tunnel Experiments on a Low Reynolds Number High Lift Section" AFOSR-TR-76-0536 1976

R - Eppler, R. and Somers, D. M. - "Low Speed Airfoil Design and Analysis" NASA Langley Advanced Technology Airfoil Research Conference March 7-9, 1978

S - Kennedy, J. L. and Marsden, D. J. - "A Potential Flow Design Method for Multicomponent Airfoil Sections" Journal of Aircraft, Vol. 15, No. 1 January 1978, pp 47-52

T - Eppler, R. - "Some New Airfoils" NASA Conference on the Science and Technology of Low Speed and Motorless Flight March 29-30, 1979

U - Phillips, W. H. - "Eppler Calculations of the Polars for Several Champine Model Airfoils" Private Communication March 1979

V - Narramore, J. C. and Yeary, R. D. - "An Airfoil Design and Analysis Methodology Using the Information Systems Approach" Bell Helicopter Textron Report, Fort Worth, Texas 1979

W - Henderson, M. L. - "Inverse Boundary Layer Technique For Airfoil Design". NASA Advanced Technology Airfoil Research, Vol. 1, NASA CP-2045, 1978

X - McMasters, J. H. and Henderson, M. L. - "Low Speed Single Element Airfoil Synthesis". NASA Conference Publication 2085, Part 1, Science and Technology of Low Speed and Motorless Flight. Hampton, VA. March 29-30, 1979

IV-Y Galloway, C. R. - "Application of Advanced Airfoils to High Altitude Long Endurance Remotely Poloted Vehicles" Air Fare Flight Dynamics Lab. Report TM-77-10-FXM, December 1976

IV-Z Liebeck, R. H. - "Superlift Airfoil Development Program" Air Force Flight Dynamics Lab Report TR-75-110, October 1975

IV-AA Eck, B. - "Everything You Ever Wanted to Know About 505 Fins" Tank Talk, 16918 Herford Road, Monkton, MD 21111, January 1979

IV-BB Sator, F. G. - "Supercritical Airfoil Sections with Slotless Fowler Flaps for Gliders and Motorgliders" Technical Soaring, Vol. VI, No. 1, September 1980

IV-CC Eggleston, B. and Surry, D. - "The Development of New A-2 Airfoils Aided by Computer" 1980 National Free Flight Symposium Report

IV-DD Draisey, S. - "Optimized Airfoils at Low Reynolds Numbers" University of Western Ontario Faculty of Engineering Science. Degree Thesis, March 1978

IV-EE McMasters, J. H., Norovik, R. H., Henderson, M. L. and Sandvig, J. H. - "Two Airfoil Sections Designed for Low Reynolds Numbers" Technical Soaring, Vol. VI, No. 4, June 1981. Published by the Soaring Society of America

IV-FF Roncz, J. - "Low Reynolds Number Airfoils Derived by the Modified Eppler Program: Unpublished to date. Private communication, July-August 1981

(D) BOOKS ON TECHNICAL AEROMODELLING

(1) Zaic, F. - Model Aeronautic Yearbook
1935-36, 37, 38, 51-52, 53, 55-56, 57-58, 59-61, 74-65
Model Aeronautic Publications, Box 135, Northridge, Calif.

(2) Grant, C. H. - "Model Airplane Design, Theory of Flight - 1941"
Notice in Free Flight Society Digest for December 1974 that it is to be republished

(3) Schmitz, F. W. - Aerodynamics of the Model Airplane - 1942
Part 1 - Airfoil Measurements - Translation by Redstone Arsenal, November 22, 1967 - Originally Published Gottingen, 1942

(4) Zaic, F. - Model Glider Design - 1944
Model Aeronautic Publications, Box 135, Northridge, Calif.

(5) Hoffman, R. J. - Model Aeronautics Made Painless - 1955
Model Aeronautic Publications, Box 135, Northridge, Calif.

(6) Zaic, F. - Circular Airflow - 1964
Model Aeronautic Publications, Box 135, Northridge, Calif.

(7) Malkin, J. - Airfoil Sections (For Model Airplanes)
Upper Hutt, New Zealand May 1971

(8) Dalby, E. and Cusick, C. - Book of Airfoils
F.A.I. Model Supply - Phoenix, Arizona 85068

(9) Eppler, R. - Model-Technik-Berater
MTB-1 Eppler Profile
MTB-2 GroBsegler - Hochliestungessegler - Special - Flugmodelle
Verlag für technik und Handwerk A&B Ledertheil
Baden-Baden, Germany 1977

(10) Pressnel, M. - Aerofoils for Aeromodellers
Pitman Publishing Corp. Fearon Pub. Inc. 6 Davis Drive
Belmont, Calif. 94002 USA 1977

(11) Simons, M. - Model Aircraft Aerodynamics
Model & Allied Publications - Argus Books Limited
14 St James Road, Watford, Herts, England 1978

(12) Althaus, D. - Profilpolaren Für Den Modellflug
N V Neckar - Verlag VS - Villingen - Schwenningen 1980

(13) Musil, M. - Aerodynamika Modernich Leteckych Modelů
Nase Vojsko - Praha 1978

(14) Althaus, D. and Wortmann, F. X. - Stuttgarter Profilkatalog 1
F. Vieweg & Sohn. Wiesbaden 1 West Germany 1981

(15) National Free Flight Society Annual Symposium Reports - 1968 through 1981. Can be obtained from Fred Terzian, 4858 Moorepark Avenue, San Jose, CA 95129

V. BOUNDARY LAYER TRIPPING DEVICES

A. Historical Review

The pioneering low Reynolds number investigations of Schmitz (Reference IV-4) included tests in which the performance of the 20% thick Gö 625 was markedly improved at R_c=82,000 by a turbulence wire placed ahead of the leading edge. Similar large performance improvements were obtained at R_c=60,000 with a wire grid placed ahead of the model.

Also in the 1940's, Pfenninger (Reference IV-5) investigated the effect of aft facing steps in the upper surface, surface waviness, and air jets blowing through the upper surface of laminar airfoils for Reynolds numbers of 250,000 to 1 x 10^6. He also noted the reduction in drag at high lift coefficient at subcritical airfoil-Reynolds number combinations. All of these devices cause early enough boundary layer transition to allow boundary layer reattachment forward of the trailing edge. The lower the Reynolds number, the further forward must the trip device be located to ensure reattachment forward of the trailing edge.

The research begun by Schmitz was continued by Kraemer including the effects of trip wires (Reference IV-13). Pfenninger (References IV-11, IV-32) investigated multiple surface mounted boundary layer trips on a thin airfoil down to R_c=21,000. Boundary layer tripping was also included in airfoil tests by Phillips (IV-26), Volkers (IV-29), Hendricks (IV-24), and Eggleston (IV-27 and IV-CC). Hacklinger has studied the effect of trips in free flight (IV-55 and IV-71).

Most recently, additional data is available from the low turbulence wind tunnels at Delft (IV-36) and at Stuttgart (IV-47) trips were used on a large number of airfoils.

The only attempt to evaluate the relative advantages of various types of surface trips was the study of Shoaf, Reference V-1.

B. Various Methods of Boundary Layer Tripping (See Figure V-1).

1. Increase the free stream turbulence by placing a wire or grid of wires in the flow ahead of the wing.
2. Beam sound energy at the forward upper wing surface with a frequency calculated to be most critical at the test Reynolds number.
3. Vibrating the wing at critical frequency.
4. Building waves of critical wave length into the upper wing surface.
5. Use of aft facing steps in the upper wing surface.
6. Bonding of multiple spanwise running tapes to the upper wing surface.
7. One or more spanwise running wires or strips bonded to the upper wing surface.
8. A spanwise row of small right cricular cylinders bonded to the upper wing surface.
9. A spanwise running strip of multiple spherical beads bonded to the upper wing surface.
10. A spanwise running raised or recessed serrated strip (Hama strip) bonded to the upper wing surface.
11. A spanwise row of holes through the wing allowing air jets to blow out normal to the upper surface.
12. A sharp leading edge at high angle of attack.
13. Normal sections at high angle of attack and low Reynolds number often automatically provide early enough transition to avoid the non-reattachment problem.

It would be desirable to know which type of boundary layer tripping would be optimum for any given Reynolds number. It is known that:

1. Laminar separation bubbles are small enough at chord RN $> 4 \times 10^6$ to make artificial tripping unnecessary.
2. It seems very difficult and perhaps impossible to effectively prevent non-reattached separated flow at lift coefficient >0.8 at chord RN $< 10{,}000$.

FIGURE V-1 VARIOUS METHODS OF BOUNDARY LAYER TRIPPING

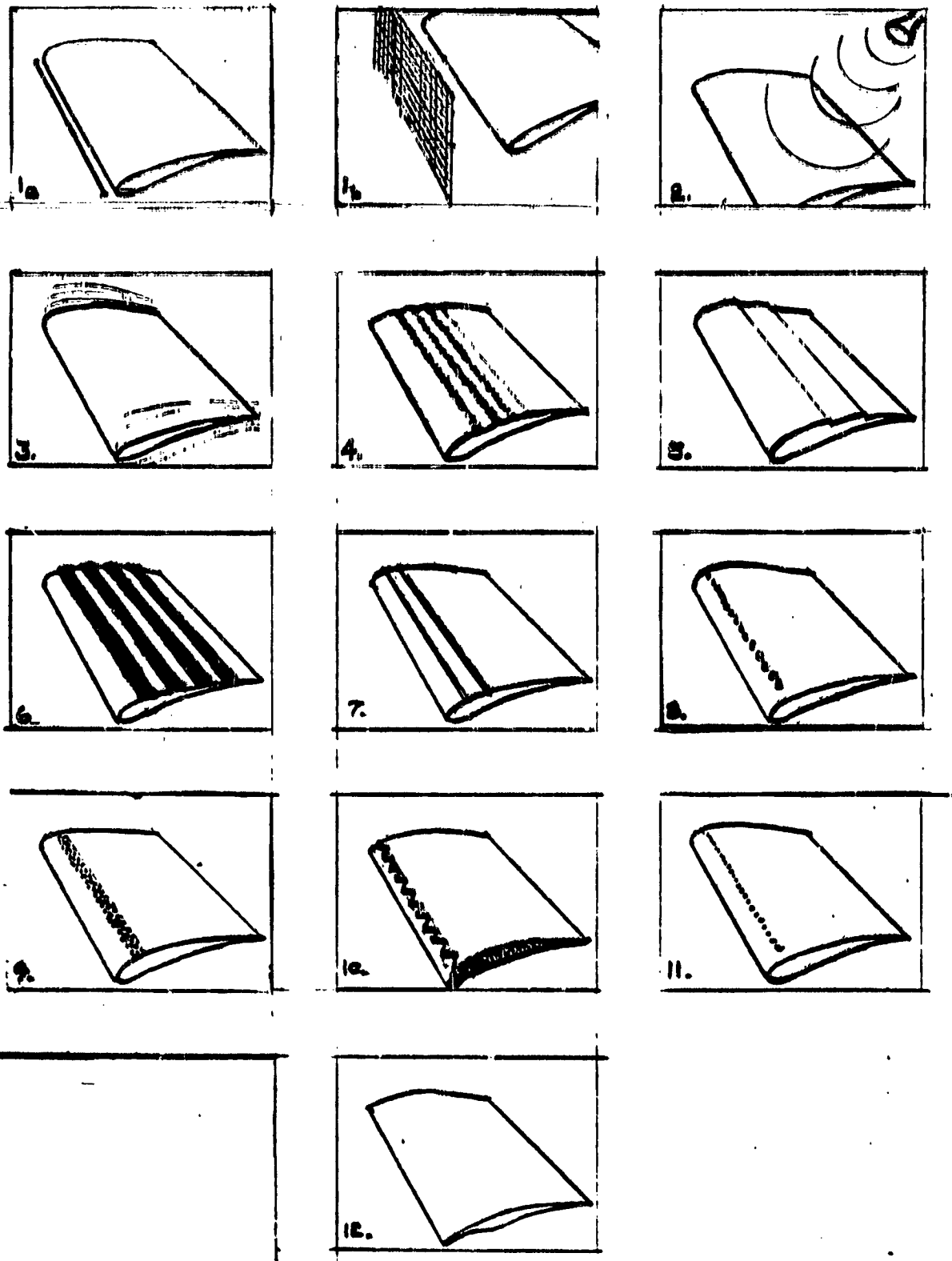

3. At 300,000 < RC < 4×10^6, the instability gradient as a tripping device IV-J seems to be an excellent method of limiting the adverse effects of laminar separation bubbles.

4. For 100,000 < R_c < 500,000, surface waviness, and aft facing steps are helpful tripping devices (IV-5).

5. A trip wire 10% chord ahead of wing leading edge improves airfoil L/D at RN at least as low as 46,000.

6. At the 1979 International Free Flight Model Airfoil Meet, the most prevalent type of b.l. tripper was a square cross-section spanwise running ridge, either single or two in series. These were found on the forward upper surfaces of wings, horizontal tails and propellers, most of which were operating in a RN range of 30,000 to 70,000. I did not see 3-dimensional trips such as a row of pins or a strip of small beads. The Israeli team had the most sophisticated trip. It was a recessed Hama strip on the forward upper wing surface. The rear edge was flush with the wing. The wing stepped down to a thinner leading portion abruptly. The face of the forward facing step was saw-toothed in plan form, thus producing a three dimensional disturbance to the boundary layer.

7. With the exception of Shoaf's paper, V-1, the writer has not seen comparative quantitative data on various types of b.l. trippers.

C. DISCUSSION

1. Two Dimensional Trip Strip on Forward Upper Surface - Stuttgart Data

   Two dimensional airfoil mounted trip strips were employed in some of the Stuttgart measurements. Trips appear on three airfoils at R_c = 40,000, nine airfoils at 60,000, and ten airfoils at 100,000 R_c.

Airfoil	Trip Location	Trip Height	Trip Width
FX 60-100	0.20 X/C	0.3 mm	2 mm
FX 60-126	0.10	0.3 mm	2 mm
FX 63-137	0.20	0.3 mm	2 mm
FX 62-K 131/17	0.205	0.3 mm	2 mm
FX M-2	0.030	0.3 mm	2 mm
AH 79-100B	0.0625	0.45 mm	2 mm
AH 79-100B	0.0875	0.3 mm	2 mm
AH 79-100C	0.23	0.5 mm	5 mm
E-193	0.10	0.3 mm	2 mm
E-193	0.23	0.3 mm	2 mm
E-203	0.083	0.15 mm	2 mm
Sokolov	0.092	0.3 mm	2 mm

In general, a performance improvement and a reduction in polar and lift curve distortion will result from tripping an airfoil at Reynolds number lower than the critical value for the bare airfoil. Performance decrements are generally found when trips are retained on airfoils at Reynolds numbers greater than the bare airfoil critical. The effect of .012 inch high by .08 inch wide rectangular cross sectioned upper surface trips located at .03 <x [illegible] 3 on (L/D) max is shown in Table 1, the effect on [illegible] is shown in Table 2, and the effect on polar and [illegible]rms appear in Table 3. The performances of all [illegible] improved at R_c = 40,000, the performance of 55% were improved at R_c = 60,000, and the performance of 33% were improved at R_c = 100,000. The effect of the trip on the FX 63-137 at 60,000 was very dramatic, bringing an airfoil which simply could not be used at that Reynolds number up to quite a commendable performance.

A somewhat unusual result was the effect of the trip at 100,000 R_c improving the AH-100C from a medium performance to top performance. The trip improved the polar and lift curve forms for the

TABLE 1 - TRIP EFFECT ON (L/D) MAX

AIR FOIL	R_c = 40,000		R_c = 60,000		R_c = 100,000	
	Bare	Trip	Bare	Trip	Bare	Trip
M-2	17	29	29	37	46.5	48.6
E-193	26	30	38	38	47.5	41
Sokolov	31.6	35	34	45.5	61	58
FX63-137			8.2	40	46	43
FX60-126			30	37.5	52	50
FX60-100			32	38	59	49
E-203			40	36.5	45	46
AH 100B			40	39	55	50
AH 100C			38	38	54	65
62K131/17 10°β					52	48
62K131/17 15°β					42	43

TABLE 2 - TRIP EFFECT ON $(L^{3/2}/D)$ MAX

AIR FOIL	R_c - 40,000		R_c - 60,000		R_c = 100,000	
	Bare	Trip	Bare	Trip	Bare	Trip
M-2	13	23	23	37	38	48
E-193	28	30	49	40	49	42.2
Sokolov	37.5	39	52	53	70.5	67
FX63-137			5.4	45	51	49
FX60-126			33	37	53	42
FX60-100			33	32	58	46
E-203			42	38	50	43
AH 100B			47	45	62	56
AH 100C			38	43	56	70
62K131/17 10°β					59.3	54
62K131/17 15°β					49	48

TABLE 3 - TRIP EFFECT ON POLAR AND LIFT CURVE FORM

AIRFOIL	BARE		TRIP		BARE		TRIP		BARE		TRIP	
	P	L	P	L	P	L	P	L	P	L	P	L
M-2	E	E	A'	B	E	E	A'	C	A'	?	A'	D
[redacted]-193	C+	C	C	B	C	C	A	A	A	B	A	A
Sokolov	D	C	C	B	C	C	B	B	B	B	A	A
FX63-137					E	E	A	A	A	A	A	A
FX60-136					A	A	A'	A	A	A	A	A
FX60-100					C	B	A'	B	A	A	A	A
E-203					C	C	A	B	A	A	A	A
AH 100B					D	D	C	C	B	A	B	B
AH 100C					C	C	A	B	A	A	A	A
62K131/17 10°β									C	B	B	A
62K131/17 15°β									C	B	B	A
	R_c = 40,000				R_c = 60,000				R_c = 100,000			

FX 62K 131/17 with deflected flap at a small decrement in (L/D) max and ($L^{3/2}$/D) max at R_c = 100,000. Detailed comparison of bare and tripped polars and lift curves should provide additional insight on optimum use of boundary layer trips.

(b) Wire Ahead of the E-61 Leading Edge--Delft Data

The effect of 0.5% chord diameter wire located 2% chord above the chord line and 10% chord in front of the leading edge on the polar and lift curve at R_c = 80,000 and 50,000 is shown in Figures V-2 and V-3. The wire completely removes the large drag increase at medium lift coefficients and takes the sag out of the lift curve. An appreciable loss in (L/D) max and $L^{3/2}$/D results. It is unfortunate we do not have data on the E-61 with an upper surface trip.

(c) Effect of Beamed Sound Pressure--Delft Data

The beneficial effect of beamed 105 db 300 cycle sound at R_c = 80,000 is shown in Figure V-2 and the effect of 104 db 145 cycle sound at R_c = 50,000 is shown in Figure V-3. The removal of the drag increase at medium lift coefficients and removal of lift-curve "sag" are now obtained with less cost in (L/D) max and ($L^{3/2}$/D) max if one does not consider the drag equivalent of the power required to produce the noise. The effect of the sound-pressure level in db at optimum frequency on the lift coefficient in the "sag" region is shown in Figure V-4. Note that the sound level in the Delft tunnel is 74 db without the tuned noise maker. This data points out once more the complexity of the aerodynamics of airfoils in the critical Reynolds number range so nobly pioneered by Schmitz and Pfenninger.

FIGURE V-2

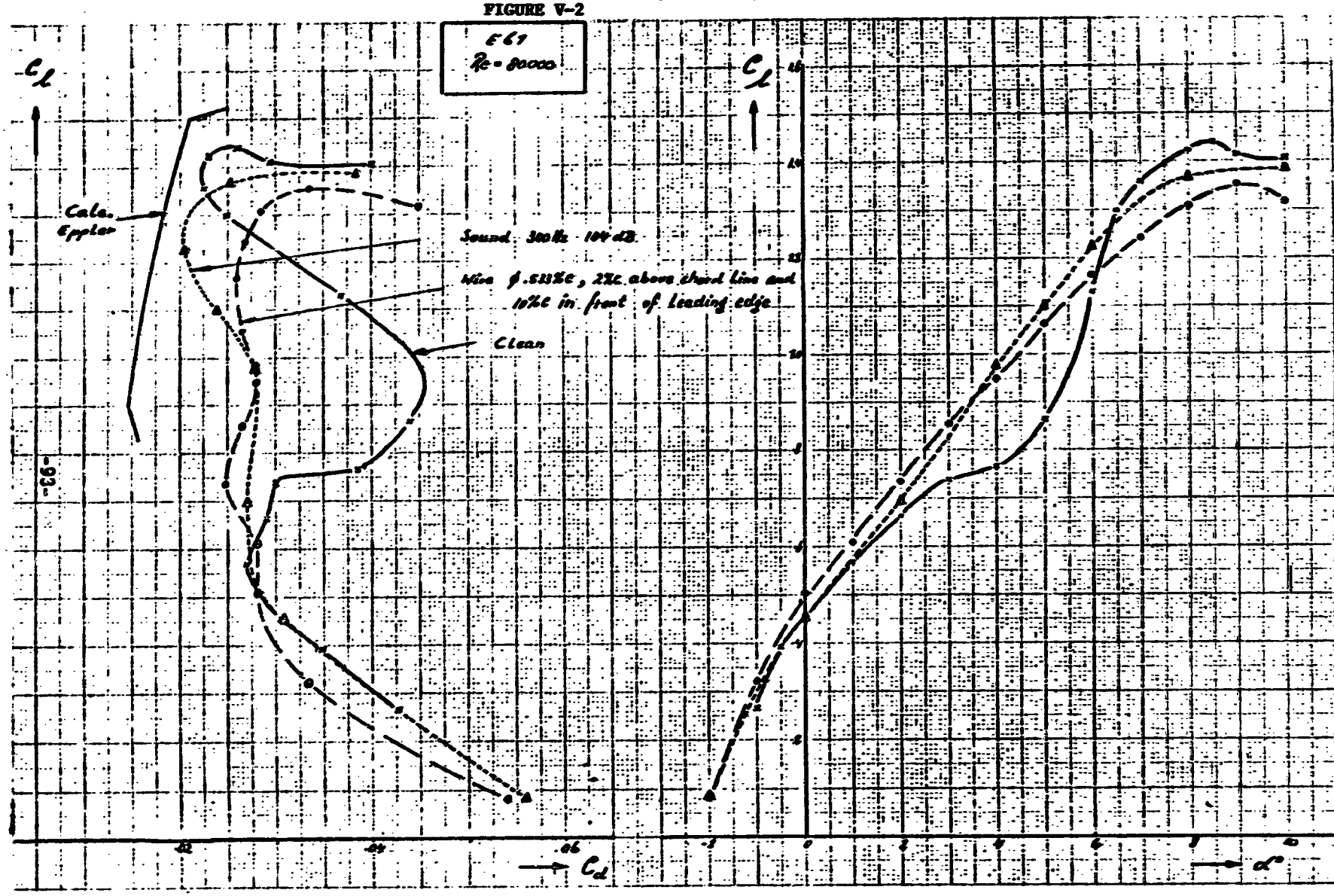

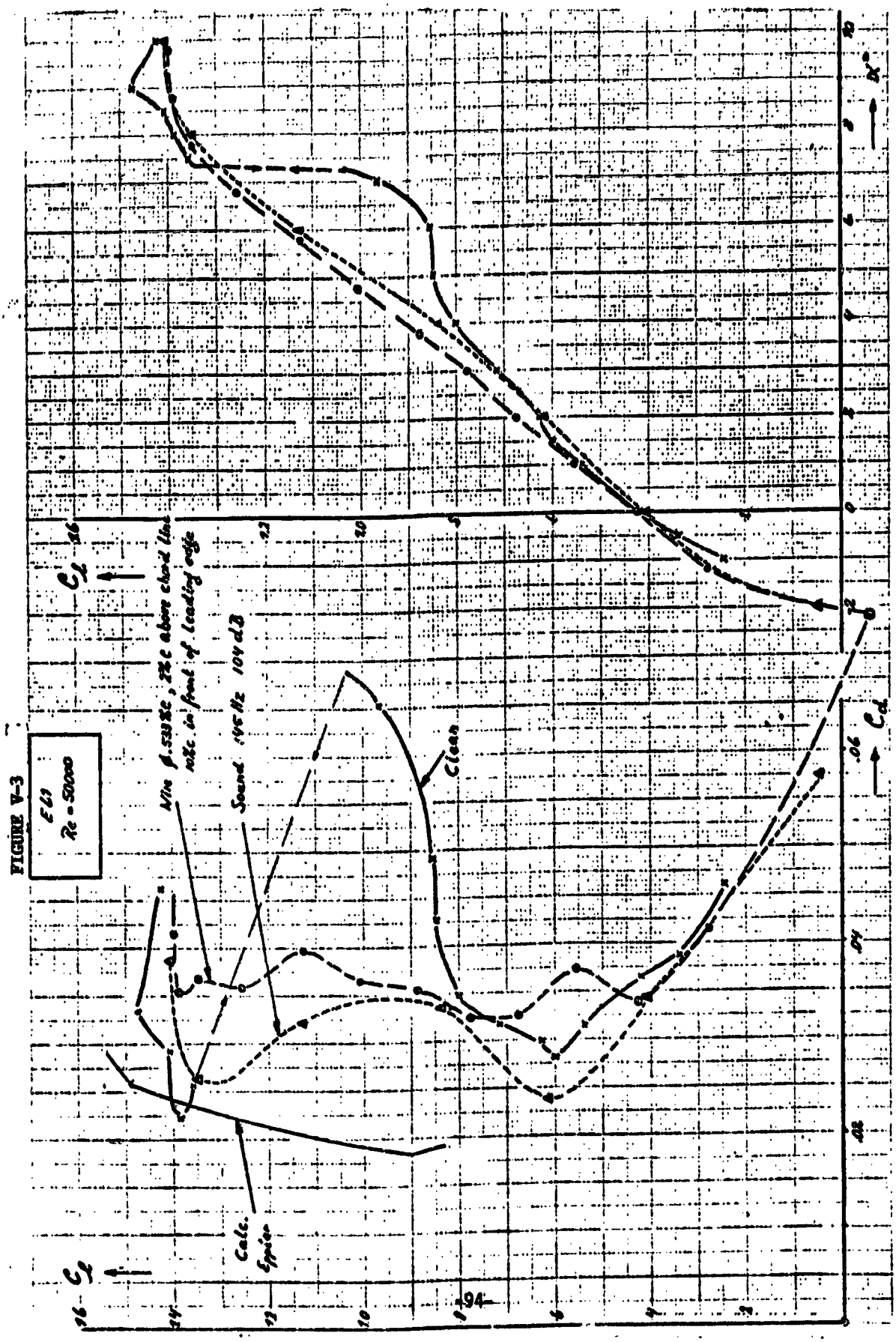

FIGURE V-3

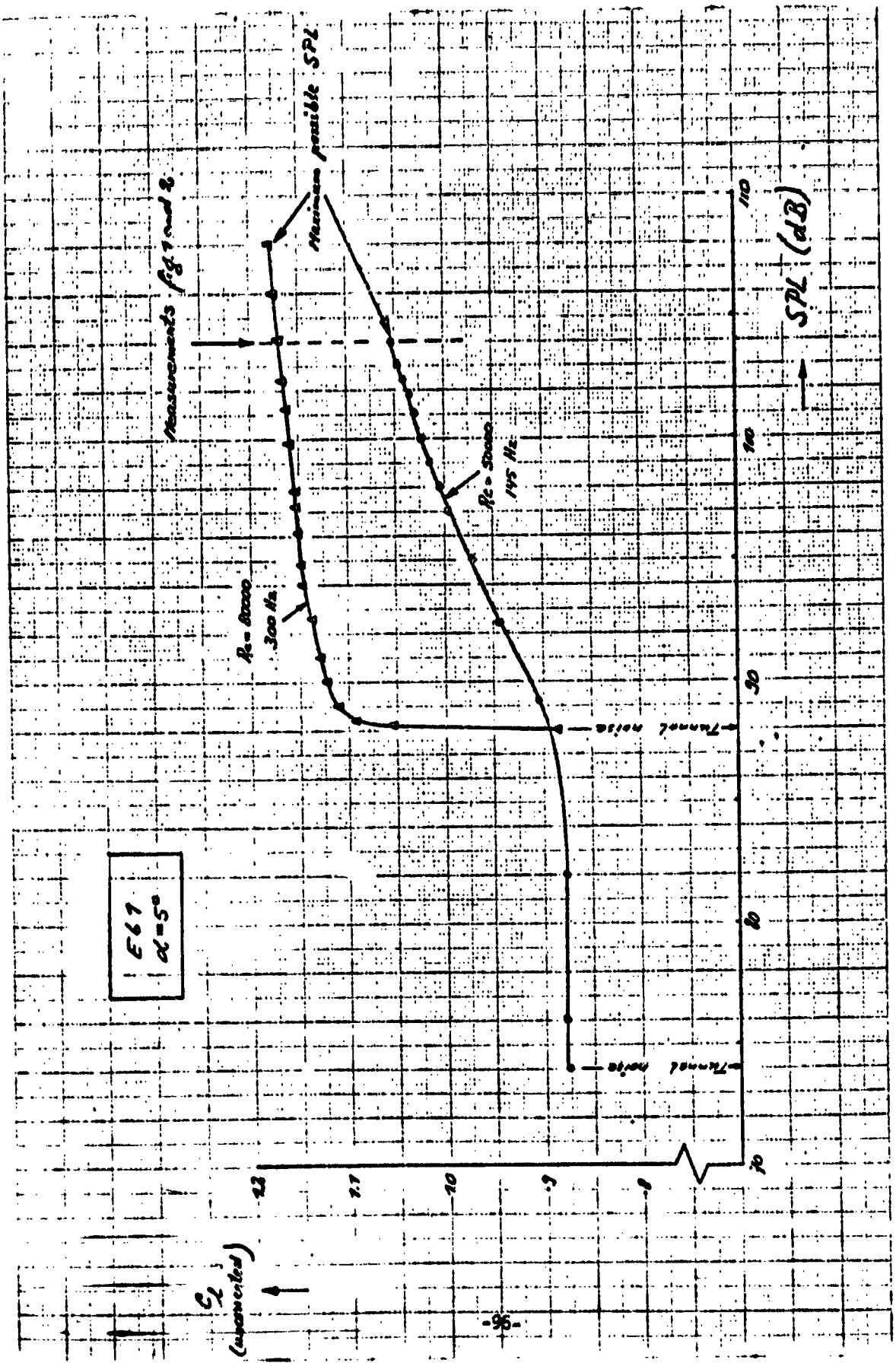

FIGURE V-4

(D) Boundary Layer Tripping Bibliography

Discussions of and in many cases data from boundary layer tripping experiments may be found in references: IV-4, IV-5, IV-8, IV-11, IV-13, IV-22, IV-24, IV-26, IV-27, IV-29, IV-30, IV-31, IV-32, IV-36, IV-43, IV-47, IV-48, IV-49, IV-55, IV-71, IV-72, IV-73, and in the books IV-3-1, 3, 10, 11, 12, 13, 15, as well as in:

V-1 Shoaf, H.C. - Characteristics of Turbulated Airfoils, Zaic 1964-65 Yearbook.

V-2 Hacklinger, M. - Artificial Turbulence, Zaic 1955-56 Yearbook.

V-3 Christi, C.M. - Turbulent Flow Airfoils, Zaic 1955-56 Yearbook.

V-4 Gillespie, W. - Rubber Power & Turbulators, Zaic 1957-58 Yearbook.

V-5 Baxter, D. - Rubber Power & Turbulators, Zaic 1957-58 Yearbook.

V-6 Pearce, F. - Airfoil Turbulators, Zaic 1959-61 Yearbook.

V-7 McBaine, C.K. - Letter on Multi Stringer Turbulator. Zaic 1959-61 Yearbook

V-8 Neustein, J. - Experiments at Low Reynolds Numbers. Part 1 - Isolated Airfoils. Cal Tech Report No. 6, March, 1957.